CANADIAN THESES ON MICROFICHE

I.S.B.N.

THESES CANADIENNES SUR MICROFICHE

National Library of Canada
Collections Development Branch

Canadian Theses on
Microfiche Service

Ottawa, Canada
K1A 0N4

Bibliothèque nationale du Canada
Direction du développement des collections

Service des thèses canadiennes
sur microfiche

NOTICE

The quality of this microfiche is heavily dependent upon the quality of the original thesis submitted for microfilming. Every effort has been made to ensure the highest quality of reproduction possible.

If pages are missing, contact the university which granted the degree.

Some pages may have indistinct print especially if the original pages were typed with a poor typewriter ribbon or if the university sent us a poor photocopy.

Previously copyrighted materials (journal articles, published tests, etc.) are not filmed.

Reproduction in full or in part of this film is governed by the Canadian Copyright Act, R.S.C. 1970, c. C-30. Please read the authorization forms which accompany this thesis.

AVIS

La qualité de cette microfiche dépend grandement de la qualité de la thèse soumise au microfilmage. Nous avons tout fait pour assurer une qualité supérieure de reproduction.

S'il manque des pages, veuillez communiquer avec l'université qui a conféré le grade.

La qualité d'impression de certaines pages peut laisser à désirer, surtout si les pages originales ont été dactylographiées à l'aide d'un ruban usé ou si l'université nous a fait parvenir une photocopie de mauvaise qualité.

Les documents qui font déjà l'objet d'un droit d'auteur (articles de revue, examens publiés, etc.) ne sont pas microfilmés.

La reproduction, même partielle, de ce microfilm est soumise à la Loi canadienne sur le droit d'auteur, SRC 1970, c. C-30. Veuillez prendre connaissance des formules d'autorisation qui accompagnent cette thèse.

THIS DISSERTATION
HAS BEEN MICROFILMED
EXACTLY AS RECEIVED

LA THÈSE A ÉTÉ
MICROFILMÉE TELLE QUE
NOUS L'AVONS REÇUE

Canada

NL-339 (r. 82/08)

STRESS ANALYSIS AND DESIGN

OF

MULTI-RING FIBRE COMPOSITE ROTORS

BY

JIMMY J.M. WONG

Thesis submitted to the School of
Graduate Studies of The University of
Ottawa in partial fulfillment of the
requirements for the degree

of

MASTER OF APPLIED SCIENCE

in

MECHANICAL ENGINEERING

February 1982

ACKNOWLEDGEMENT

The author would like to express his deepest gratitude and appreciation to Dr. R.C. Flanagan for his valuable supervision and guidance throughout the work. Also, he wishes to extend his very sincere thanks to Dr. M.B. Munro for providing material information and valuable suggestions. Furthermore, the author would like to take this opportunity to thank the members of the Flywheel Research Team of the University of Ottawa for their interesting and motivating discussion throughout the work. In particular, his sincere appreciation goes to Dr. A. Miyase and Mr. Jack McCrea.

In addition, he wishes to thank Dr. R.C. Flanagan for his financial support from NRC (Canada) - Contract No. OSU80-00043, NSERC Grant No. A-7516 and teaching assistantships from the Department of Mechanical Engineering, University of Ottawa.

Finally, the author is indebted to his overseas family, Miss Suzie Kong and his housemates for their endless love and care that encouraged his completion of the work. Also, his sincere thanks go to Mrs. Susan Flanagan for her carefulness and patience in typing this thesis.

ABSTRACT

The sensitivity and behaviour of both the radial and tangential stress distributions in hoop-wound fibre composite rotors were analyzed. Both physical and material parameters, representative of the glass, graphite and kevlar fibre families were explored. The controlling parameters were found to be ring thickness ratio, interfacial pressure, material modulus ratio (E_θ/E_r) and specific modulus (or strength).

The three main categories of flywheel design concepts identified by the Flywheel Research Team [1], namely, (i) Single Material Multi-Ring-On-Ring, (ii) Multi-Material Biannular and (iii) Multi-Material Multi-Ring-On-Ring, were studied and evaluated. The five recommended materials: (i) E-glass, (ii) S2-glass, (iii) Kevlar 29, (iv) Kevlar 49, and (v) AS-Carbon were used for the analysis. In addition, the recommended SMC hub and manufactured aluminum hub were also included in the study for estimating the cost of material, weight and dimensions of full size flywheel designs.

Six designs were selected as holding considerable promise for a 1 KW-Hr (usable, 2:1 speed range) anisotropic material flywheel including three biannular designs, one triannular, one multi-material multi-ring and one single-material multi-ring. Several of these designs can meet all the design objectives/constraints imposed for the transportation application even for the 1.0 KW-Hr usable energy requirement.

S2-glass, AS-Carbon and Kevlar 49 were identified as the most desirable materials for the advanced data base material tests.

TABLE OF CONTENTS

LIST OF FIGURES

LIST OF CHARTS

LIST OF TABLES

NOMENCLATURE

a	-	outside radius of a single ring
a_m	-	outside radius of ring 'm'
a_{m-1}	-	inside radius of ring 'm'
b	-	outside radius of a single ring
c	-	radius ratio of a single ring; (a/b)
c_m	-	radius ratio of ring 'm'; (a_{m-1}/a_m)
E_θ, E_r	-	Young's modulus in the tangential, radial direction
g	-	gravitational constant
k	-	modulus ratio, $(E_\theta/E_r)^{\frac{1}{2}}$
N	-	numbers of rings in a rotor
P_a, P_b	-	internal, external pressure on a single ring
P_{m-1}, P_m	-	internal, external pressure on ring 'm'
P1	-	interfacial pressure between Ring #1 and Ring #2
PN	-	interfacial pressure between Ring #N and Ring #(N+1). (N = 1,.....N-1)
r	-	radial position
RO	-	inside radius of Ring #1
R1	-	outside radius of Ring #1
RN	-	outside radius of Ring #N (N = 1,.....N)
t	-	ring thickness, $(a_m - a_{m-1})$
T	-	change of temperature
T(r)	-	winding tension function

u	-	radial displacement
$u^m(r)$	-	radial displacement of mandrel
v	-	displacement in tangential direction
V_f	-	volume fraction of fibre
θ	-	angular position
ρ_m	-	density of ring 'm'
α_θ, α_r	-	thermal coefficient of expansion in the tangential radial direction
ν_θ, ν_r	-	poisson ratio in the tangential, radial direction
ε_θ, ε_r	-	strain in the tangential, radial direction
$\varepsilon_{\theta o}$, ε_{ro}	-	free shrinkage strain in the tangential, radial direction
σ_θ, σ_r	-	stress in the tangential, radial direction
$\sigma_{\theta R}$, σ_{rR}	-	residual stress in the tangential, radial direction
$\sigma_{\theta m}$, σ_{rm}	-	stress in the tangential, radial direction of the mandrel
$\tau_{r\theta}$	-	shear stress in r-θ plane
ω	-	rotor angular speed (rad/s)

CHAPTER 1
INTRODUCTION

1.1 LITERATURE SURVEY

Flywheel technology has become an area of national interest due to the promise of substantial energy conservation, especially in the urban road transport sector [1,2,3,4].

While the storage of mechanical energy is not a new idea [5], the successful development and manufacture of such a unit, suitable for mass production and implementation into the market place, is yet to be accomplished.

The area of current interest of many prominent researchers in the field is that of fibre composite rotor design. Due to the fibre's high specific strength, the fibre composite flywheel has the potential of becoming a high energy density storage system. Further, it greatly reduces the hazard of catastrophic failure common to conventional steel rotors [6,7].

The first composite material flywheels to be constructed were in the form of flat circumferentially wound thick rings or disks [8]. These rotors developed circumferential cracks at relatively low rotational speeds. This is to be expected since, although fibre-reinforced composite materials possess very high longitudinal strengths, they have very low transverse strengths. In an attempt to reduce the radial tensile stresses, the axial thickness of the disk was varied with the radius [9], however, the radial stresses were not reduced significantly. Reedy [10] conducted a optimization study after which he constructed a thick rim carbon/epoxy "Wagon Wheel" flywheel. He noted that, in order to prevent circumferential cracks, as found in thick ring or solid disk flywheels, it was necessary to select the proper inner to outer rim radius ratio.

To overcome this problem, as well as that of poor volumetric efficiency, several multi-ring flywheels have been proposed. The simplest design consists of nested individually wound rings. The radial thickness of each ring is chosen to avoid a radial tensile failure. There is, however, a radial displacement incompatibility between the rings. As such, bonding is required to prevent separation at the ring interface. This gives rise to a stress pattern similar to that of a thick single ring. An attempt to alleviate this problem by separating the composite material rings with thin inter-rings of soft rubber has been made by Danfelt et.al. [6]. Thus, stress patterns can be redistributed by varying the material density and modulus. Apart from manufacturing problems, tension still exists at the inner side of the low modulus ring. Kirk [11, 12] suggested the use of interfacial pressure, a physical parameter, to redistribute the stress pattern. The major disadvantages are the difficulty of manufacture and the high compressive loading at static or low speed operation. However, Huddleston et.al. [13] were successful in producing a residual pre-stress in a thick ring flywheel by winding individual layers at different winding tensions. Post [14] suggested the use of an inner ring material with a lower modulus to density ratio than the outer rings. Pardoen [15] investigated the possibility of achieving the desirable stress states by varying material density with respect to the radial coordinate. In theory, this permits ring compatibility and a suitable stress distribution, however, in practice, material constraints do not allow for the range of material properties required.

The above options were explored using a computer analysis of the radial and tangential stress patterns and the radial displacement. The program, established in parameter form, can accept single, multi or hybrid ring designs with varying thicknesses and materials.

One of the task objectives of the work was to explore the sensitivity of stress to changes in the physical parameters and material

properties. The physical parameters are the diameter ratio, the overall internal and external diameter and the external pressure. The material properties are the modulus in the tangential and radial direction, Poisson's ratio and the density of the composite material. In addition, the work included a search for all the feasible designs of the different flywheel design concepts that were identified and recommended [1]. The computer results estimated the cost, weight, configuration and swept volume as well as the stress patterns for each of the different flywheel design concepts.

While part of this work was to explore hoop-wound fibre composite stress patterns and to establish the controlling physical and material parameters, it is first necessary, for any practical design concept to emerge, to identify the application and design objective. For the hybrid power train road vehicle application, the following design objectives and constraints were established [1].

1. Usable energy storage of 0.75 to 1.0 KW-Hr with a 2:1 speed range.

2. Maximum design speed of 25,000 rpm.

3. Maximum outside diameter of 61 cm (24 inches).

4. Swept volume of about 0.025 cubic meters (1500 cubic inches).

5. Flywheel weight of about 30 to 32 Kg (65 to 70 pounds).

1.2 THESIS OVERVIEW

Chapter 1 is a general literature survey of flywheel technology development and a statement of the thesis objective. In Chapter 2,

flywheel design concepts are reviewed and a more in-depth literature survey on existing flywheel concepts and flywheel systems was conducted. Then, in order to meet the identified design objectives/constraints [1], flywheel technology and materials are assessed and selected for further study. Before the design analyses were conducted, design parameters of single and multi-ring rotors were explored in Chapter 4 to give better insight into the sensitivity of flywheel rotor design with respect to material and physical parameters. In Chapter 5, the thesis proceeds to study and discuss the results of the computer analysis of the identified flywheel designs that give a 1 KW-Hr usable energy with a 2:1 speed range. Thereafter, final rotor designs are selected. Final conclusions and R & D recommendations are then presented.

CHAPTER 2

REVIEW AND SELECTION OF FLYWHEEL DESIGN CONCEPTS

2.1 FLYWHEEL TERMINOLOGY IDENTIFICATION

This chapter is mainly an extension of the literature survey of Chapter 1. Various existing flywheel design concepts are reviewed and discussed. Thereafter, various feasible existing and non-existing flywheel designs are assessed so as to identify the types of flywheels that appear most suitable for the road vehicle transportation application.

For ease of reading and better systematic analysis, the various existing flywheel design concepts are divided into four groups which consist of nine categories as follows:

Group I	-	1. Single Material Multiring on Ring
		2. Multi-material Multiring on Ring
		3. Wound Disk
Group II	-	4. Single/Multiring with Overwrap
		5. Tape Wrap
		6. Thick Rim with Bandwrap
Group III	-	7. Laminated Disk
		8. Laminated Disk/Rim
Group IV	-	9. Bare Filament/Tape

Figures and details of the nine categories are given in Table A-1 (see Appendix A).

2.2 REVIEW AND ASSESSMENT OF EXISTING FLYWHEEL DESIGN CONCEPTS

While different flywheel design concepts are categorized in Section 2.1, the actual design details and performance of these systems are reviewed and discussed in this section.

The first group of flywheels is composed of three main design categories consisting of a hoop-wound fibre composite rim, namely; design concept (1) Single Material Multiring on Ring, (2) Multi-material Multiring on Ring, and (3) Wound Disk. As mentioned earlier, Morganthaler [8] designed and spin tested the first single material thick ring rotor and reported circumferential cracks at relatively low speeds due to the poor transverse strength of fibre composite material. In order to reduce the transverse radial stress, Garrett [16, 17] designed a single material multiring on ring rotor using E-glass (for details refer to Tables A-2 and A-3 in Appendix A). As expected the specific energy storage of this design was relatively low because of the low specific strength of E-glass. On the other hand, a rotor made of eight thin rings of Kevlar 49 [16, 17, 18] had a significantly higher energy density because of the high specific strength of Kevlar -49. However, the non-optimal usage of material and the requirement of high interfacial pressure to prevent ring separation are still the main disadvantages [19] of this category of design.

In order to obtain a higher energy density in multiring rotors, one approach is to achieve failure (or working stress) simultaneously in each individual ring at the same design speed. In this regard, the multi-material multiring rotor design was judged promising [20]. Not only will this concept allow the designer to achieve a desirable stress pattern across the full radial dimension of the ring, but it will also allow efficient usage of material and provide better radial dilation compatibility between the rings [20]. The typical multimaterial multiring design is achieved by stacking a material of higher specific

strength or moduli with increasing radial position. The relative dilation of the inner and outer rings alleviate the radial compatibility problem. Never-the-less, separation between the inner S2-glass ring and the outer Kevlar 49 ring in Garrett's multimaterial multiring on ring flywheel [16, 17, 18, 21] is a typical failure mode of this category of design (see Table A.3 in Appendix A). In addition, Garrett's multiring rotor [21] design consists of an oversize star-hub for hub-rim assembly. Consequently, the sub-circular shape of the rim would likely require the use of a thin ring design concept [19]. Unfortunately, such a design approach results in a large swept volume for the flywheel system and a large number of rings to be wound. Alternate designs such as tension-balanced spokes for supporting the fibre composite rim by Brobeck [22, 23] permits the use of thicker rings and rim. However, the questionable rigidity and high manufacturing cost for the tension-balanced spokes will definitely hold down the ratings of the design for the road transportation application.

Other than designing a multimaterial multiring on ring flywheel to achieve high energy density and optimal usage of material, a constant stress wound disk (ring) made of a contoured filament-wound fibre composite also looks promising. Hercules [24, 25] continuously wound a contoured AS-carbon disk (ring) as a typical design of this category. The major drawbacks of the design were premature radial circumferential failure; high cost and manufacturing technology.

The second flywheel design group consists of a hoop-wound fibre composite rim that is reinforced radially with an overwrap on bandwrap, namely; design concept (4) Single/multiring with Overwrap, (5) Tape Wrap, and (6) Thick Rim with Bandwrap (see Table A-1 in Appendix A for diagrams of wrap). This group of flywheel designs is characterized by the use of a fibre composite overwrap or bandwrap in attaching the hoop-wound fibre composite rim to the metallic hub (usually aluminum). The major flywheel manufacturers for single/multiring with overwrap are Aerospatiale [26], MAN [27] and Rocketdyne [28, 29]; for tape wrap is

again Rocketdyne [29, 30, 31]; and for thick rim with band wrap are Union Carbide [13, 33, 39] and Sandia Lab's 'Wagon Wheel' and 'pin-wrapped' flywheels [10, 34, 35] (see Table A-2 for flywheel design details). On the whole overwrap or bandwrap flywheels have the disadvantages of high cost of manufacturing and poor rigidity of hub/rim attachment. This is supported by the fact that failure of flywheels of this group was caused by creep in the bonding of hub and overwrap [27]; dynamic instability [29]; bowing of bandwrap [32] and band failure [13, 25, 36] (see Table A-3 for performance details). Furthermore, bandwrap failure could possibly pierce the containment which is a major drawback from the safety point of view.

The third flywheel design group consists of a disk made of a quasi-isotropic laminate layup. This includes design concepts (7) Laminated Disk, and (8) Laminated Disk with Rim. Generally the laminated disk is manufactured by stacking layers of composite laminate at prescribed angles of orientation. The manufacturing and design analysis of a laminated disk are complicated by the fact that thick-laminate technology is in its infancy [37]. Quasi-isotropic laminates are not isotropic in strength [37] and interlaminar stresses cannot be accurately predicted due to the empirical nature of laminate strength theories [37, 38]. In addition, the reported catastrophic failures [37, 39] of laminated disks presents a critical containment and safety problem, (see Table A-3 in Appendix A). On the other hand, a laminated disk reinforced by a hoop-wound fibre composite rim [40] seems to be promising in providing both higher energy density and better failure modes. However, the infancy of laminate technology [37] and the unidentified failure modes [1], combined with the relatively low rigidity of hub/disk attachment by elastomeric bonding [41], will still hold down the rating of this design.

The last flywheel design group is the Bare Filament/Tape design where bare fibre filament is continuously wound and attached to hub with radial wraps. The principle feature of this flywheel configuration, other than being a filament wound structure, is that the wound filaments are held together by a minimum amount of resin or, in most applications,

only by a radial wrap without the use of resin [42]. In addition, the design has demonstrated the feasibility of providing a low cost flywheel system [43] by using low-cost materials such as vinyl impregnated glass, steel wire and 'Metglas' Amorphous Metal Ribbon. These designs hold considerable promise as a low-cost home energy-storage system (basement flywheel) to eliminate the daytime load peaks or as a backup for home solar photovoltaic or wind energy systems over cyclic non-operating periods. Combining the disadvantages of relatively poor swept volume, weight and rotor stability [1] of the bare filament flywheel off-sets the cost advantage and it can be seen that the design is not too suitable for the road vehicle transportation application (see Table B-3 in Appendix B).

2.3 FLYWHEEL DESIGN CONCEPTION: IDENTIFICATION AND SELECTION

After reviewing the flywheel technology in Section 2.2, the main objective of this section is to identify and select the most promising flywheel design concepts that will satisfy the design objectives/constraints outlined in Chapter 1.

Generally speaking, anisotropic material flywheel design is a new high technology field with many unanswered questions and is yet in its embryonic stages. Both the maturity of thought and the manufacturing technology required for absolute assessment and R & D program definition remain fragmented and controversial. It seems that there are many generation's of design maturity yet to come. Also, there is no clear design direction, at this stage of development, which has been identified as the across the board leader. Therefore, decision analysis techniques are used to evaluate all existing and non-existing flywheel design concepts for further study.

For the decision analysis rating, a series of twenty existing and non-existing flywheel design concepts were identified and assessed [1],

relative to each other, against a set of fourteen 'Impact Parameters' (see Table B-1) which cover the areas of safety, geometry, cost and technology. The twenty 'flywheel design concepts' are as follows (see Table B-3 in Appendix B):-

A (i)	Single Material, Thin Ring
~~(ii)~~	Single Material, Thick Ring
B	Single Material Ring with Overwrap or Bandwrap
C	Single Material Multi-Ring with Overwrap or Bandwrap
D	Single Material Multi-Ring with Low-Modulus Inter-Ring Wrap
E	Single Material Multi-Ring-On-Ring
F	Multi-Material Multi-Ring with Overwrap or Bandwrap
G	Multi-Material Multi-Ring with Low Modulus Inter-Ring Wrap
H	Multi-Material Multi-Ring-on-Ring
I	Shaped Central Core with Tape-wrap
J	Bare Filament/Tapes
K	Wound Disc
L	Laminated Disc
M	Shaped Laminated Disc
N	Laminated Disc with Ring
O	Shaped Laminated Disc/Ring
P	SMC Disc
Q	Shaped SMC Disc
R	SMC Disc with Ring
S	Shaped SMC Disc/Ring

Design concepts'A' to 'O' are similar to the nine categories of existing flywheel designs discussed earlier in the previous section. Exceptions being designs 'D' and 'G' which have thin, low modulus (elastomeric material) inter-ring wraps that separate the composite rings [4]. These two designs were judged to be difficult for manufacturing and potentially unstable [20]. Further, the ratings are low for designs 'P' to 'S' that are made of an SMC (Sheet Moulding Compound) disc.

This can be expected because of the low specific strength of the SMC material (see Table B-3).

From the decision analysis rating (see Table B-3 and B-4), on the basis of either a restriction violation or a below average score, all but three were eliminated from the transportation application. The three judged meritorious were:

1. Design 'E' — Single-Material Multi-Ring-On-Ring
2. Design 'F' — Multi-Material Multi-Ring with Overwrap or Bandwrap
3. Design 'H' — Multi-Material Multi-Ring-On-Ring. (n-ring or bianular)

For the ring type flywheels selected, nine hub designs were identified. As with the flywheel design concepts, decision analysis ratings were used to identify the most promising hub designs. Tables B-5 and B-6 in Appendix B provide the technical summary and numerical ratings for each hub.

From the ratings, the manufactured metallic (aluminum) hub with integral shaft appears to be the most desirable design approach. However, SMC hubs appear very attractive especially in the light that the ratings assigned to 'integrity', 'ease of containment', 'quality control/inspection' and 'technical risk' are held down due to the lack of appropriate data. A moderate R & D program in SMC hub design could well result in substantially higher ratings.

2.4 FIBRE ASSESSMENT AND SELECTION

Detailed data analysis and assessment of fibre composite material is beyond the scope of this thesis. However, for consistency and ease of reading, a summary of fibre assessment and selection is included in this section.

The candidate fibres selected for assessment were E-glass, S2-glass, high modulus carbon, high strength carbon, intermediate properties carbon, Kevlar 29 and Kevlar 49.

The above mentioned candidate fibres were assessed [1] in a very similar manner to that of the flywheel design concept reviewed in Section 2.3. Material cost, tensile fatigue, transverse tensile strength and resistance to creep were identified as the four key impack parameters for rating the candidate fibres.

All candidate fibres were rated against the impact parameters (Table B-7) according to the values reported in the appropriate data bases by the Flywheel Research Team [1]. According to the rating and the present status of the R & D program the following materials were recommended for evaluation:

(i) E-glass (Type 3709, Fibreglas Canada)

(ii) S2-glass

(iii) Kevlar 29

(iv) Kevlar 49

(v) Carbon (Grafil Type E/AS).

CHAPTER 3

STRESS EQUATIONS DEVELOPMENT

3.1 INTRODUCTION

In studying the stress developed in a high-speed fibre composite rotor, other than the stress induced by the centrifugal loading at high-speed rotation, pre-stress due to winding tension and residual stress due to chemical setting and thermal curing are also important. However, to develop a theory (or model) to account for all these stresses will be complicated by the fact that the pre-stress and residual stress are functions of many parameters [13] during the manufacturing process. Pre-stress due to winding tension, for example is a function of resin flow, tension relaxation, winding speed, mandrel stiffness, etc. Residual stress due to chemical setting is also complicated by the local irregularity [61] during the bonding between resin and fibre, interface material properties, etc.

In view of the complex range of parameters that could influence the stress developed in a high-speed fibre composite rotor, and also the fact that stress due to spinning is the most important for the first generation rotor design analysis, only centrifugal stresses will be studied in detail in the next chapter.

However, the following section will discuss the development of stress equations for anisotropic material rotors. Pre-stress due to winding tension, residual stress due to anisotropic chemical setting, thermal residual stress due to curing or elevated temperatures due to aerodynamic drag [72] will be introduced. Finally, the most important stress in a high-speed rotor, centrifugal stress, will be presented.

3.2 PRE-STRESS DUE TO WINDING TENSION

Although fibre composite materials possess very high longitudinal strengths, the relatively low transverse strength will not allow a rotor of high outside to inside diameter ratio (thick ring) to be utilized without premature delamination failure. From the safety viewpoint, transverse premature delamination could be desirable compared with the longitudinal catastropic failure. But, on the other hand, energy density of the whole flywheel system will be dramatically decreased because of the transverse failure at low speed.

One of the practical manufacturing methods to solve the premature delamination in a thick ring design is to pre-stress the rim by constant or variable winding tension. The compressive pre-stress by winding tension will balance the rotational tensile radial stress (transverse direction) at a desirable rotational speed. Theoretically, the pre-stressed ring could be manufactured by winding tension control so that it will fail both transversly and longitudinally at the same time. In addition, the ring could also be prestressed so that delamination would occur just before longitudinal failure at design speed to give a more desirable failure mode.

Liu and Chammis [51] developed a theory to calculate the pre-stress due to winding tension in the filament-wound composite ring. But this theory assumed that the residual stresses were directly a result of winding tension alone and did not take into consideration other variables in the filament-winding process. In the actual process, rather than winding tension alone, the problem could be complicated by tension relaxation, resin flow, resin shrinkage and orthotropic thermal stresses during curing.

The stress equations due to winding tension [61] were developed in Appendix C-1. Equation (3.2.1) and (3.2.2) give the radial and tangential residual stress of a filament-wound composite ring after removal from the mandrel due to winding tension.

$$\sigma_r(r) = \frac{2KB^{2K}C^{K-1}f(b_m)}{C^{2K} - b_m^{2K}} \left[\left(\frac{c}{r}\right)^{K+1} - \left(\frac{r}{c}\right)^{K-1} \right]$$

$$- b_m^{K-1} f(r) \left[\alpha \left(\frac{b_m}{r}\right)^{K+1} + \beta \left(\frac{r}{b_m}\right)^{K-1} \right] \quad \text{.....(3.2.1)}$$

$$\sigma_\theta(r) = T(r) + Kb_m^{K-1} f(r) \left[\alpha \left(\frac{b_m}{r}\right)^{K+1} - \beta \left(\frac{r}{b_m}\right)^{K-1} \right]$$

$$- \frac{2K^2 b_m^{2K} C^{K-1} f(b_m)}{C^{2K} - b_m^{2K}} \left[\left(\frac{c}{r}\right)^{K+1} + \left(\frac{r}{c}\right)^{K-1} \right] \quad \text{.....(3.2.2)}$$

Where $\alpha = K - \nu_\theta - B$

$\beta = K + \nu_\theta + B$

$$B = \frac{E_\theta}{E_m(b_m^2 - a_m^2)} \left[(1-\nu_m) b_m^2 + (1+\nu_m) a_m^2 \right]$$

$$f(r) = \int_r^C \frac{\rho^K T(\rho)}{B\rho^{2K} + \alpha b_m^{2K}} \, d\rho$$

a_m = inside radius of mandrel

b_m = outside radius of mandrel

c = outside radius of filament-wound composite ring

ρ = radial position

Although the theory looks straight forward, it remains to be proven experimentally. As mentioned earlier, residual stress due to filament-winding is a result of many variables, such as: resin flow,

resin strinkage and orthotropic thermal stress. Also, a significant amount of tension relaxation at the winding surface affects the accuracy of the theory by Liu and Chamis.

Huddlestion and Knight [13, 33] took into consideration tension relaxation and conducted experiments to determine the residual stresses in filament-wound composite rings. Because of the scattered and small amount of experimental data, it is still difficult to correlate experimental and theoretical results.

3.3 RESIDUAL STRESS DUE TO ANISOTROPIC SHRINKAGE

It is very common to find cracks occuring somewhere near the middle of a relatively thick filament-wound composite ring. Shiratori [62, 63] reported that these cracks occur almost at the same place in the same size of rings, and concluded that the cracks were developed by residual stress due to anisotropic shrinkage.

Anisotropic shrinkage was considered to be composed of two components [62]. First, the chemical shrinkage due to the chemical setting of resin, and second, the thermal shrinkage due to the drop of temperature following the curing process. In the beginning of gelation of resin, because of the liquidity of resin, no stress will be developed due to the shrinkage of resin. However, as soon as some elasticity developed between the resin and fibre, shrinkage would induce a residual stress in the ring. Similarly, after the chemical setting, a thermal stress would develop in the ring when cooled from elevated temperature to room temperature in the curing process.

Shiratori [62] studied theoretically and experimentally the residual stress in a filament-wound composite ring due to anisotropic shrinkage. The experimental results of the study approximated the theory proposed by Shiratori [62]. The radial and circumferential residual stresses, σ_{rR} and $\sigma_{\theta R}$, are given by equation (3.3.1) and (3.3.2). Both equations are derived in Appendix C-2.

$$\sigma_{rR} = \frac{(\varepsilon_{ro}-\varepsilon_{\theta o})E_\theta}{K^2-1}\left[\frac{C^{K+1}-1}{C^{2K}-1}\ C^{K-1}\ \left(\frac{r}{a}\right)^{K-1}\right.$$

$$\left.+\left(\frac{C^{K-1}-1}{C^{2K}-1}\right)\ \left(\frac{r}{a}\right)^{-K-1}-1\right] \qquad \ldots\ldots(3.3.1)$$

$$\sigma_{\theta R} = \frac{(\varepsilon_{ro}-\varepsilon_{\theta o})KE_\theta}{K^2-1}\left[\left(\frac{C^{K+1}-1}{C^{2K}-1}\right)\ C^{K-1}\ \left(\frac{r}{a}\right)^{K-1}\right.$$

$$\left.-\left(\frac{C^{K-1}-1}{C^{2K}-1}\right)\ \left(\frac{r}{a}\right)^{-K-1}-\frac{1}{K}\right] \qquad \ldots\ldots(3.3.2)$$

Where $C = \frac{a}{b}$

$$K = \sqrt{\frac{E_\theta}{E_r}}$$

In equation (3.3.1) and (3.3.2), ε_{ro} and $\varepsilon_{\theta o}$ are the radial and tangential free shrinkage of an infinitestinal element of the filament-wound composite ring. Furthermore, the free shrinkage strains are composed of strains due to chemical setting and thermal shrinkage. The difference of free shrinkage strain, $(\varepsilon_{ro} - \varepsilon_{\theta o})$, were determined experimentally by substituting the measured residual strain ε_{rR} and $\varepsilon_{\theta r}$ of the composite ring into equation (3.3.3) and (3.3.4). Then, the residual stresses, σ_{rR} and $\sigma_{\theta R}$ were obtained by substituting the values of ε_{ro} and $\varepsilon_{\theta o}$ into equation (3.3.1) and (3.3.2) respectively.

$$\varepsilon_{rR} = \frac{K^2(\varepsilon_{ro} - \varepsilon_{\theta o})}{K^2-1}\left[\left(1-\sqrt{\nu_r\nu_\theta}\right)\ \frac{C^{K+1}-1}{C^{2K}-1}\ C^{K-1}\left(\frac{r}{a}\right)^{K-1}\right.$$

(Equation continued)....

$$+ (1+\sqrt{\nu_r \nu_\theta})\left(\frac{C^{K-1}-1}{C^{2K}-1}\right)\left(\frac{r}{a}\right)^{-K-1} + (\nu_r - 1)\Big] \quad \ldots\ldots (3.3.3)$$

$$\varepsilon_{\theta R} = \frac{\varepsilon_{ro}-\varepsilon_{\theta o}}{K^2-1}\Big[(K-\nu_\theta)\,\frac{C^{K+1}-1}{C^{2K}-1}\,C^{K-1}\left(\frac{r}{a}\right)^{K-1}$$

$$- (K+\nu_\theta)\left(\frac{C^{K-1}-1}{C^{2K}-1}\right)\left(\frac{r}{a}\right)^{-K-1} + (\nu_\theta - 1)\Big] \quad \ldots\ldots (3.3.4)$$

Even though the experimental results of Shiratori's work [62] quite agree with the results of equations (3.3.1) to (3.3.4), the agreement between theoretical and experimental results needs to be proven further since the stresses and strains due to winding tension and curing should be treated individually. This could be supported by the fact that the free shrinkages in equations (3.3.1) to (3.3.4), ε_{ro} and $\varepsilon_{\theta o}$, should be varying with respect to different winding tension and curing temperatures since, in an actual winding process, winding tension and temperature may not be held constant for all cases. The assumption that constant ε_{ro} and $\varepsilon_{\theta o}$ for all rings is not generally valid. In other words, the assumption of constant ε_{ro} and $\varepsilon_{\theta o}$ may not be valid in predicting residual stress where winding tension and thermal shrinkage may be studied and controlled individually.

3.4 THERMAL STRESS

As mentioned earlier, thermal stresses could be induced in a filament-wound composite ring when cooled from its curing temperature or from aerodynamic heating [64]. Even in the case of a uniform temperature change, as different from that of an anisotropic material, residual stresses will be developed in the cylindrical orthotropic material.

Literature pertaining to thermal stresses in anisotropic thick wall cylinders under various temperature distributions [65,66,67,68, 69] is so vast that an in-depth review would far exceed the scope of this section. However, the special case of a uniform temperature change in a cylindrical orthrotropic composite ring [70, 71] will be discussed in more detail. Further, a uniform temperature change in plane stress cylindrical orthotropic composite ring is a more appropriate model for a composite ring flywheel.

The thermal radial stress, tangential stress and radial displacement due to a uniform temperature change and hydrostatic external loading are derived in Appendix C-3. They are presented here as equations (3.4.1), (3.4.2) and (3.4.3) respectively.

$$\sigma_r = \frac{E_r(K^2-\nu_\theta^2)(\alpha_\theta-\alpha_r)T}{(1-\nu_r\nu_\theta)(1-K^2)}\left[\frac{1-C^{K-1}}{1-C^{-2K}}\left(\frac{r}{a}\right)^{K-1}\right.$$

$$\left. + \frac{1-C^{K-1}}{1-C^{2K}}\left(\frac{r}{a}\right)^{-K-1} - 1\right] - Pa\left[\frac{1}{1-C^{-2K}}\left(\frac{r}{a}\right)^{K-1}\right.$$

$$\left. + \frac{1}{1-C^{2K}}\left(\frac{r}{a}\right)^{-K-1}\right] - P_b\left[\frac{1}{1-C^{2K}}\left(\frac{r}{b}\right)^{K-1} + \frac{1}{1-C^{-2K}}\left(\frac{r}{b}\right)^{-K-1}\right] \quad \text{.....(3.4.1)}$$

$$\sigma_\theta = \frac{E_r(K^2-\nu_\theta^2)(\alpha_\theta-\alpha_r)T}{(1-\nu_r\nu_\theta)(1-K^2)}\left[K\frac{1-C^{-K-1}}{1-C^{-2K}}\left(\frac{r}{a}\right)^{K-1} - K\frac{1-C^{K-1}}{1-C^{2K}}\left(\frac{r}{a}\right)^{-K-1}\right.$$

$$\left. - 1\right] - kP_a\left[\frac{1}{1-C^{-2K}}\left(\frac{r}{a}\right)^{K-1} - \frac{1}{1-C^{2K}}\left(\frac{r}{a}\right)^{-K-1}\right]$$

$$- KP_b\left[\frac{1}{1-C^{2K}}\left(\frac{r}{a}\right)^{K-1} - \frac{1}{1-C^{-2K}}\left(\frac{r}{b}\right)^{-K-1}\right] \quad \text{.....(3.4.2)}$$

$$u = \frac{aT}{1-K^2}\left\{(\alpha_\theta-\alpha_r)(K-\nu_\theta)\frac{1-C^{-K-1}}{1-C^{-2K}}\left(\frac{r}{a}\right)^K - (\alpha_\theta-\alpha_r)\right.$$

$$\left.(K+\nu_\theta)\frac{1-C^{K-1}}{1-C^{2K}}\left(\frac{r}{a}\right)^{-K} + [\nu_\theta(\alpha_\theta-\alpha_r)+\alpha_r-K^2\alpha_\theta]\left(\frac{r}{a}\right)\right\}$$

$$-\frac{P_a(1-\nu_r\nu_\theta)}{E_r}\,a\left[\frac{1}{(\nu_\theta+K)(1-C^{-2K})}\left(\frac{r}{a}\right)^K + \frac{1}{(\nu_\theta-K)(1-C^{2K})}\left(\frac{r}{a}\right)^{-K}\right]$$

$$-\frac{P_b(1-\nu_r\nu_\theta)b}{E_r}\left[\frac{1}{(K+\nu_\theta)(1-C^{2K})}\left(\frac{r}{b}\right)^K + \frac{1}{(\nu_\theta-K)(1-C^{-2K})}\left(\frac{r}{b}\right)^{-K}\right]$$

.....(3.4.3)

The terms P_a and P_b are the internal and external pressures exerted on the inner and outer radial position of the ring. From the above equations, it can be easily seen that stresses are proportional to $(\alpha_\theta-\alpha_r)$, K and E_r. Furthermore, for the same kind of material, stresses are only dependent on the diameter ratio. Preliminary inhouse analysis [19] showed that the inside radius of a Kevlar 49 ring will expand after cooling which agrees with the above equation and with the observed results from fabrication of composite rings. However, the validity and accuracy of the theory must be proven experimentally by measuring the thermal residual stress.

3.5 CENTRIFUGAL STRESS

Basically, the stresses in a hoop-wound fibre composite ring due to centrifugal loading are analyzed by using the following assumptions: (1) stress distribution is symmetrical with respect to the axis of rotation; (2) the axial thickness of the disc or ring is constant; (3) a plane stress analysis is representative; (4) radial stress is equal to zero at a free surface and (5) in a multi-ring rotor, radial displacement and radial stress are continuous at the inter-ring boundaries. The solution of the problem is well-established in the literature, [6,8,9,11,12,72,73]. Details of stresses and displacement equation due to centrifugal loading were derived in Appendix C-4. Equations (3.5.1) to (3.5.3) show respectively the radial displacement, radial stress and tangential stress due to centrifugal loading.

$$u^{(m)} = \frac{\gamma_m \omega^2 a_m^3}{g E_\theta^{(m)} (9-K_m^2)} \Bigg\{ (3+\nu_\theta^{(m)}) \left[(K_m - \nu_\theta^{(m)}) \frac{1-c_m^{k_m+3}}{1-c_m^{2k_m}} \left(\frac{r}{a_m}\right)^{k_m} \right.$$

$$\left. - (K_m + \nu_\theta^{(m)}) \frac{1-c_m^{k_m-3}}{1-c_m^{2k_m}} c_m^{k_m+3} \left(\frac{a_m}{r}\right)^{k_m} \right]$$

$$- \left[(K_m^2 - \nu_\theta^{(m)})^2 \right] \left(\frac{r}{a_m}\right)^3 \Bigg\} + \frac{q_{m-1} a_m c_m^{k_m+1}}{E_\theta^{(m)} (1-c_m^{2k_m})}$$

$$\times \left[(K_m - \nu_\theta^{(m)}) \left(\frac{r}{a_m}\right)^{k_m} + (K_m + \nu_\theta^{(m)}) \left(\frac{a_m}{r}\right)^{k_m} \right]$$

(Equation continued)....

$$- \frac{q_m a_m}{E_\theta^{(m)}(1-c_m^{2k_m})} \left[(K_m - \nu_\theta^{(m)}) \left(\frac{r}{a_m}\right)^{k_m} \right.$$

$$\left. + (K_m + \nu_\theta^{*(m)})\, c_m^{2k_m} \left(\frac{a_m}{r}\right)^{k_m} \right] \qquad \text{.....(3.5.1)}$$

$$\sigma_r^{(m)} = \frac{\gamma_m \omega^2}{g} a_m^2 \frac{3+\nu_\theta^{(m)}}{9-K_m^2} \left[\frac{1-c_m^{K_m+3}}{1-c_m^{2K_m}} \left(\frac{r}{a_m}\right)^{K_m-1} \right.$$

$$+ \frac{1-c_m^{K_m-3}}{1-c_m^{2K_m}} c_m^{K_m+3} \left(\frac{a_m}{r}\right)^{K_m+1} \left. - \left(\frac{r}{a_m}\right)^2 \right]$$

$$+ \frac{p_{m-1}\, c_m^{K_m+1}}{1-c_m^{2K_m}} \left[\left(\frac{r}{a_m}\right)^{K_m-1} - \left(\frac{a_m}{r}\right)^{K_m+1} \right]$$

$$+ \frac{p_m}{1-c_m^{2K_m}} \left[- \left(\frac{r}{a_m}\right)^{K_m-1} + c_m^{2K_m} \left(\frac{a_m}{r}\right)^{K_m+1} \right]$$

$$\text{.....(3.5.2.)}$$

$$\sigma_\theta^{(m)} = \frac{\gamma_m \omega^2}{g} \cdot \frac{a_m^2}{9-K_m^2} \left\{ (3+\nu_\theta^{(m)})\, K_m \left[\frac{1-c_m^{K_m+3}}{1-c_m^{2K_m}} \left(\frac{r}{a_m}\right)^{K_m-1} \right.\right.$$

$$\left.\left. - \frac{1-c_m^{K_m-3}}{1-c_m^{2K_m}} c_m^{K_m+3} \left(\frac{a_m}{r}\right)^{K_m+1} \right] - (K_m^2 - 3\nu_\theta^{(m)}) \left(\frac{r}{a_m}\right)^2 \right\}$$

(Equation continued)....

$$+\frac{p_{m-1}\,c_m^{K_m+1}}{1-c_m^{2K_m}}\left[\left(\frac{r}{a_m}\right)^{K_m-1}\left(\frac{a_m}{r}\right)^{K_m+1}\right]$$

$$-\frac{p_m K_m}{1-c_m^{2K_m}}\left[\left(\frac{r}{a_m}\right)^{K_m-1}+c_m^{2K_m}\left(\frac{a_m}{r}\right)^{K_m+1}\right] \quad \ldots\ldots(3.5.3)$$

In order to meet the design objectives/constraints of the 1.0 KW-Hr rotor (mentioned in chapter 1), in-house analytical studies [31] has identified that the physical size and weight of the rotor are critical. Thus, aside from manufacturing problems, a rotor of contoured axial thickness will violate the swept volume and diameter design objectives/constraints for the road vehicle application. Logically, inspite of the potentially better stress distribution of a contoured rotor, only constant thickness rotors are considered.

CHAPTER 4

FLYWHEEL DESIGN BY PARAMETRIC SENSITIVITY ANALYSIS

4.1 INTRODUCTION

The main purpose of this chapter is to evaluate the effect and sensitivity of the design parameters, both physical and material, on the stress patterns of the hoop-wound fibre composite high speed rotors.

The sensitivity and behaviour of both the radial and tangential stress patterns in hoop-wound fibre composite rotors were analyzed by varying sensitive parameters, such as: thickness ratio, interfacial pressure, and the material modulus ratio (E_θ/E_r). Further, in an actual rotor design, specific swept volume and specific energy storage must be maximized by using practical manufacture techniques and available fibre materials. Several feasible rotor design concepts are explored in this chapter, including: Multimaterial Multiring and Single-Material Multiring with low modulus interfacial wraps; Single Material and Multimaterial Ring-On-Ring with manufacture controlled interfacial pressure; and the Multimaterial Bi-annular Ring-On-Ring Flywheel Rotor.

The sensitivity results obtained in this chapter provide a valued insight into the design analysis of the full size rotor discussed in the following chapter. The sensitivity of both material and physical parameters together with the manufacturing feasibility, give insight into the advantages and disadvantages of each flywheel design concept.

4.2 PARAMETER SENSITIVITY ANALYSIS

4.2.1 GEOMETRIC CONFIGURATION

While the primary interest of this section is to explore hoop-wound fibre composite ring stress patterns and to establish the controlling physical and material parameters, it is first necessary, before any detail study can be made, to identify the geometric configuration of the flywheel rotor. Figures 4.1 and 4.2 show a typical geometric requirement, at different speeds, for a disc type rotor with a ten inch diameter manufactured aluminum hub and solid SMC hub respectively. For the design objectives stated earlier, the working speed and physical sizes can be readily identified from these figures. It is clear that rotors with an outer diameter larger than 11.0 inches and speeds in excess of 22,000 rpm will be required.

4.2.2 SINGLE-RING SENSITIVITY ANALYSIS

One of the primary objectives of the single-ring analysis is to explore the sensitivity of the ring with respect to material and physical parameters. Then, this knowledge and controlling techniques are applied to multi ring rotor designs. Figure 4.3 shows the non-dimensionalized radial and tangential stress patterns in a hoop-wound fibre composite ring as a function of diameter ratio. As is well established, the radial stress maximizes somewhat inside of the ring center and is highly dependent on the diameter ratio. Since the longitudinal to traverse working stress ratios of hoop-wound fibre composite are usually in the order of 50 to 100, a thick ring will encounter premature delamination (radial failure) at low speed while the tangential stress level is still far below failure. This will not allow optimal utilization of material and will result in undesirably low specific energy. While it is clear that a thin ring can approach the desired stress level, it cannot meet the geometric requirement of most applications.

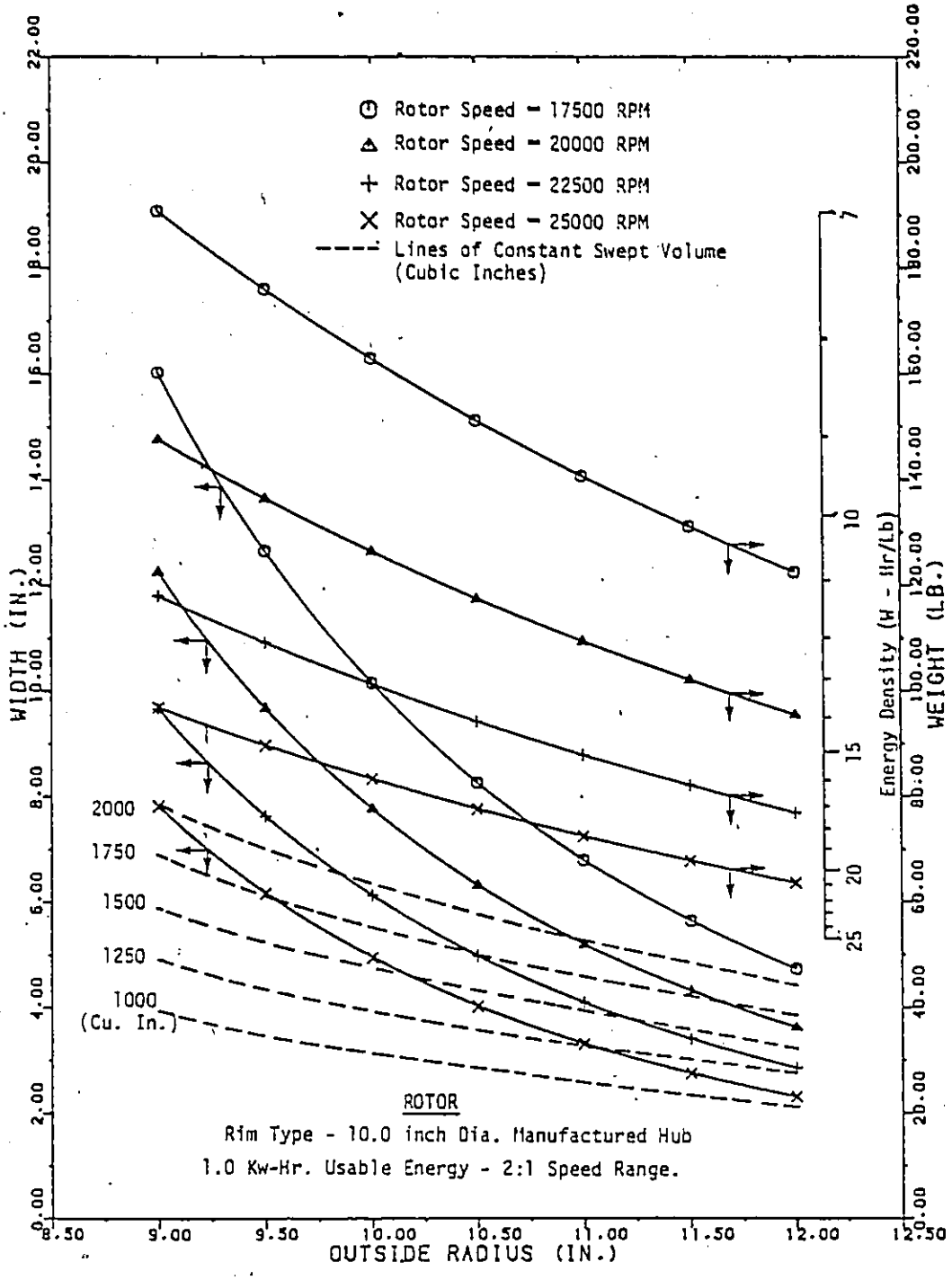

Fig. 4.1: Projected Geometry of a Rim Type Rotor vs. Rotor Outside Diameter for a Range of Design Speeds up to 25,000 RPM.

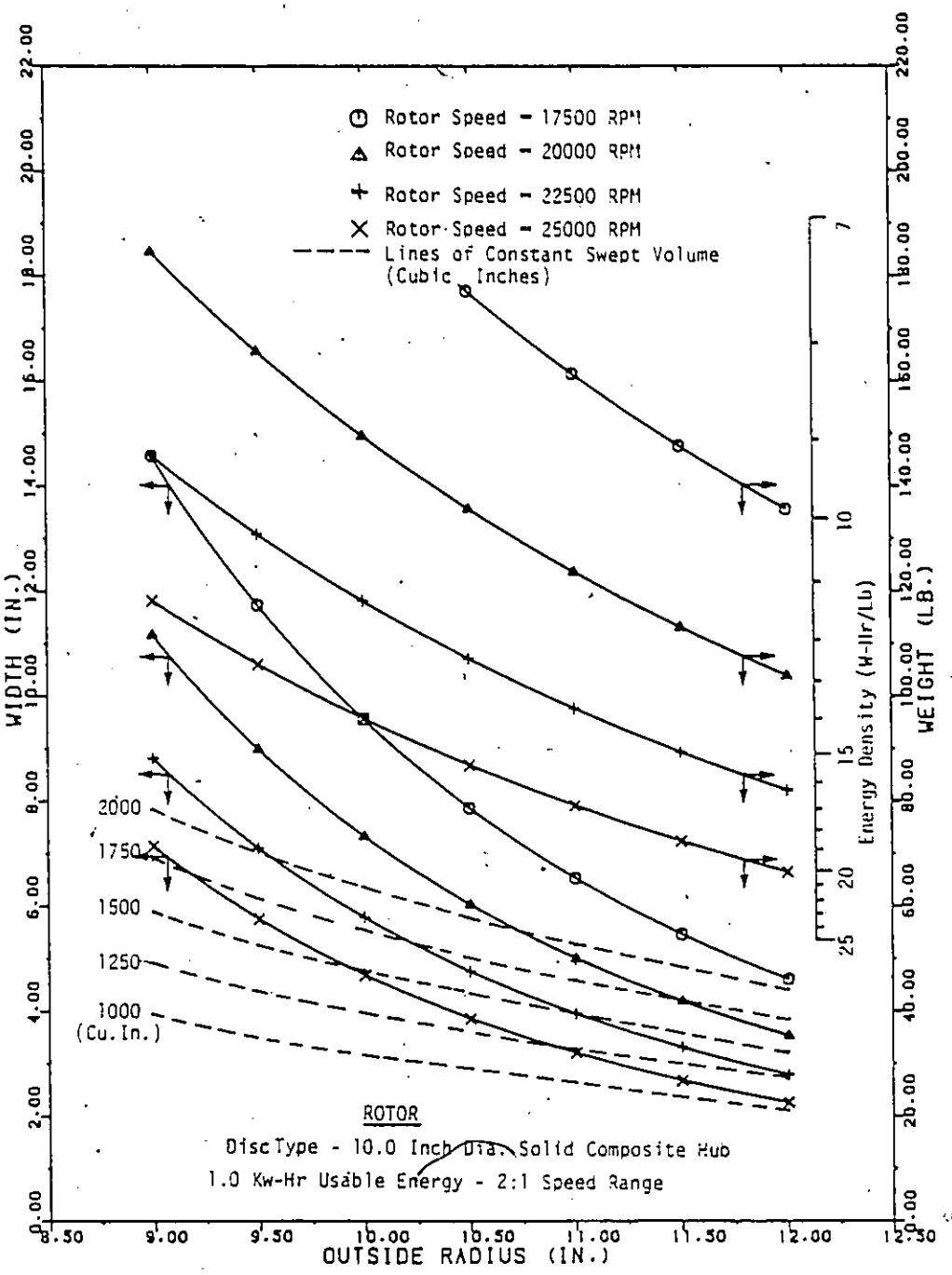

Fig. 4.2: Projected Geometry of a Disc Type Rotor vs. Rotor Outside Diameter for a Range of Design Speeds up to 25000 RPM.

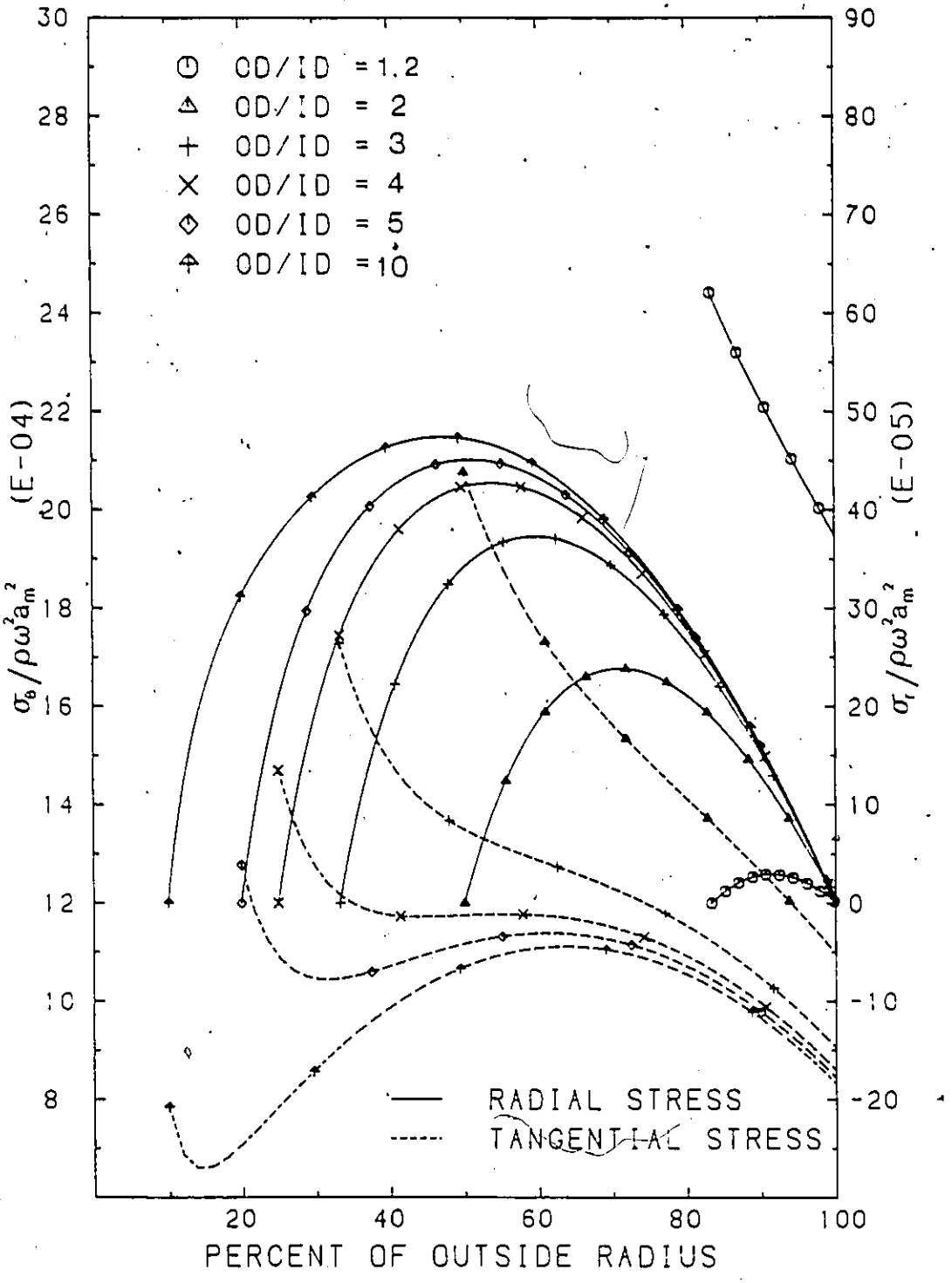

Fig. 4.3: Non-dimensional Tangential and Radial Stress Distribution in an Anisotropic Disc with Various Diameter Ratios, K=1.8.

To control the stress pattern, the material and physical parameters were explored. Ring interfacial pressure, ring diameter, diameter ratio, material density and material modulus ratio 'K' were found to be the controlling parameters. The stress distribution of five thin rings, with varying diameter ratio, are shown in Figure 4.4. As expected, radial stress is extremely sensitive to the diameter ratio (ring thickness). The relative effect of interfacial pressure (2,000 psi) on these five rings is shown in Figure 4.5. From the figures, not only can radial stress patterns be altered, but also more desirable tangential stress patterns can be obtained by such ring interfacial pressure control.

The effect of material modulus ratio 'K' is shown in Figure 4.6. The values of 'K' used in the figure are representative of those found in the glass, graphite and kevlar fibre families. Apparently, holding all the other material properties constant, the higher values of 'K' provide the more desirable radial and tangential stress patterns.

Not only will the single-ring analysis provide necessary reference for multi ring rotor design, but it is also valuable in estimating the stress patterns and maximum stresses in rings for the in-house study [1]. Figure 4.7 shows the projected stress patterns in POC (Proof of Concept) rings due to hydrostatic loading. It can be seen that very thin rings (0.1 inch thick) should be used to achieve the desirable logitudinal failure [1]. By the same method, the geometric configuration of composite rings for spin-tests can be projected. Figure 4.8 to Figure 4.10 shows the projected maximum tangential stress in a 0.1 inch thick POC specimen rings, with various inside diameters, for S2-glass, Kevlar 49 and Grafil-AS respectively. Clearly, it can also be seen from the figures that S2-glass has the highest stress level. Logically, because of its relatively low strength, S2-glass will be restricted to inside rings for the 0.75 or 1.0 KW-Hr multi-ring flywheel rotor [1]. On the other

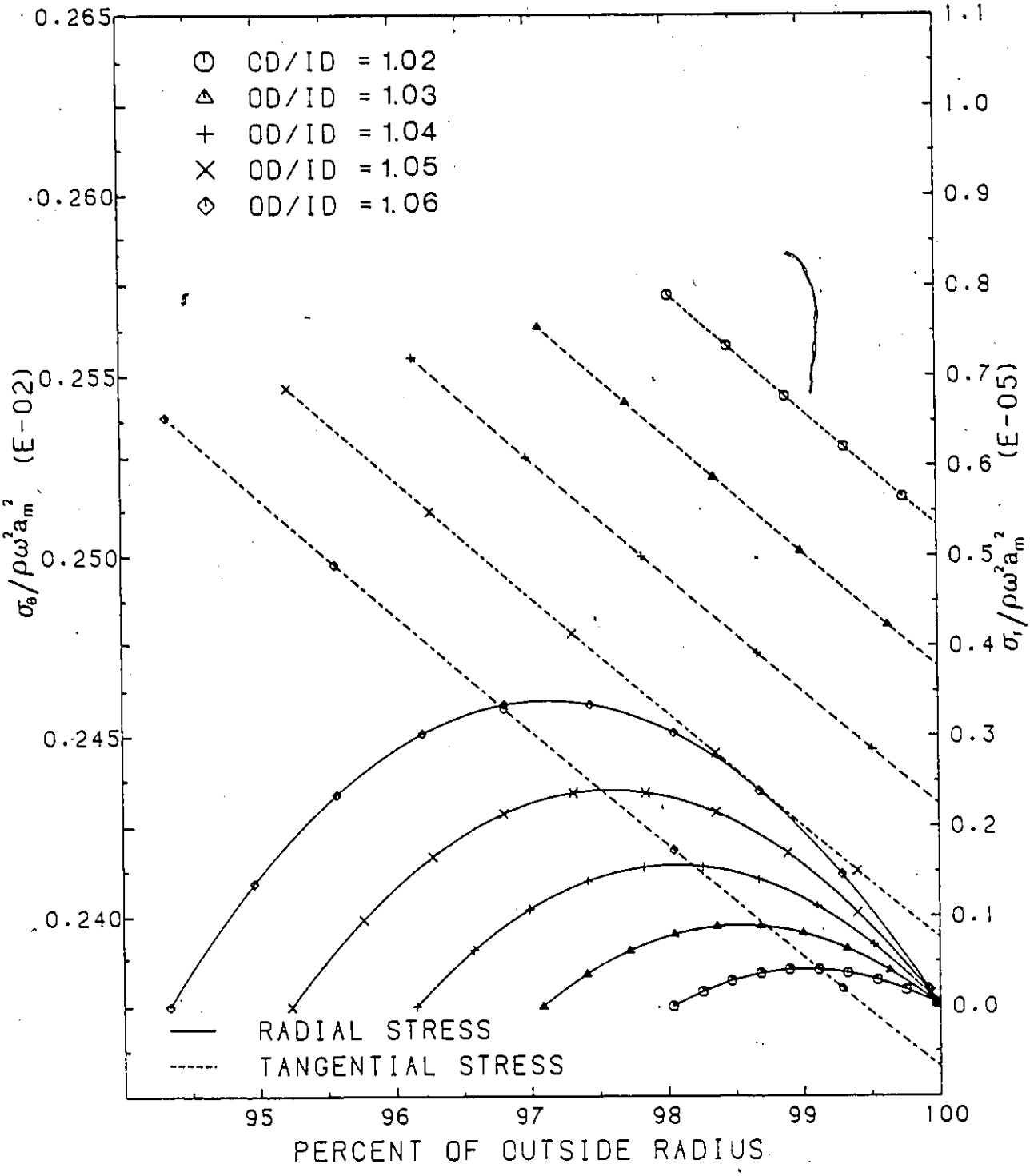

Fig. 4.4: Non-dimensional Tangential and Radial Stress Distribution in Thin Hoop-Wound Fibre Composite Ring (K=1.8) for a Range of Thin Ring Diameter Ratios from 1.02 to 1.06.

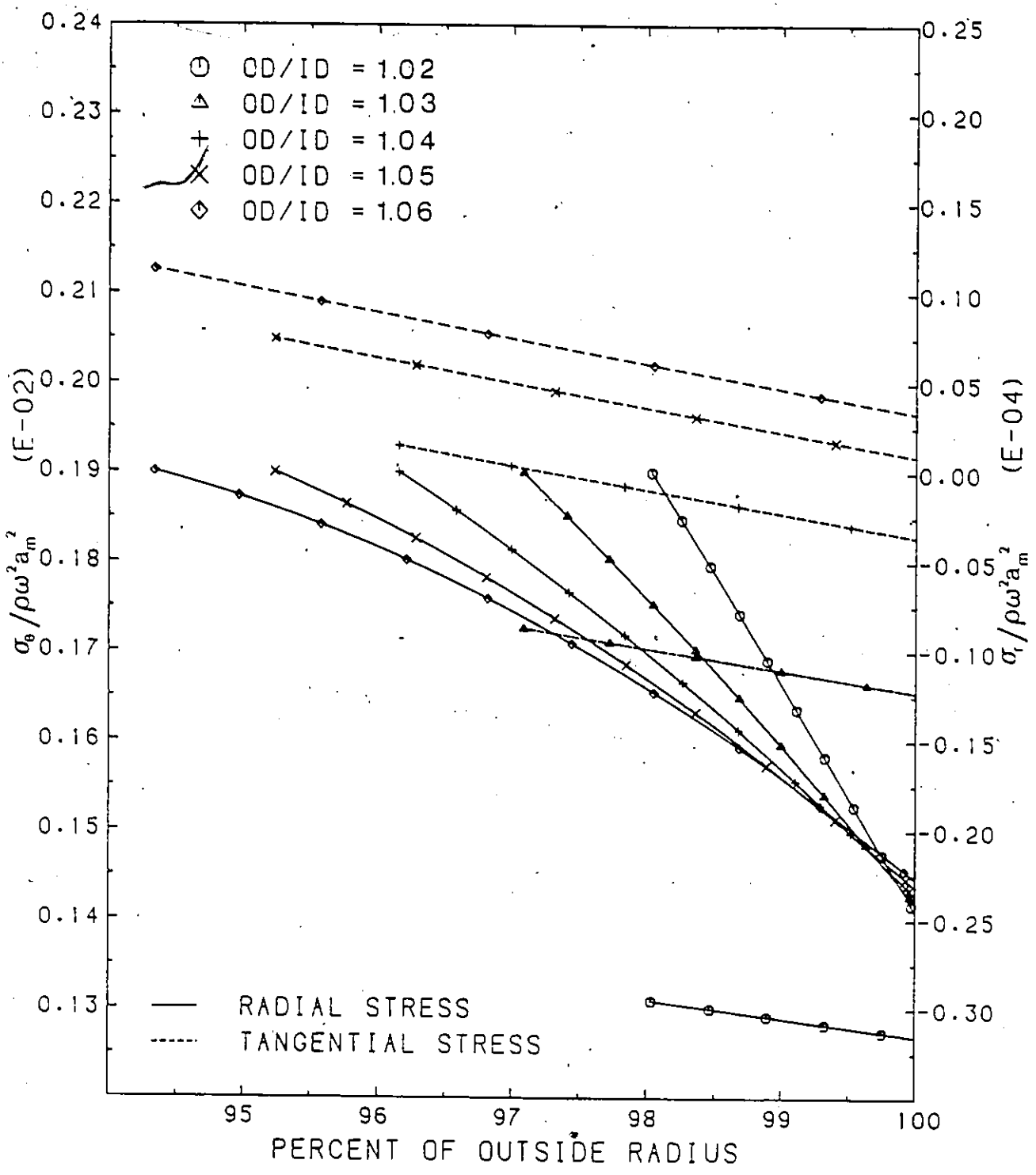

Fig. 4.5: Relative Effect of Interfacial Pressure (2000 psi external) on Stress Patterns of Rings Shown in Figure 4.4.

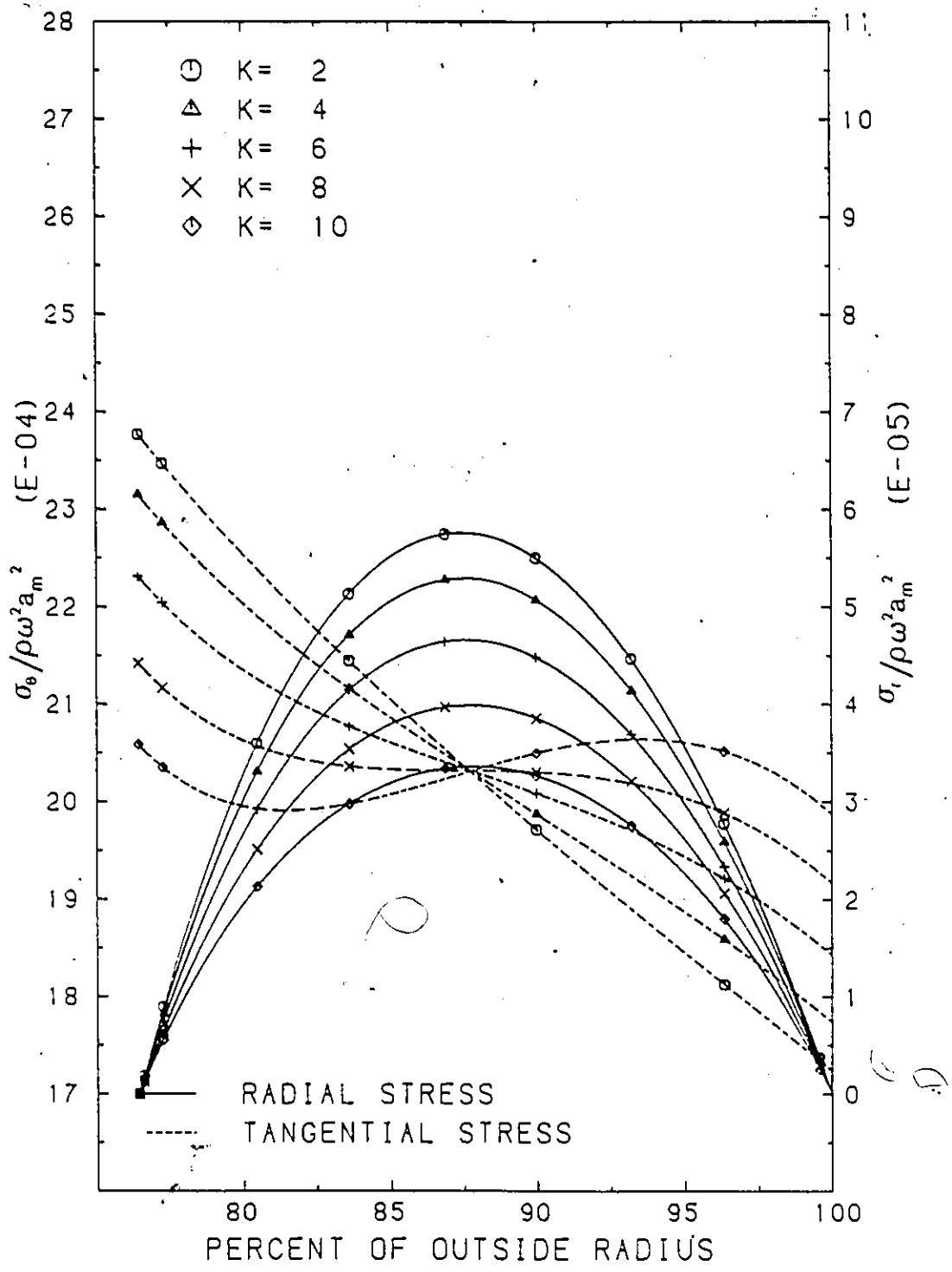

Fig. 4.6: Effect of Material Modulus Ratio on the Tangential and Radial Stress Distribution of a Thin Composite Ring.

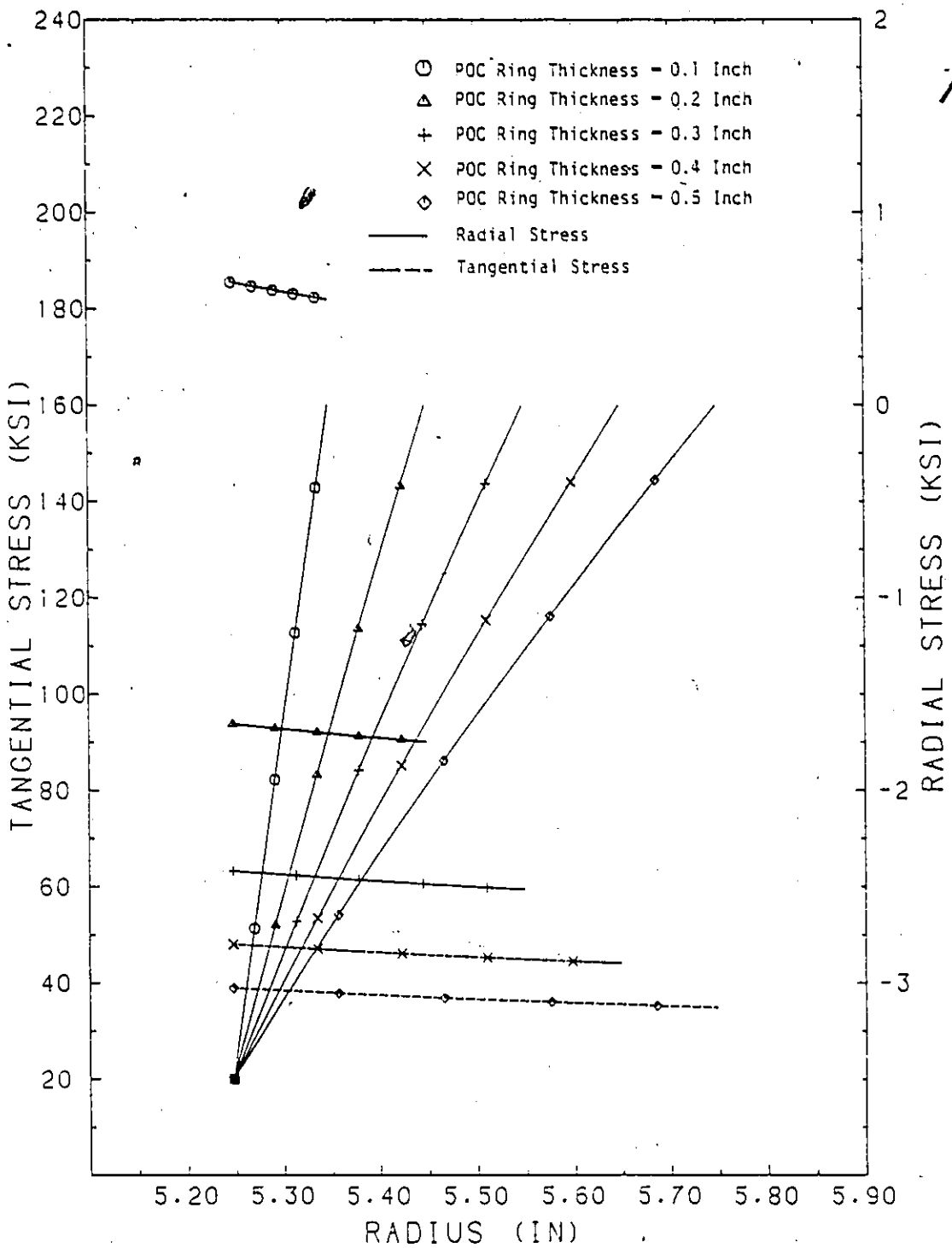

Fig. 4.7: Typical Stress Patterns in POC Rings Due to Hydrostatic Loading. Test Case: 10.5 inch I.D.; 3500 psi; E-Glass.

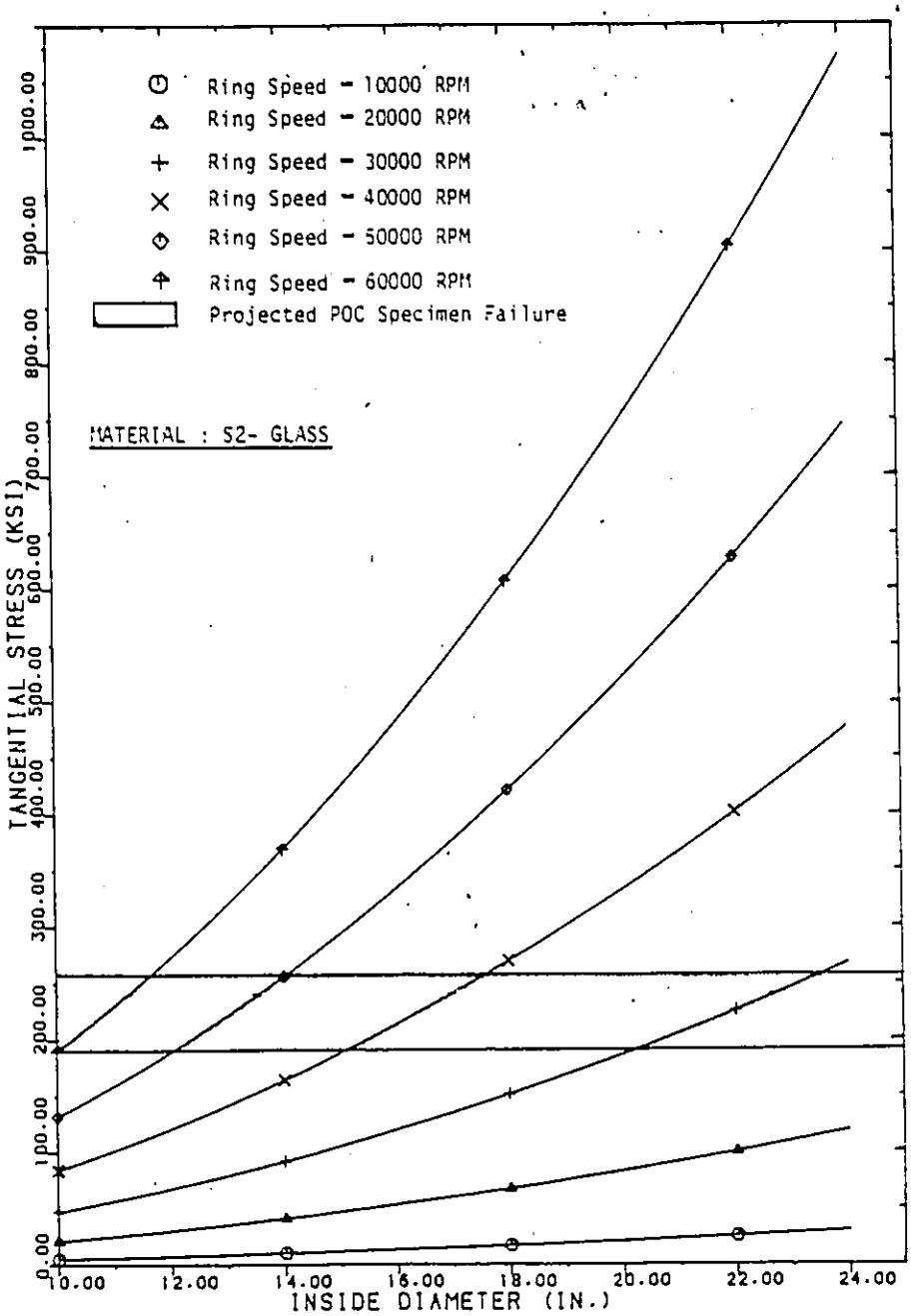

Fig. 4.8: Projected Maximum Tangential Stress in 0.1 Inch Thick POC Specimen Rings vs. Ring Inside Diameter for Range of Test RPM.

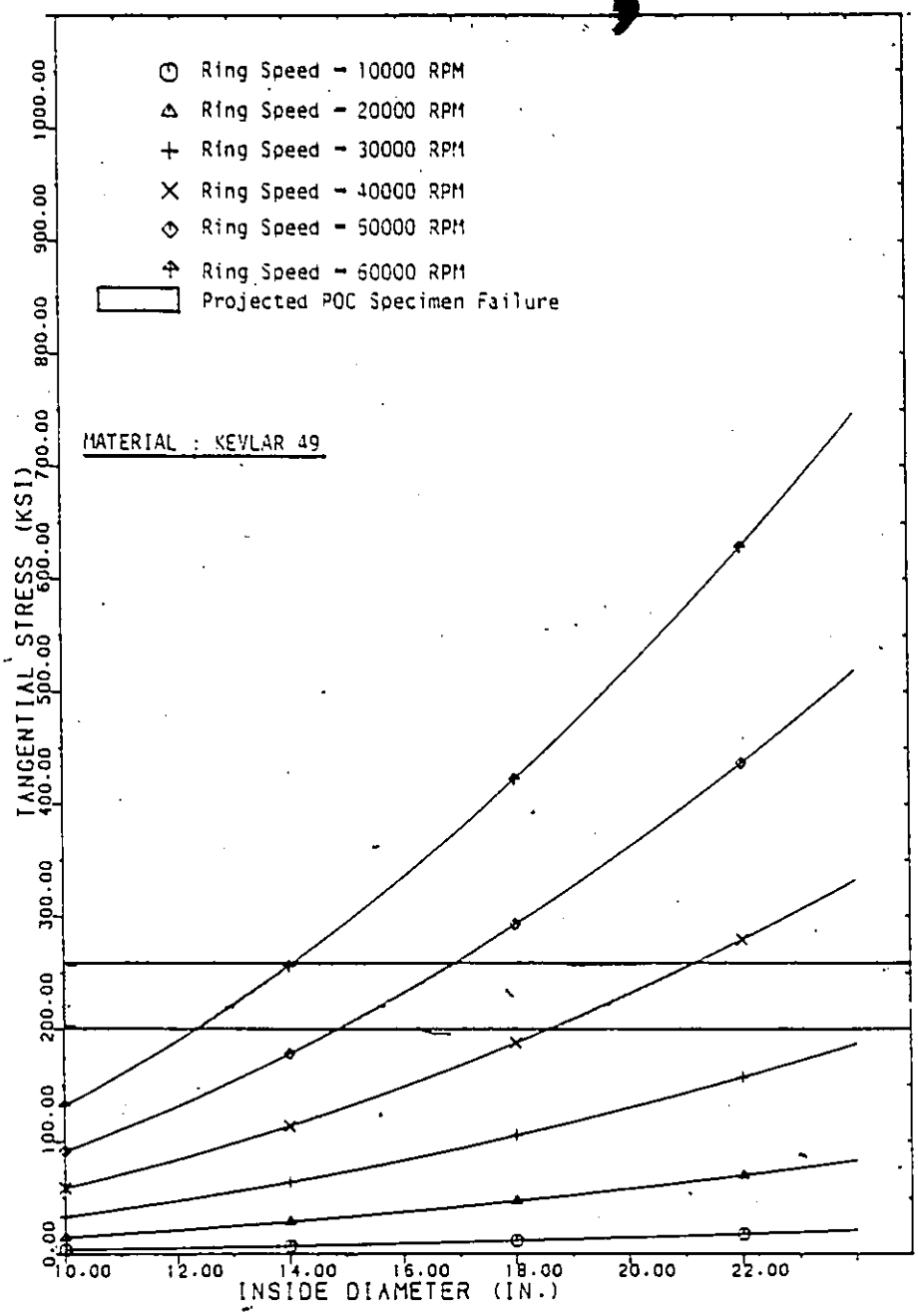

Fig. 4.9: Projected Maximum Tangential Stress in 0.1 Inch Thick POC Specimen Rings vs. Ring Inside Diameter for Range of Test RPM.

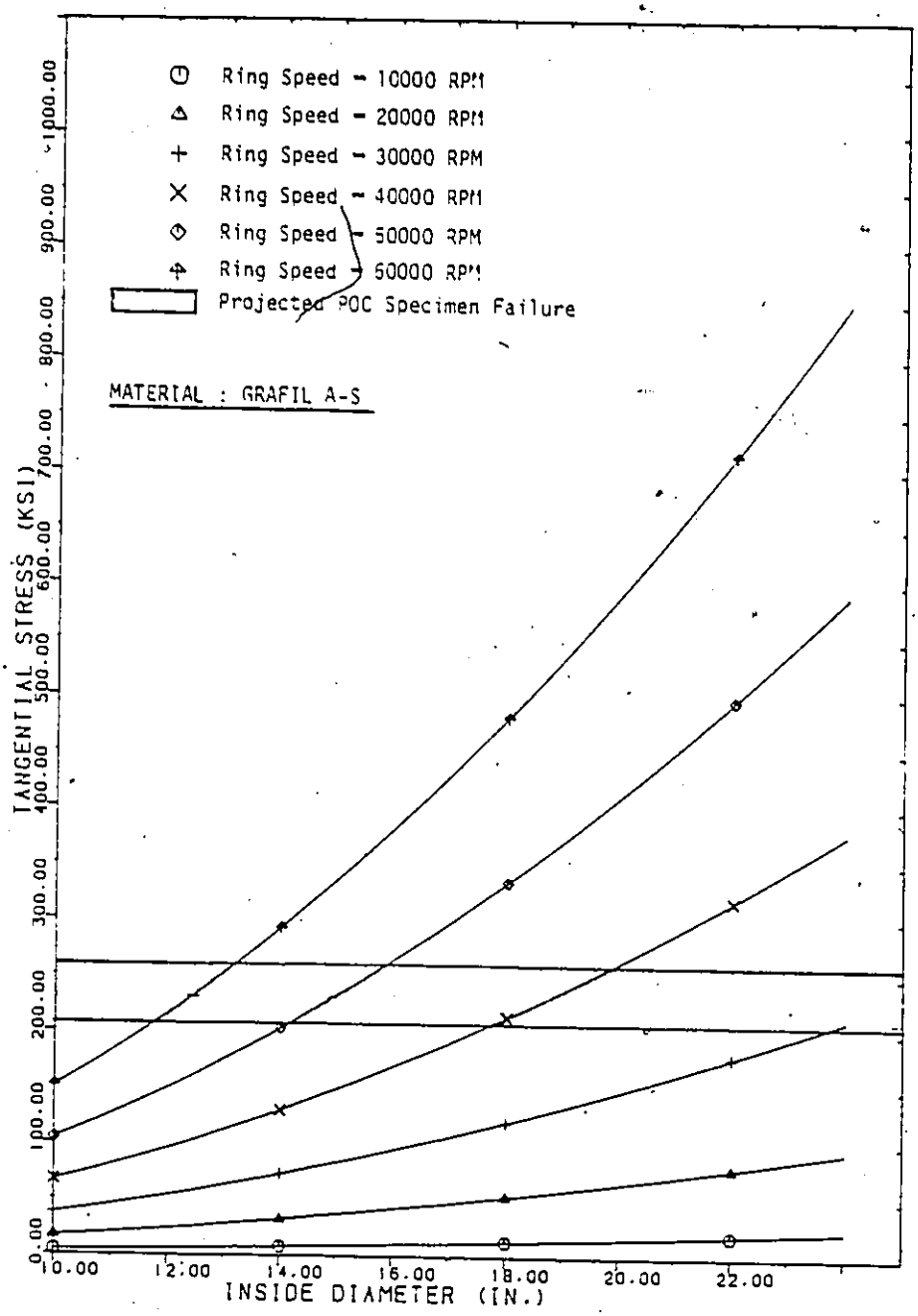

Fig. 4.10: Projected Maximum Tangential Stress in 0.1 Inch Thick POC Specimen Rings vs. Ring Inside Diameter for Range of Test RPM.

hand, the relatively low stress levels and high strength of Kevlar 49 and AS-Carbon allow them to be utilized as exterior rings.

4.2.3 MULTI-RING ROTOR SENSITIVITY ANALYSIS

From the previous section, it is clear that material and physical parameters can effectively control the stress distribution in a multiring flywheel rotor.

For high energy density flywheel rotors, an in-house analytical study [20] has identified that the primary objective for hoop-wound fibre composite flywheel design is to achieve a relatively constant tangential stress distribution across the radial dimension of the flywheel while maintaining a suitably low radial stress and radial compatibility. Obviously, this could be achieved by stacking a certain number of rings by several techniques mentioned earlier. However, manufacture and material availability must be carefully considered.

A rotor consisting of ten nested fibre composite rings with thin inter-rings designed to prevent high tensile forces across the ring boundaries is shown in Figure 4.11. The sensitivity of stress patterns with respect to inter-ring modulus is studied. In order to achieve the desirable radial stress pattern, a very low modulus bonded inter-ring material is required. Further, the undesirable tangential stress pattern (as projected from Figure 4.11) would result in low system shape factors or low specific energy. By decreasing the material density across the radial position, an optimal pattern can readily be achieved as shown in Figure 4.12. However, there is no practical way to achieve such a design. On the other hand, the appropriate choice of fibre material can provide a reasonable design with tensile stresses approximately matched to the design working stress of the material as shown in Figure 4.13. Here five E-glass inner rings with fibre Kevlar 49 outer rings are used.

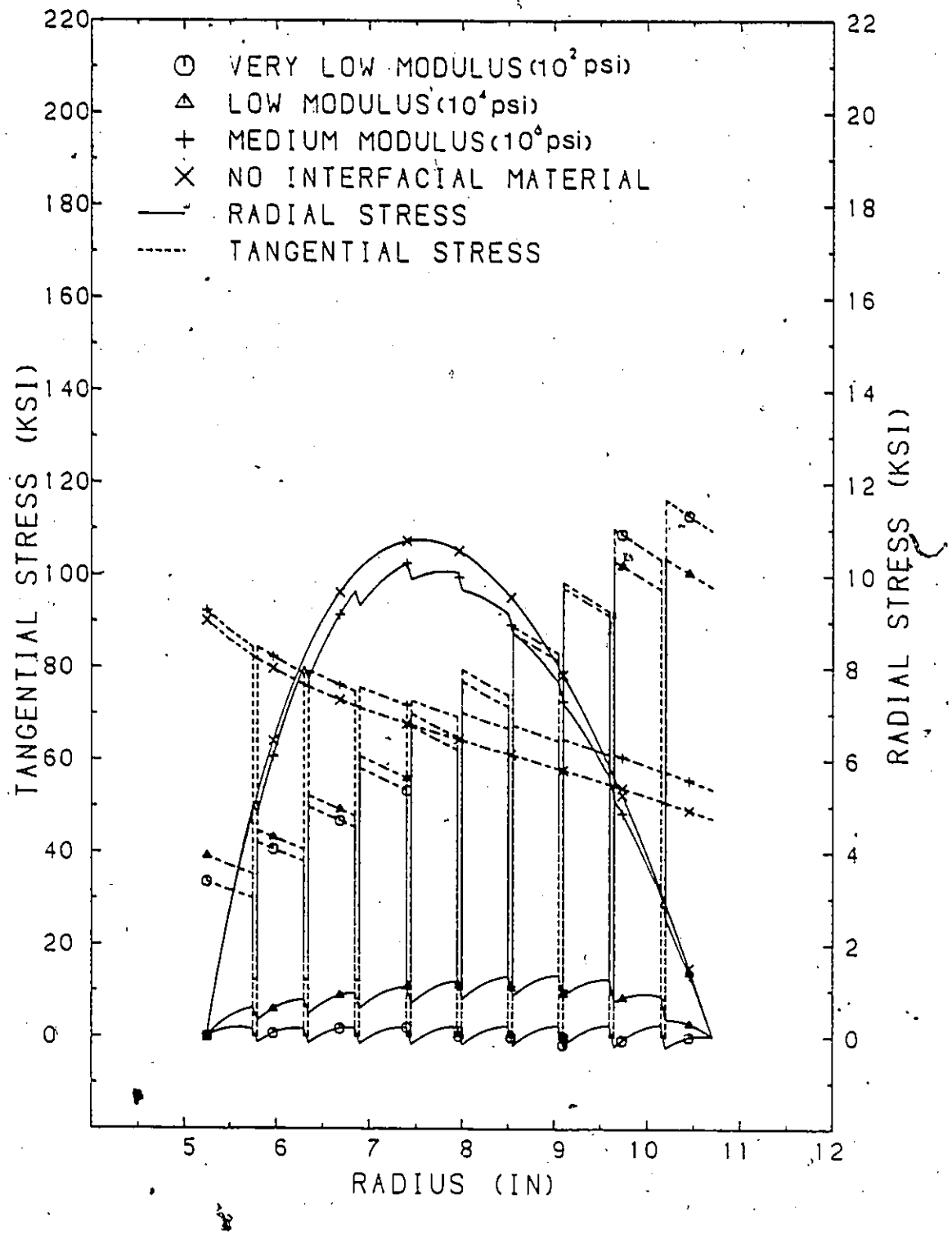

Fig. 4.11: The Effect of Inter-ring Material Modulus on the Stress Patterns of a Nested Multi-ring Flywheel Rotor. Test Speed = 22,000 RPM, E-glass Hoop-wound Composite Rings.

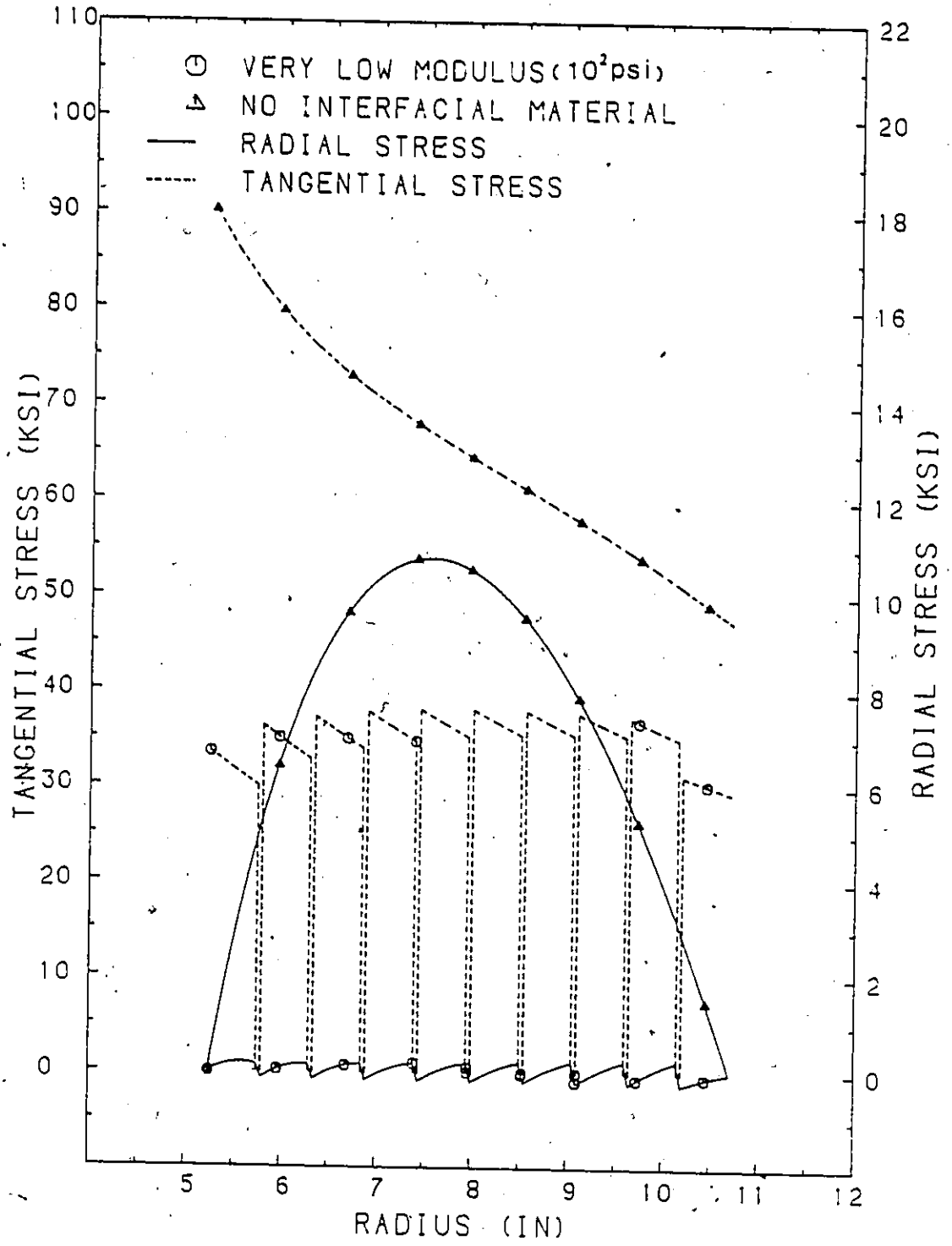

Fig. 4.12: Control of Tangential Stress Patterns in a Nested Multi-ring Rotor by Varying Material Density. Test Speed = 22,000 RPM.

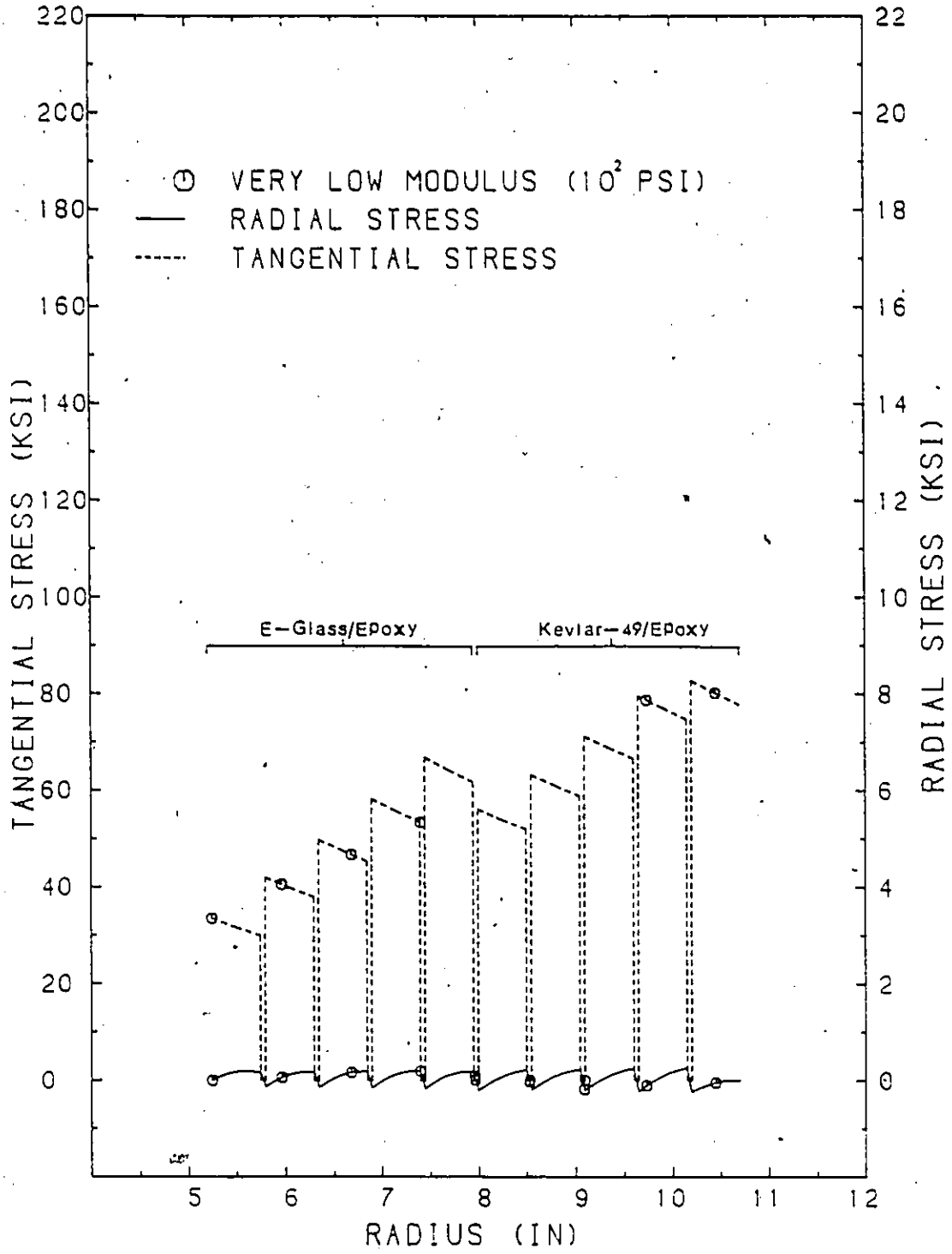

Fig. 4.13: Control of Tangential Stress Patterns in a Nested Multi-ring Rotor by Fibre Material Selection.

In general, rotor designs with low modulus thin inter rings were judged to be impractical because of dynamic instability and manufacture difficulty. On the other hand, hoop-wound ring-on-ring designs would appear to lend themselves to easier manufacture and greater rotor stability. Through winding tension control or shrink fitting, interfacial pressure could be achieved across the boundaries of multi-ring rotors. Figure 4.14 examines the stress profile at operating speed of such a design. It could be noted that maximum compressive loads will occur at static conditions and, if carefully chosen, will all approach zero at maximum design speed, after which (in principle) ring separation or dynamic instability will occur as in the design shown in Figure 4.15 when the rotational speed exceeds 23,000 rpm. However, the static compressive loads can become prohibitively high leading to difficult manufacturing, or compressive material failure.

Rather than applying static loading between ring boundaries, interfacial compressive loading can also be achieved by centrifugal loading between rings (dynamic loading). This design concept could be achieved through the selection of higher modulus to density ratio (specific modulus) materials with increasing radial position. Figure 4.16 gives an example of such a design. In this case, the outer high specific modulus Grafil A-S ring dilates less than the lower specific modulus S2-glass ring. Therefore, compressive loading was induced across the boundary of these rings by centrifugal loading. Figure 4.17 shows the effect of outer ring thickness on the stress profile of a biannular rotor. It can be seen from the figure that an optimal stress profile occurs when the outside ring thickness, t, is equal to 1.3 inches. This shows that an optimum ring thickness ratio does exist wherein both radial and tangential stress can be minimized for a a given design condition.

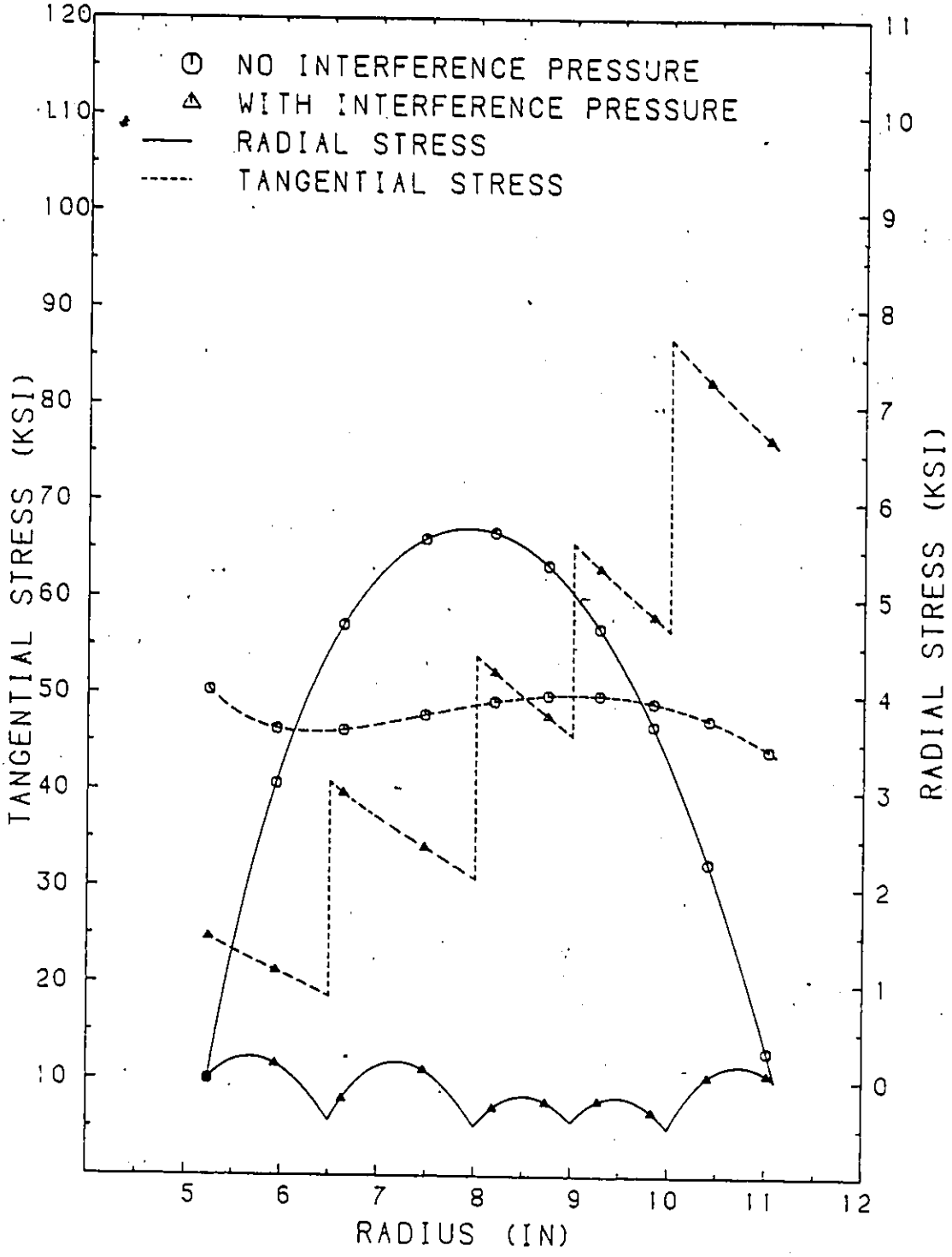

Fig. 4.14: Single Material Multi-ring Flywheel Rotor with Manufacture Controlled Interfacial Pressure. Rotor Stress Patterns Shown at the Design Speed of 22,000 RPM.

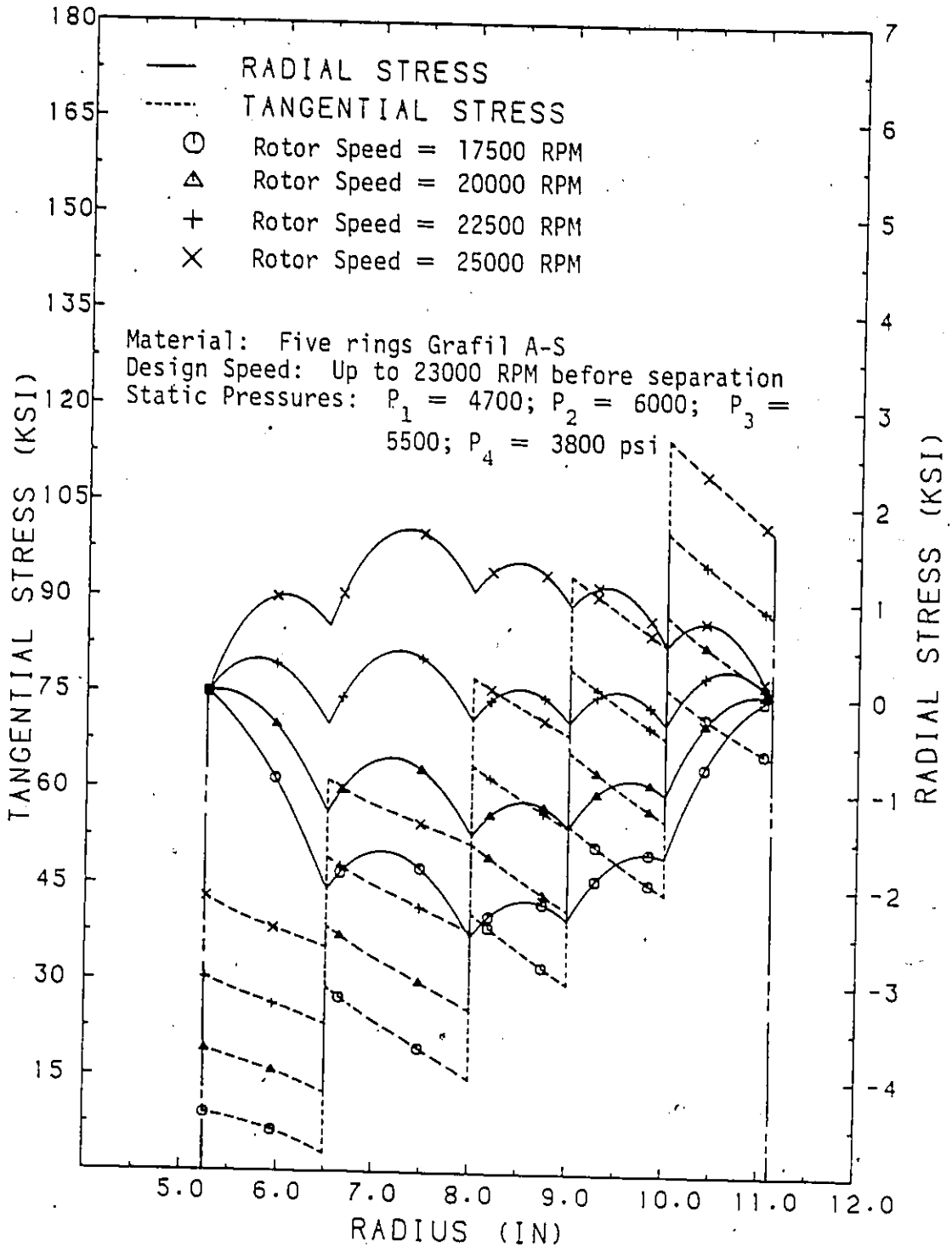

Fig. 4.15: Tangential and Radial Stress Patterns in a Single Material Multi-Ring-On-Ring Rotor with Controlled Static Inter-ring Pressures for Speed Range to 25000 RPM.

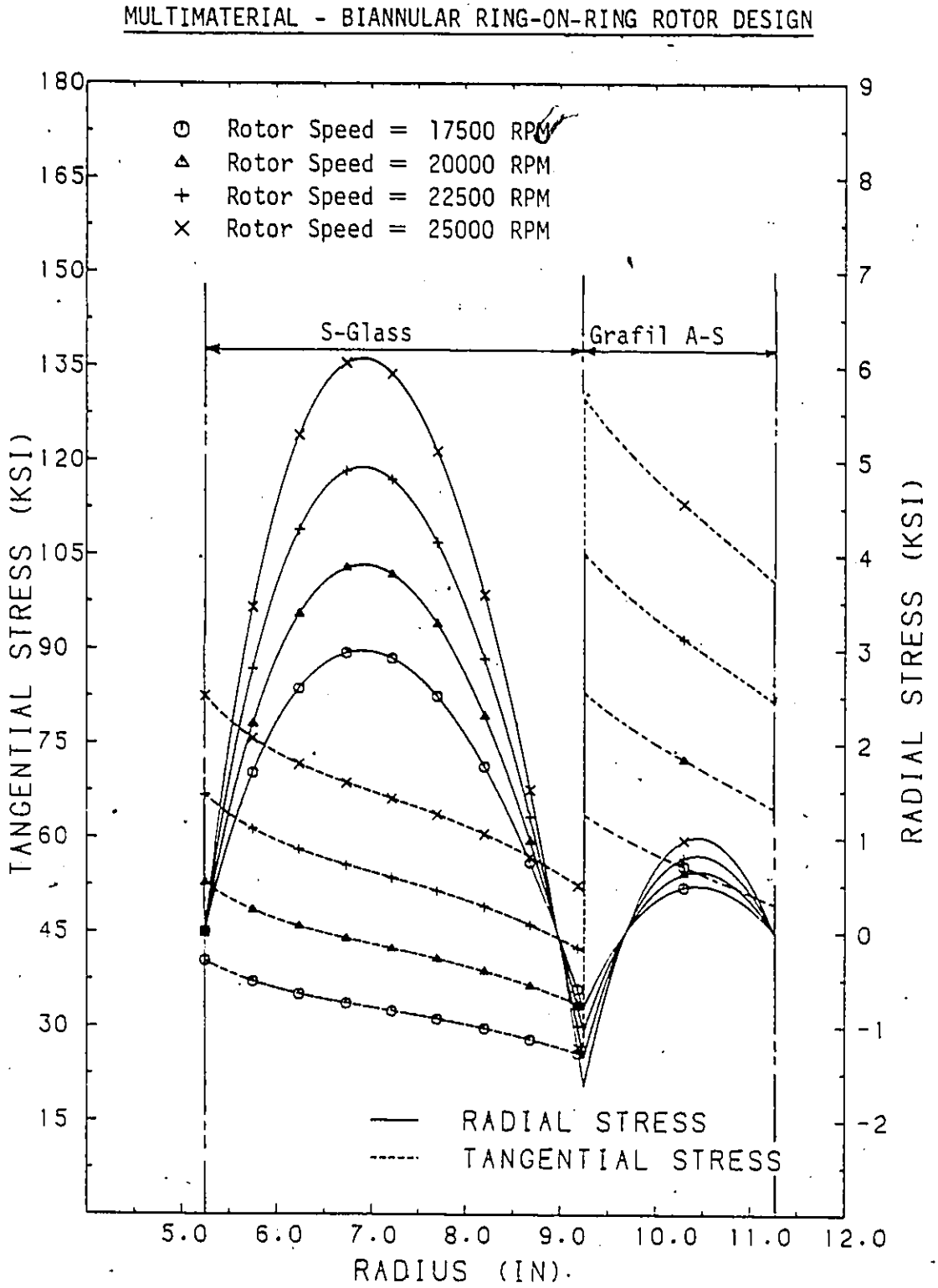

Fig. 4.16: Radial and Tangential Stress Patterns in a Multi-material Biannular Ring-On-Ring Rotor using Dynamic Loading for Inter-ring Pressure/Radial Compatibility Control. Speed Range to 25000 RPM.

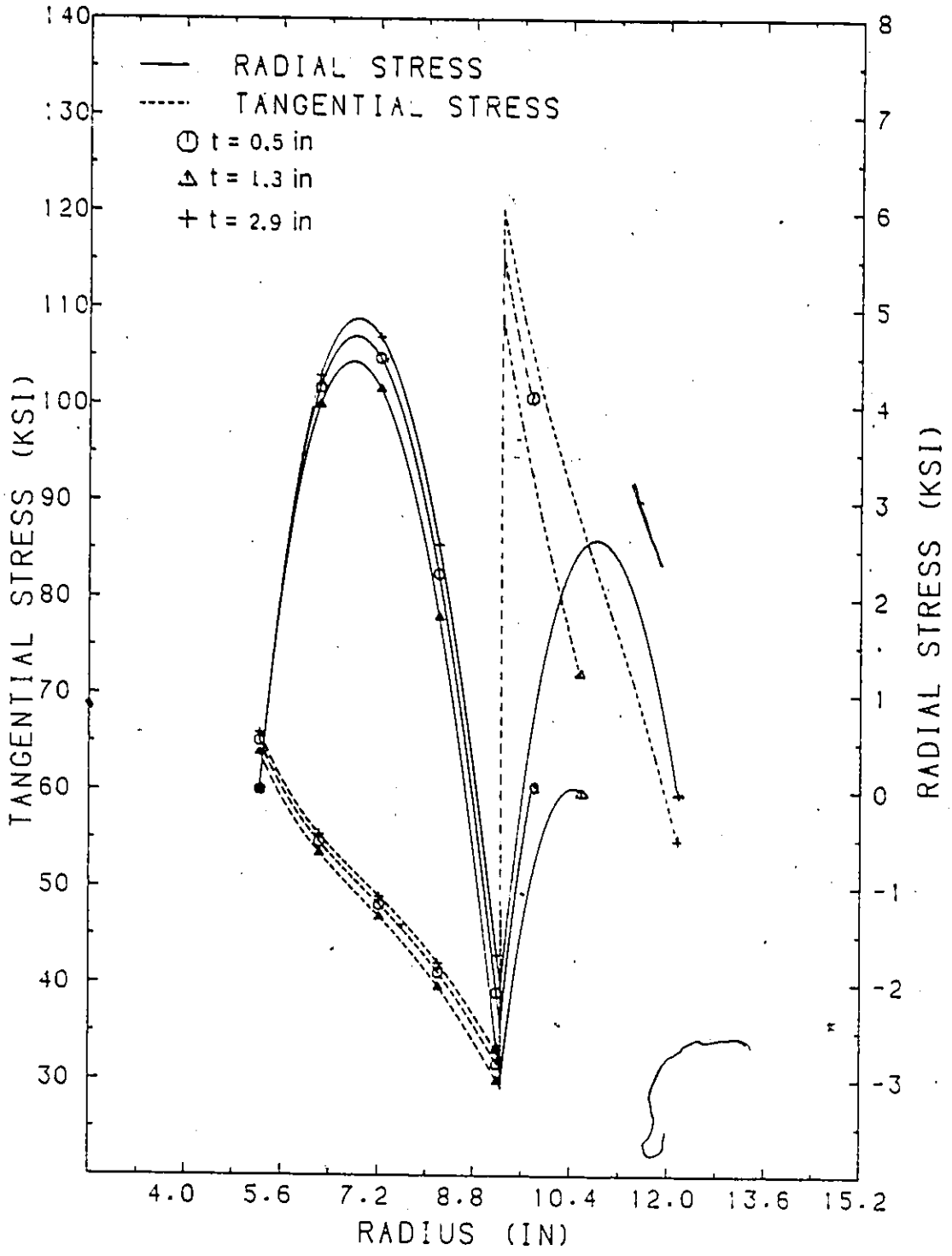

Fig. 4.17: Effect of Ring Thickness on Maximum Stress for the Multimaterial Biannular Rotor. Test Speed = 22,000 RPM.

Even though some of the design concepts explored above are hard to be achieved in manufacturing, the above sensitivity analysis provides valuable insight into different design concepts for multiring flywheel rotors.

CHAPTER 5
DESIGN ANALYSIS

5.1 INTRODUCTION

After reviewing and assessing the flywheel design concepts in Chapter 2, three types of flywheel designs with manufactured aluminum hub or SMC hub were considered to be the most promising of the twenty design concepts evaluated. It was also recommended that the five materials: (1) E-glass, (2) S2-glass, (3) Kevlar 29, (4) Kevlar 49, and (5) AS-Carbon be used in the present stage of the analysis.

The task objective of the flywheel design analysis is to set up a preliminary full size rotor data base to serve as (i) a guideline for choosing full size rotor designs and (ii) a reference for future iterations. As a result, some of the fifty-six rotor designs listed in this chapter have similar dimensions and material arrangements. The similarities are deliberately recorded to indicate the sensitivities of different flywheel designs with respect to geometry, material, interference pressure, etc., such that stress patterns, costs and other factors could be projected from the data base.

This chapter mainly focuses on the two designs previously recommended. They are design 'E': Single Material Multi-Ring-On-Ring and design 'H': Multimaterial Multi-Ring-On-Ring. However, design 'H' is divided into two groups: the multi-ring and the biannular ring. The recommended design 'F': Multi-Material Multi-Ring-On-Ring with Overwrap or Bandwrap is not included in this study because of the following reasons:

i) This design is a particular case of design 'H': Multi-Material Multi-Ring-On-Ring. Therefore, it should be studied only after the preliminary search is finished.

ii) Also, referring to the task objectives mentioned before, exploration of this design is not valued at this stage of the analysis.

5.2 ROTOR DESIGN ANALYSIS

During the search for feasible designs by computer analysis, the design objectives/constraints specified in Chapter 1 were imposed. Generally, all designs that could not meet the design objectives/constraints were eliminated. However, in some cases weight and swept volume constraints were relaxed to a reasonable extent so as to include more feasible designs for a final selection.

Chart I gives the properties used in this analysis for the selected materials. Material cost, density, moduli, specific moduli and poisson's ratio are listed in the chart for the materials at different fibre volume fractions. All the appropriate material properties and costs are calculated from the rule of mixtures [Ref. 19]. (Appendix D and E).

In addition to the constraints specified above, all stress levels (tangential and radial) in each ring of a particular flywheel design must fall below or within a reasonable range of the working strengths (both compressive and tensile) of that particular material. The working strengths listed in Chart II provide a reasonable data test programs in the flywheel research project provided that material is selected for the Advanced Data Base. For these reasons, stress-levels of some flywheel designs that are above the working strengths in Chart II will also be considered to be feasible provided the level falls within a reasonable range.

In the following sections, the three identified designs are studied. Charts III, IV and V give the data bases for Single Material Multi-Ring-On-Ring, Multi-Material Biannular Ring-On-Ring and Multi-Material Multi-Ring-On-Ring flywheel designs respectively. In all, fifty-six possible designs are listed which provide a 1 KW-Hr usable energy storage from a 2:1 speed range, operate within 25,000 rpm and a 24 inch diameter and in general meet the stress patterns, radial compatibilities and working strengths of the materials. However, as stated, some flexibility in weight, swept volume and ultimate stress

CHART I [Ref. 19]

MATERIAL PROPERTIES OF SELECTED FIBRE COMPOSITES

COMPOSITE	VOLUME FRACTION (%)	COST/LB (1985 $/LB)	DENSITY, ρ (LB/CU.IN)	LONGITUDINAL MODULUS, E_{11} (MSI)	TRANSVERSE MODULUS, E_{22} (MSI)	SPECIFIC LONGITUDINAL MODULUS, E_{11}/ρ	SPECIFIC TRANSVERSE MODULUS, E_{22}/ρ	MAJOR POISSON'S RATIO[1] (60%)
E-GLASS	55.	1.102	0.0736	7.992	1.313	108.6	17.8	.335
	60.	1.074	0.0763	8.441	1.682	110.6	22.1	
	65.	1.049	0.0790	8.891	2.052	112.5	26.0	
	70.	1.025	0.0818	9.340	2.422	114.2	29.6	
S2-GLASS	55.	3.071	0.0690	7.265	2.118	105.3	30.7	.25
	60.	3.150	0.0713	7.960	2.350	111.6	32.9	
	65.	3.224	0.0736	8.654	2.582	117.5	35.1	
	70.	3.294	0.0760	9.342	2.814	123.1	37.0	
KEVLAR-29	55.	14.177	0.0481	6.171	0.544	128.2	11.3	.35
	60.	15.195	0.0486	6.802	0.580	140.1	11.9	
	65.	16.195	0.0490	7.433	0.616	151.7	12.6	
	70.	17.177	0.0494	8.064	0.653	163.2	13.2	
KEVLAR-49	55.	8.771	0.0481	9.206	0.544	191.3	11.3	0.37
	60.	9.351	0.0486	10.182	0.580	209.7	11.9	
	65.	9.920	0.0490	11.157	0.616	227.8	12.6	
	70.	10.478	0.0494	12.132	0.653	245.5	13.2	
AS-CARBON	55.	12.384	0.0557	16.281	1.023	292.4	18.4	0.29
	60.	13.130	0.0568	17.405	1.102	306.5	19.4	
	65.	13.847	0.0579	18.529	1.182	319.9	20.4	
	70.	14.537	0.0590	19.653	1.262	332.9	21.4	

Note: 1. Poisson's ratio was assumed to be constant for volume fraction ranging from 55% to 70%.

CHART II [Ref. 19]

WORKING STRENGTHS OF SELECTED COMPOSITES[1,2]

COMPOSITE[2]	σ_{11TW} (Note 3,4)	σ_{22TW} (Note 3,5)	σ_{11CW} (Note 3,6)	σ_{22CW} (Note 3,7)
E-GLASS	300 (43.5)	3 (0.435)	100 (14.5)	20 (2.9)
S2-GLASS	400 (58)	20 (2.9)	150 (21.75)	30 (4.35)
KEVLAR-29	1000 (145)	5 (0.725)	100 (14.5)	25 (3.625)
KEVLAR-49	1000 (145)	5 (0.725)	100 (14.5)	25 (3.625)
AS-CARBON	800 (116)	30 (4.35)	350 (50.75)	150 (21.75)

Notes: 1. Estimated from current literature (10^6 cycles).[19]

2. Volume fraction of composite approximately 60%.

3. Stress in MPA (KSI).

4. σ_{11TW} = working tensile stress in fibre direction.

5. σ_{22TW} = working tensile stress in transverse direction.

6. σ_{11CW} = working compressive stress in fibre direction.

7. σ_{22CW} = working compressive stress in transverse direction.

may be allowed. A final chart provides a first cut of all those designs that were selected and are recommended on the basis that they are a good representative of each category investigated. A final selection of designs will be taken from the chart or new design approaches recommended for further study.

5.2.1 SINGLE MATERIAL MULTI-RING-ON-RING

This category of flywheel design consists of a number of rings of the same material nested together by interference fit.

According to the in-house report [1], Garrett AiResearch (in-house), [16,17] had designed and spin tested a single material multi-ring flywheel made of four thin E-glass rings that gave a low energy storage of only 0.2 KW-Hr at a maximum speed of 17,000 rpm. Further, Garrett's single material multiring flywheel had a relatively large outside diameter of twenty-six inches.

Comparing with our design constraints, it could be judged intuitively that two of the selected materials, E-glass and S2-glass, cannot meet the identified design objectives/constraints. The results of the design analysis proved this to be the case. Neither of the materials could even come close to reaching the design objectives/constraints even though relaxations on the objectives, constraints and working strengths were allowed.

In Chart III, nine single material multiring designs are presented. Only Kevlar 49 and AS-Carbon were found to qualify as feasible design materials because of their high specific strengths. Kevlar 29 was also found to be inferior in this analysis because of its low specific modulus and higher cost compared with that of Kevlar 49.

The SMC S2-Glass hub diameter is limited to about twelve inches [1] at the working speeds being considered. Thus, in order to establish a design using the SMC hub/single material ring concept, very

high inter-ring interfacial pressures are required in order to maintain radial compatibility.

In spite of the high tangential working strength of Kevlar 49, its low working compressive and tensile strengths in the radial direction eliminate the possibility of using SMC hubs. In Chart III, designs one to seven give some of the feasible designs of Kevlar 49 with manufactured aluminum hubs. On the other hand AS-Carbon has the advantages of having high compressive and tensile working radial strengths as well as having reasonably high working hoop strengths. All these advantages allow the possibility of using either an SMC hub or a manufactured Aluminum hub for the AS-Carbon single material multi-ring flywheel. Designs eight and nine in Chart III give the flywheel configurations for AS-Carbon with a manufactured aluminum hub and an SMC hub respectively.

Generally speaking, for the aluminum hub, Kevlar 49 is the most desirable material to use (designs 1 to 7) while carbon is the only material suitable for single material SMC hub designs (No. 9).

For all the aluminum hub designs, very large swept volumes (poor geometric compatibility), all well in excess of the 1500 cu. inch objective, were found. However, several designs are quite attractive from a rotor weight/material cost point of view. The SMC hub/carbon-ring design can meet the geometric requirements but does exceed the weight objective.

Designs five and nine were selected as representative of this design concept for further consideration (see Chart VI). Design five, although exceeding the swept volume constraint, does offer the best geometric compatibility of all the aluminum hub rotors together with desirable weight/material cost properties. Design nine meets all the design objectives except the weight constraint. Further, it is the only rotor of this design concept which uses an SMC hub.

CHART [I]

SINGLE MATERIAL MULTI-RING-ON-RING DATA BASE

DESIGN NO.	MATERIAL	NO. OF RINGS	DIMENSIONS AND DETAILS	DESIGN SPEED (RPM)	STRESS (KSI) MAX σ_θ	STRESS (KSI) MIN σ_θ	STRESS (KSI) MAX σ_r	STRESS (KSI) MIN σ_r	STATIC INTERFERENCE PRESSURE (KSI)	POLAR INERTIA[1] (LB-IN/SEC^2)	HEIGHT (IN)	WEIGHT[4] (LB)	SPECIFIC ENERGY (W-HR/LB)	SWEPT VOLUME (CU.IN.)	COST[3] OF RINGS (1985$)	COST OF MATERIAL[2] (1985$)	HUB TYPE
1	KEVLAR-49	6 Six 0.50 inch thick. rings	R0 = 9.0 R1 = 9.5 R2 = 10.0 R3 = 10.5 R4 = 11.0 R5 = 11.5 R6 = 12.0	25,000	125.7	69.9	0.05	-0.1	P1 = 1.8 P2 = 2.6 P3 = 2.8 P4 = 2.4 P5 = 1.5	2.8596	4.335	52.3	25.5	1961	393	393	ALU
2	KEVLAR-49	7 Seven 0.40 inch thick rings	R0 = 9.2 R1 = 9.6 R2 = 10.0 R3 = 10.4 R4 = 10.8 R5 = 11.2 R6 = 11.6 R7 = 12.0	25,000	126.7	72.3	0.02	-0.1	P1 = 1.4 P2 = 2.2 P3 = 2.6 P4 = 2.5 P5 = 2.0 P6 = 1.2	2.7395	4.525	52.0	25.6	2047	387	387	ALU
3	KEVLAR-49	7 Five 0.40 inch thick rings plus two 0.50 inch thick rings	R0 = 9.0 R1 = 9.4 R2 = 9.8 R3 = 10.2 R4 = 10.6 R5 = 11.0 R6 = 11.5 R7 = 12.0	25,000	125.7	69.2	0.05	-0.1	P1 = 1.5 P2 = 2.4 P3 = 2.8 P4 = 2.8 P5 = 2.4 P6 = 1.5	2.8596	4.335	52.3	25.5	1961	393	393	ALU
4	KEVLAR-49	10 Ten 0.30 inch thick rings	R0 = 9.0 R1 = 9.3 R2 = 9.6 R3 = 9.9 R4 = 10.2 R5 = 10.5 R6 = 10.8 R7 = 11.1 R8 = 11.4 R9 = 11.7 R10= 12.0	25,000	128.1	68.2	0.02	-0.1	P1 = 1.2 P2 = 2.0 P3 = 2.5 P4 = 2.8 P5 = 2.9 P6 = 2.7 P7 = 2.3 P8 = 1.8 P9 = 1.0	2.8596	4.335	52.3	25.5	1961	393	393	ALU
5	KEVLAR-49	12 Twelve 0.30 inch thick rings	R0 = 8.4 R1 = 8.7 R2 = 9.0 R3 = 9.3 R4 = 9.6 R5 = 9.9 R6 = 10.2 R7 = 10.5 R8 = 10.8 R9 = 11.1 R10= 11.4 R11= 11.7 R12= 12.0	25,000	128.1	59.2	0.02	-0.1	P1 = 1.4 P2 = 2.4 P3 = 3.1 P4 = 3.6 P5 = 3.8 P6 = 3.8 P7 = 3.6 P8 = 3.2 P9 = 2.7 P10= 2.0 P11= 1.2	3.1748	3.905	53.7	25.0	1767	413	413	ALU

Notes: 1. Polar inertia/inch thickness about the rotational axis of the rotor.
2. Cost of aluminum hub was not included.
3. Constant Dollars.
4. Total Rotor Weight including hub. (Estimated for aluminum)

CHART III

SINGLE MATERIAL MULTI-RING-ON-RING DATA BASE

DESIGN NO.	MATERIAL	NO. OF RINGS	DIMENSIONS AND DETAILS	DESIGN SPEED (RPM)	STRESS (KSI) MAX σ_θ	STRESS (KSI) MIN σ_θ	STRESS (KSI) MAX σ_r	STRESS (KSI) MIN σ_r	STATIC INTERFERENCE PRESSURE (KSI)	POLAR INERTIA[1] (LB-IN/SEC^2)	HEIGHT (IN)	WEIGHT[4] (LB)	SPECIFIC ENERGY (W-HR/LB)	SWEPT VOLUME (CU.IN.)	COST[3] OF RINGS (1985$)	COST OF MATERIAL[2] (1985$)	HUB TYPE
6	KEVLAR-49	11 Eleven 0.30 inch thick rings	R0 = 8.7 R1 = 9.0 R2 = 9.3 R3 = 9.6 R4 = 9.9 R5 = 10.2 R6 = 10.5 R7 = 10.8 R8 = 11.1 R9 = 11.4 R10= 11.7 R11= 12.0	25,000	128.1	63.6	0.02	-0.1	P1 = 1.3 P2 = 2.2 P3 = 2.9 P4 = 3.2 P5 = 3.4 P6 = 3.3 P7 = 3.0 P8 = 2.5 P9 = 1.9 P10= 1.1	3.0253	4.098	52.8	25.3	1854	403	403	ALU
7	KEVLAR-49	10 Ten 0.20 inch thick rings	R0 = 10.0 R1 = 10.2 R2 = 10.4 R3 = 10.6 R4 = 10.8 R5 = 11.0 R6 = 11.2 R7 = 11.4 R8 = 11.6 R9 = 11.8 R10= 12.0	25,000	130.4	82.5	0.03	-0.1	P1 = 0.6 P2 = 1.0 P3 = 1.3 P4 = 1.4 P5 = 1.4 P6 = 1.3 P7 = 1.2 P8 = 0.9 P9 = 0.6	2.1746	5.701	52.1	25.6	2579	361	361	ALU
8	AS-CARBON	11 Eleven 0.30 inch thick rings	R0 = 8.7 R1 = 9.0 R2 = 9.3 R3 = 9.6 R4 = 9.9 R5 = 10.2 R6 = 10.5 R7 = 10.8 R8 = 11.1 R9 = 11.4 R10= 11.7 R11= 12.0	22,500	120.9	59.8	0.001	-0.1	P1 = 1.3 P2 = 2.2 P3 = 2.8 P4 = 3.1 P5 = 3.3 P6 = 3.2 P7 = 2.9 P8 = 2.5 P9 = 1.8 P10= 1.1	3.5134	4.356	63.6	21.0	1970	700	700	ALU
9	AS-CARBON	7 Seven 0.90 inch thick rings	R0 = 5.2 R1 = 6.1 R2 = 7.0 R3 = 7.9 R4 = 8.8 R5 = 9.7 R6 = 10.6 R7 = 11.5	23,500	116.1	25.3	0.25	-0.1	P1 = 4.7 P2 = 6.8 P3 = 7.6 P4 = 7.4 P5 = 6.1 P6 = 3.7	4.0765	3.442	83.8	15.9	1430	851	907	SHC

Notes: 1. Polar inertia/inch thickness about the rotational axis of the rotor.
2. Cost of aluminum hub was not included.
3. Constant Dollars.
4. Total rotor weight including hub. (Estimated for aluminum)

5.2.2 MULTIMATERIAL MULTI-RING-ON-RING

This category of design includes all the flywheels that consist of numbers of rings of different materials nested together with or without an interference-fit. In this thesis, this category of design is also sub-divided into two concepts, (1) Multimaterial Biannular Ring-On-Ring and (2) Multimaterial Multi-Ring-On-Ring.

5.2.2.1 MULTIMATERIAL BIANNULAR RING-ON-RING

This type of flywheel design consists of two distinct rings of different material. The inner and outer ring materials are chosen in such a manner that the inner ring dilates concurrent with the outer ring. Because of the compatible dilation, the inner ring will grow with the outer ring with increasing rotor speed. Consequently, radial compatibility is maintained and even dynamic induced compression can be built up at the interface of the two rings. This compression will reduce the hoop stress of the inner ring and consequently will reduce the radial tensile stress in both the inner and outer rings, In designing the multimaterial biannular ring-on-ring flywheel, the rule of thumb is to use a material of high specific modulus for the outer ring.

Chart IV lists thirty-three possible designs of the Multimaterial Ring-On-Ring. In the first thirty designs, S2-glass was used as the inner ring material with Kevlar 49 and AS-Carbon as outer ring materials. Designs 40-42 use Kevlar 29 and Kevlar 49 as inner and outer ring materials respectively. These three combinations were found to be the most compatible among the five materials being investigated since the difference of specific moduli between the inner and outer ring materials is large enough to induce dynamic compression across the boundary. Consequently, radial stresses can be reduced by careful parameter selection to satisfactory levels. Further, depending

on the materials and rotor geometry, static interference pressure between the rings may or may not be required for radial compatibility throughout the operating range of the rotor.

Designs ten through seventeen list the most promising rotor configurations found for the S2-Glass/Kevlar 49 material combinations. This can be subdivided into those suited for an SMC hub (Nos. 10-15) and those using an aluminum hub (Nos. 16-17).

In general, this design concept will yield maximum material stress states (in either ring material for even under static conditions) at an operating speed of 22,500 RPM for the 22-24 inch diameter rotors being evaluated.

For S2-Glass/Kevlar 49/SMC hub designs, no rotor configuration was found that could meet all the design objectives. All exceed the design weight and all exceed the S2-Glass working stress in the fibre direction. Further, it should be noted that all these designs require a static interference pressure at the limit of the transverse compressive stress of Kevlar 49, and hub diameters are at the upper limit for SMC. However, these rotors offer attractive geometric parameters and the lowest potential material costs of all rotor designs of all the design concepts evaluated. As such, this design concept will not be eliminated at this stage of the analysis and design eleven is recommended.

Similarly, for the S2-Glass/Kevlar 49/aluminum hub designs, no rotor configuration was found that could meet all the design criteria. While the larger hub diameters permit desirable stress levels/rotor weight/interference pressures; rotor geometry, in particular swept volume, becomes unacceptably large. Further, this design is not amendable to the subcircular hub attachment due to the very thick rings involved. Of the two, design seventeen is recommended because of its more favourable stress patterns.

Designs eighteen through thirty-nine represent the most promising biannular ring-on-ring rotor configurations found using S2-glass and AS-Carbon as the inner and outer ring material respectively. In general, AS-carbon is better than Kevlar 49 as an outer ring material due to its high compressive and tensile radial working stresses. This permits the use of thicker outside rings and consequently the size of the inner S2-glass ring and/or SMC hub could be reduced, which is favourable in reducing the stress in the inner S2-glass ring and SMC hub.

All designs from eighteen through thirty-eight can be used with an SMC hub with inside radius ranging from 5.0 inches to 6.5 inches. Again, none of these rotors can meet all the design objectives. However, a number of these designs violate only the weight constraint (about 85 pounds vs. the desired 65-70 pounds). This is principally due to the use of the SMC hub and is not considered to be a serious problem especially in view of the very favourable stress patterns and geometric parameters. Material costs tend to be high compared with the S2-Glass/Kevlar 49/SMC counterparts but it must be recognized that the latter rotors do not meet the desired stress patterns at this stage of development. Of those rotors in the 85 pound class, design twenty is preferred because of its relative low projected costs, desirable stress patterns and geometric parameters. Further, it has the advantage of a small SMC hub.

It is desirable, from a manufacturing point of view, to have a design that does not require interfacial pressures between the rings. The S2-Glass/AS-Carbon biannular configuration is the only design concept found to date which meets this objective and permits the use of SMC hubs. Further, no evidence of this design approach has been found in the literature. Of those listed, design number thirty-four is selected because it offers the best stress patterns together with a desirable geometry.

Designs 39-41 are biannular rotors, using aluminum hubs, which do not require static interfacial pressures. The limiting factor in these designs is swept volume, all are large but are the best such

CHART IV

MULTI-MATERIAL BIANNULAR-RING-ON-RING DATA BASE

DESIGN NO.	MATERIAL	NO. OF RINGS	DIMENSION AND DETAIL	DESIGN SPEED (RPM)	MAX. STRESS (KSI)				STATIC INTERFERENCE PRESSURE (KSI)	POLAR INERTIA[1] (LB-IN/SEC²)	HEIGHT (IN)	WEIGHT[4] (LB)	SPECIFIC ENERGY (W-HR/LB)	SWEPT VOLUME (CU.IN.)	COST[5] OF RINGS (1985$)	COST OF MATERIAL[2] (1985$)	HUB TYPE
					S-GLASS		KEV-49/AS CAR.										
					σ_θ	σ_r	σ_θ	σ_r									
10	S2-GLASS AND KEVLAR -49	2	RO = 6.5 R1 = 9.65 R2 = 12.0	22,500	76.157	2.75	107	0.7347	3.661	4.862	3.148	87.5	15.2	1424	343	423	SMC
11	S2-GLASS AND KEVLAR -49	2	RO = 6.6 R1 = 9.65 R2 = 12.0	22,500	75.945	2.473	107	0.7099	3.603	4.859	3.149	87.5	15.2	1425	340	423	SMC
12	S2-GLASS AND KEVLAR -49	2	RO = 5.7 R1 = 8.7 R2 = 11.0	22,500	61.225	2.513	89	0.7561	3.553	3.403	4.497	104.5	12.8	1710	430	518	SMC
13	S2-GLASS AND KEVLAR -49	2	RO = 6.1 R1 = 9.3 R2 = 11.5	22,500	70.253	2.897	99	0.5976	3.630	4.119	3.716	95.2	14.0	1544	373	457	SMC
14	S2-GLASS AND KEVLAR -49	2	RO = 6.2 R1 = 9.2 R2 = 11.5	22,500	68.847	2.439	98	0.7052	3.505	4.089	3.743	95.4	14.0	1555	378	465	SMC
15	S2-GLASS AND KEVLAR -49	2	RO = 6.1 R1 = 9.2 R2 = 11.5	22,500	68.702	2.662	98	0.7052	3.658	4.091	3.741	95.4	14.0	1554	381	465	SMC
16	S2-GLASS AND KEVLAR -49	2	RO = 8.5 R1 = 9.8 R2 = 12.0	22,500	63.109	-3.788	117	0.2767	2.500	3.485	4.392	66.1	20.2	1987	377	377	ALU
17	S2-GLASS AND KEVLAR -49	2	RO = 8.5 R1 = 9.7 R2 = 12.0	22,500	59.842	-3.740	116	0.3762	2.500	3.452	4.434	66.1	20.2	2006	387	387	ALU
18	S2-GLASS AND AS-CARBON	2	RO = 5.0 R1 = 8.0 R2 = 12.0	22,500	52.236	2.781	102	3.911	3.603	5.023	3.047	85.7	15.6	1379	657	702	SMC
19	S2-GLASS AND AS-CARBON	2	RO = 5.5 R1 = 8.5 R2 = 11.5	22,500	59.640	2.758	102	2.162	2.215	4.328	3.537	93.0	14.3	1470	603	668	SMC
20	S2-GLASS AND AS-CARBON	2	RO = 5.5 R1 = 8.5 R2 = 12.0	22,500	59.640	2.758	107	3.02	2.774	5.080	3.013	85.5	15.6	1363	597	652	SMC
21	S2-GLASS AND AS-CARBON	2	RO = 6.0 R1 = 8.5 R2 = 11.5	22,500	55.969	1.194	107	1.825	2.500 (c[3])	4.318	3.544	92.8	14.4	1473	590	667	SMC
22	S2-GLASS AND AS-CARBON	2	RO = 6.0 R1 = 8.5 R2 = 11.5	22,500	57.871	1.413	105	1.963	2.000 (c)	4.318	3.544	92.8	14.4	1473	590	667	SMC

Notes: 1. Polar inertia/inch thickness about the rotational axis of the rotor.
2. Cost of aluminum hub was not included.
3. Compression at interface when no interference pressure was applied.
4. Total rotor weight including hub. (Estimated for aluminum)
5. Constant dollars.

CHART IV

MULTI-MATERIAL BIANNULAR-RING-ON-RING DATA BASE

DESIGN No.	MATERIAL	NO. OF RINGS	DIMENSION AND DETAIL	DESIGN SPEED (RPM)	MAX. STRESS (KSI) S-GLASS σ_0	MAX. STRESS (KSI) S-GLASS σ_r	MAX. STRESS (KSI) AS CARBON σ_0	MAX. STRESS (KSI) AS CARBON σ_r	STATIC INTER-FERENCE PRESSURE (KSI)	POLAR INER-TIA[1] (LB-IN /SEC^2)	HEIGHT (IN)	WEIGHT[4] (LB)	SPE-CIFIC ENERGY (W-HR) /LB)	SWEPT VOLUME (CU.IN.)	COST OF RINGS[5] (1985$)	COST OF MATE RIAL[2] (1985$)	HUB TYPE
23	S2-GLASS AND AS-CARBON	2	RO = 6.0 R1 = 8.75 R2 = 11.5	22,500	59.765	1.647	110	1.419	2.500 (c)	4.355	3.515	92.7	14.4	1460	560	637	SMC
24	S2-GLASS AND AS-CARBON	2	RO = 6.1 R1 = 8.5 R2 = 11.5	22,500	57.199	1.164	106	1.915	2.000 (c)	4.316	3.546	92.8	14.4	1473	587	667	SMC
25	S2-GLASS AND AS-CARBON	2	RO = 6.0 R1 = 8.5 R2 = 11.5	22,500	65.478	2.429	96	2.594	0 (c)	4.318	3.544	92.8	14.4	1473	590	667	SMC
26	S2-GLASS AND AS-CARBON	2	RO = 6.0 R1 = 9.0 R2 = 12.0	22,500	67.842	2.785	112	2.181	1.761	5.147	2.974	85.3	15.6	1345	535	599	SMC
27	S2-GLASS AND AS-CARBON	2	RO = 6.0 R1 = 8.7 R2 = 12.0	22,500	63.409	2.13	109	2.679	1.803	5.099	3.001	85.3	15.6	1358	566	631	SMC
28	S2-GLASS AND AS-CARBON	2	RO = 6.2 R1 = 8.5 R2 = 11.5	22,500	64.687	1.869	97	2.478	0.0 (c)	4.314	3.548	92.7	14.4	1474	585	667	SMC
29	S2-GLASS AND AS-CARBON	2	RO = 6.3 R1 = 9.0 R2 = 12.0	22,500	72.915	2.786	106	2.584	0.0 (c)	5.140	2.918	85.2	15.7	1347	528	599	SMC
30	S2-GLASS AND AS-CARBON	2	RO = 6.5 R1 = 9.0 R2 = 12.0	22,500	72.119	2.188	107	2.462	0.0 (c)	5.135	2.981	85.1	15.7	1348	525	599	SMC
31	S2-GLASS AND AS-CARBON	2	RO = 6.5 R1 = 8.5 R2 = 12.0	22,500	65.102	1.337	103	3.306	0.0 (c)	5.058	3.026	85.2	15.6	1369	574	651	SMC
32	S2-GLASS AND AS-CARBON	2	RO = 6.5 R1 = 8.8 R2 = 12.0	22,500	69.318	1.828	106	2.799	0.0 (c)	5.103	2.999	85.2	15.7	1357	544	620	SMC
33	S2-GLASS AND AS-CARBON	2	RO = 6.5 R1 = 8.9 R2 = 12.0	22,500	70.719	2.01	107	2.630	0.0 (c)	5.118	2.990	85.1	15.7	1353	533	610	SMC
34	S2-GLASS AND AS-CARBON	2	RO = 6.5 R1 = 8.3 R2 = 12.0	22,500	62.271	1.043	101	3.645	0.0 (c)	5.031	3.042	85.2	15.6	1376	594	672	SMC
35	S2-GLASS AND AS-CARBON	2	RO = 6.5 R1 = 9.3 R2 = 12.0	22,500	76.320	2.771	110	1.969	0.0 (c)	5.187	2.951	85.0	15.7	1335	491	566	SMC

Notes:
1. Polar inertia/inch thickness about the rotational axis of the rotor.
2. Cost of aluminum hub was not included.
3. Compression at interface when no interference pressure was applied.
4. Total rotor weight including hub. (Estimated for aluminum)
5. Constant dollars.

CHART IV

MULTI-MATERIAL BIANNULAR-RING-ON-RING DATA BASE

DESIGN NO.	MATERIAL	NO. OF RINGS	DIMENSION AND DETAIL	DESIGN SPEED (RPM)	MAX. STRESS (KSI) S2-GL/KEV.29 σ_0	MAX. STRESS (KSI) S2-GL/KEV.29 σ_r	MAX. STRESS (KSI) AS-CAR/KEV.49 σ_0	MAX. STRESS (KSI) AS-CAR/KEV.49 σ_r	STATIC INTER-FERENCE PRESSURE (KSI)	POLAR INER-TIA [1] (LB-IN /SEC^2)	HEIGHT (IN)	WEIGHT [4] (LB)	SPE-CIFIC ENERGY (W-HR) /LB)	SWEPT COLUME (CU.IN.)	COST OF RINGS [5] (1985$)	COST OF MATE RIAL [2] (1985$)	HUB TYPE
36	S2-GLASS AND AS-CARBON	2	RO = 6.5 R1 = 9.5 R2 = 12.0	22,500	72.018	2.174	123	1.036	2.0	5.225	2.929	84.8	15.7	1325	469	544	SMC
37	S2-GLASS AND AS-CARBON	2	RO = 6.5 R1 = 9.2 R2 = 12.0	22,500	67.295	1.586	119	1.511	2.0	5.169	2.961	85.0	15.7	1340	501	577	SMC
38	S2-GLASS AND AS-CARBON	2	RO = 6.5 R1 = 9.2 R2 = 12.0	22,500	74.918	2.571	109	2.131	0.0 (c)	5.169	2.961	85.0	15.7	1340	501	577	SMC
39	S2-GLASS AND AS-CARBON	2	RO = 8.5 R1 = 9.3 R2 = 11.5	22,500	58	-2.1	113	0.767	0.0 (c)	3.008	5.089	69.9	19.1	2114	598	598	ALU
40	KEVLAR-29 AND KEVLAR-49	2	RO = 9.05 R1 = 10.2 R2 = 12.0	25,000	77.6	0.08	125.1	0.73	0.0	2.830	4.380	52.2	25.5	1981	479	479	ALU
41	KEVLAR-29 AND KEVLAR-49	2	RO = 8.60 R1 = 10.35 R2 = 12.00	25,000	82.8	0.70	124.2	0.65	0.0	3.077	4.029	52.9	25.2	1823	526	526	ALU
42	KEVLAR-29 AND KEVLAR-49	2	RO = 7.6 R1 = 9.9 R2 = 12.0	25,000	66.6	.695	131.8	.676	2.90	3.502	3.540	55.4	24.1	1601	568	568	ALU

1. Polar inertia/inch thickness about the rotational axis of the rotor.
2. Cost of aluminum hub was not included.
3. Compression at interface when no interference pressure was applied.
4. Total rotor weight including hub. (Estimated for aluminum).
5. Constant dollars.

configurations generated by the study. Further, since these relatively thick rings are not amendable to a sub-circular hub mount, hub-ring attachment could be a major problem. Design forty is recommended for this design class. Further, no SMC/ Kevlar 29/Kevlar 49 rotor configuration could be found. Design forty-two represents the smallest inside radius (RO = 7.6 inches) which could be generated.

5.2.2.2 MULTI-MATERIAL MULTI-RING-ON-RING

This type of design consists of any number of rings of different materials nested together and generally require an interference fit. Optimum usage of material can be achieved in this design by appropriately arranging the rings of different materials with respect to radial position. The rule of thumb to achieve an optimal result is to arrange the fibre composite material with increasing specific strength (or specific modulus). In so doing, all materials in the multi-ring rotor can achieve their design stress at the same rotor design speed.

Chart V lists fourteen feasible designs of the multimaterial multi-ring-on-ring flywheel. In general, this design concept holds considerable promise to meet all the design objectives including rotor weight even with a relatively heavy SMC hub.

Designs forty-three and forty-four are similar to the single material (AS-Carbon) multi-ring rotors but use one or more outer reinforcing rings of Kevlar 49. Such reinforcement allows higher rotational speeds and consequently more desirable physical and geometric parameters while maintaining the stress within the material design limits. Design forty-three uses an aluminum hub which characteristically results in a light weight but large swept volume geometry. This parameter relationship is reversed in design forty-four which uses an SMC hub. However, the high material costs and

CHART V

MULTI-MATERIAL MULTI-RING-ON-RING DATA BASE

DESIGN NO.	MATERIAL	NO. OF RINGS	DIMENSION AND DETAILS	DESIGN SPEED (RPM)	MAX STRESS IN EACH TYPE OF RING (KSI)						STATIC INTERFERENCE PRESSURE (KSI)	POLAR INERTIA[1] (LB-IN/SEC²)	HEIGHT (IN)	WEIGHT[3] (LB.)	SPECIFIC ENERGY (W-HR/LB)	SWEPT VOLUME (CU.IN.)	COST OF RINGS[4] (1985$)	COST OF MATERIAL[2] (1985$)	HUB TYPE
					S-GLASS		AS-CAR		KEV-49										
					σ_θ	σ_r	σ_θ	σ_r	σ_θ	σ_r									
43	AS-CARBON AND KEVLAR-49	8 Six AS carbon plus two Kevlar -49	RO = 8.5 R1 = 8.9 R2 = 9.3 R3 = 9.7 R4 = 10.1 R5 = 10.5 R6 = 10.8 R7 = 11.1 R8 = 11.5	25,000	-	-	116.6	O.K.	116	0.02	P1 = 1.9 P2 = 3.1 P3 = 3.7 P4 = 3.8 P5 = 3.5 P6 = 2.9 P7 = 1.8	2.753	4.503	57.2	23.3	1871	571	571	ALU
44	AS-CARBON AND KEVLAR-49	8 Seven AS carbon plus one Kevlar -49	RO = 5.2 R1 = 6.1 R2 = 7.0 R3 = 7.9 R4 = 8.8 R5 = 9.7 R6 = 10.6 R7 = 11.5 R8 = 12.0	23,500	-	-	114	O.K.	111	0.04	P1 = 4.9 P2 = 7.3 P3 = 8.4 P4 = 8.5 P5 = 7.6 P6 = 5.9 P7 = 2.6	4.723	2.971	77.7	17.2	1344	785	833	SMC
45	S2-GLASS AS-CARBON AND KEVLAR -49	3	RO = 8.7 R1 = 9.5 R2 = 11.3 R3 = 12.0	22,500	54	-2.8 (c)	115.0	0.14	101	0.10	P1 = 0.7 P2 = 1.93	3.5068	4.364	64.7	20.6	1974	531	531	ALU
46	S2-GLASS AS-CARBON AND KEVLAR -49	3	RO = 5.5 R1 = 8.0 R2 = 11.2 R3 = 12.0	25,000	65.1	2.1	116.0	2.98	124	0.18	P1 = 3.5 P2 = 3.96	4.853	2.554	70.4	18.9	1156	498	544	SMC
47	S2-GLASS AS-CARBON AND KEVLAR -49	3	RO = 5.3 R1 = 8.0 R2 = 11.2 R3 = 12.0	25,000	66.4	2.85	114.0	3.14	124	0.18	P1 = 3.5 P2 = 3.99	4.856	2.553	70.5	18.9	1154	501	545	SMC
48	S2-GLASS AS-CARBON AND KEVLAR -49	3	RO = 5.5 R1 = 8.1 R2 = 11.3 R3 = 12.0	25,000	66.9	2.36	118.0	3.0	124.3	0.13	P1 = 3.5 P2 = 3.52	4.883	2.539	70.3	19.0	1148	493	540	SMC
49	S2-GLASS AS-CARBON AND KEVLAR -49	3	RO = 5.4 R1 = 8.1 R2 = 11.3 R3 = 12.0	25,000	67.5	2.70	117	3.08	124.6	0.13	P1 = 3.5 P2 = 3.54	4.885	2.538	70.3	19.0	1148	495	540	SMC

Notes: 1. Polar inertia/inch thickness about the rotational axis of the rotor.
2. Cost of aluminum was not included.
3. Total rotor weight including hub. (Estimated for aluminum)
4. Constant dollars.

CHART V

MULTI-MATERIAL MULTI-RING-ON-RING DATA BASE

DESIGN NO.	MATERIAL	NO. OF RINGS	DIMENSION AND DETAILS	DESIGN SPEED (RPM)	MAX STRESS IN EACH TYPE OF RING (KSI)						STATIC INTERFERENCE PRESSURE (KSI)	POLAR INERTIA[1] (LB-IN/SEC²)	HEIGHT (IN)	WEIGHT[3] (LB.)	SPECIFIC ENERGY (W-HR/LB)	SWEPT VOLUME (CU.IN.)	COST OF RINGS (1985$)	COST OF MATERIAL[2] (1985$)	HUB TYPE
					S-GLASS		AS-CAR		KEV-49										
					σ_θ	q_r	σ_θ	q_r	σ_θ	q_r									
50	S2-GLASS AS-CARBON AND KEVLAR -49	3	RO = 6.0 R1 = 8.0 R2 = 11.3 R3 = 12.0	25,000	60.1	0.62	122	2.86	124	0.13	P1 = 3.5 P2 = 3.49	4.862	2.550	70.1	19.0	1153	492	547	SHC
51	S2-GLASS AS-CARBON AND KEVLAR -49	3	RO = 5.8 R1 = 8.0 R2 = 11.3 R3 = 12.0	25,000	62.3	1.14	120	2.99	125	0.13	P1 = 3.5 P2 = 3.51	4.866	2.548	70.2	19.0	1152	496	547	SHC
52	S2-GLASS AS-CARBON AND KEVLAR -49	5 Two S-Glass, Two AS carbon One Kev-49	RO = 6.0 R1 = 7.0 R2 = 8.0 R3 = 9.65 R4 = 11.3 R5 = 12.0	25,000	57.6	0.4	121	0.99	124	0.13	P1 = 2.36 P2 = 2.8 P3 = 5.79 P4 = 3.49	4.8623	2.550	70.1	19.0	1153	492	547	SHC
53	S2-GLASS AS-CARBON AND KEVLAR -49	5 Two S-Glass, Two AS carbon One Kev-49	RO = 5.5 R1 = 6.8 R2 = 8.1 R3 = 9.7 R4 = 11.3 R5 = 12.0	25,000	60.0	0.8	121	0.9	124	0.13	P1 = 4.45 P2 = 4.35 P3 = 6.02 P4 = 3.5	4.883	2.539	70.3	19.0	1148	493	540	SHC
54	S2-GLASS AS-CARBON AND KEVLAR -49	5 Two S-Glass, Two AS carbon One Kev-49	RO = 5.8 R1 = 6.9 R2 = 8.0 R3 = 9.65 R4 = 11.3 R5 = 12.0	25,000	57.0	0.56	121	0.9	124	0.13	P1 = 3.05 P2 = 3.5 P3 = 5.94 P4 = 3.5	4.8663	2.548	70.2	19.0	1152	496	549	SHC
55	S2-GLASS AS-CARBON AND KEVLAR -49	5 Two S-Glass, Two AS carbon One Kev-49	RO = 5.7 R1 = 6.85 R2 = 8.0 R3 = 9.65 R4 = 11.3 R5 = 12.0	25,000	58.7	0.61	121	0.99	124	0.13	P1 = 3.416 P2 = 3.6 P3 = 6.02 P4 = 3.53	4.868	2.547	70.2	19.0	1152	498	547	SHC
56	S2-GLASS AS-CARBON AND KEVLAR -49	5 Two S-Glass, Two AS carbon One Kev-49	RO = 5.8 R1 = 6.95 R2 = 8.1 R3 = 9.7 R4 = 11.3 R5 = 12.0	25,000	56.7	0.62	121	0.93	124	0.13	P1 = 3.3 P2 = 3.8 P3 = 5.77 P4 = 3.5	4.878	2.541	70.2	19.0	1150	489	539	SHC

Note: 1. Polar inertia/inch thickness about the rotational axis of the rotor.
2. Cost of aluminum was not included.
3. Total rotor weight including hub. (Estimated for aluminum)
4. Constant dollars.

and very high interring-interfacial pressures render this design (No. 44) undesirable.

Design forty-five through fifty-one are all triannular configurations using S2-Glass/AS Carbon/Kevlar 49 rings and, with the exception of design forty-five, all use SMC hubs. The concept is similar to the biannular design with a Kevlar 49 reinforcing ring. This concept was explored using E-Glass as the inner ring material, no suitable designs were found principally due to the low working strengths being used.

In general the triannular designs provide very attractive physical and geometric parameters, reasonable material costs but slightly higher working stresses in the S2-Glass/AS Carbon rings than projected in Chart II. However, depending on the design failure mode, this stress pattern may be desired. Design forty-six was selected for further study.

The stress patterns, in particular the radial stress in the S2-Glass/AS Carbon rings, can be controlled by using two thinner rings for each material. These are represented by designs fifty-two through fifty-six. These five rings, three material rotors again offer very attractive parameters and best meet all design objectives at reasonable material costs. Design fifty-five was selected for further study.

5.3 DESIGN ANALYSIS SUMMARY

The three flywheel design concepts together with the five candidate materials as recommended by the in-house study [1] were numerically analyzed. Fifty-six possible designs were presented together with their geometric and physical properties, stress patterns and material costs. All designs were for a 1.0 KW-Hr usable energy (2:1 speed range). Rotor configurations, for each of the three design concepts, can generally meet the overall design

objectives/constraints for the vehicular application (see Section 1.1), the principal exception being swept volume for designs using aluminum hubs and rotor weight for those using SMC hubs.

Chart VI summarizes the results of the analysis. Eleven designs that appear to be the most promising for each rotor class (design concept/ring material/hub type), as identified in the previous section, are shown. The chart shows the range of values of ring cost, rotor weight and swept volume for each class as well as the specific value (in brackets) of the actual rotor recommended. Further, Figures 5.1 through 5.11 give the detailed stress patterns for the eleven recommended rotor configurations. As discussed earlier, both E-glass and S2-glass did not qualify as candidate materials for the single material multi-ring-on-ring flywheel because of their low working tensile stress in the fibre direction. Further, Kevlar 49 was preferred over Kevlar 29 for this design class due to its lower cost and more amenable properties.

One of the common characteristics of the Single Material Multi-Ring-On-Ring design is the non-optimal usage of material due to the increasing stress distribution with radial position. However, this will give rise to a sequential failure mode (outside ring) which has proven desirable from a containment point of view. However, if the total ring thickness remains small, fairly efficient usage of material can still be achieved as is apparent from the weight/ring-material-cost of design five. However, large swept volumes and the need for metallic hubs naturally result. On the other hand, if a thicker ring structure is used, (or smaller hubs as is required for SMC) then very high ring interfacial pressures are required to achieve radial compatibility under operating conditions. Under such conditions, only AS-Carbon had sufficient radial compressive strength to qualify for such a design. However, the non-optimal use of material results in high cost/heavy rotors. Further, achieving the high interfacial pressures in manufacture may prove difficult.

The second category of flywheel design is the Biannular Ring-On-Ring. This design class is built up of two distinct annular rings of different materials. The difference in specific strength and modulus of the inner ring material and the outer ring material, together with an appropriate geometry, permits not only an optimal stress distribution but also the use of thick rings with controlled radial stress. As such, they are well suited to small SMC hubs and offer the lowest cost (ring material) designs found in this analysis (see rotor number eleven). Such designs would appear to offer distinct manufacturing advantages, especially those designs not requiring any static interfacial pressures (which must be built-in at the time of manufacture), eg. design number thirty-four. Further, most rotors in this design category offer the possibility of lower speed operation. Several disadvantages can be cited however, the first being that these rotors tend to run 15-18 pounds over the guide weight of 70 pounds. This results, in part, from the choice of reducing operating speed as opposed to rotor diameter for the design. Secondly, there is a tendency for stresses in the inner S2-glass ring to be high. From the S2-Glass stress point of view, AS-Carbon is a better candidate for the outer ring material than Kevlar 49, however, firm conclusions on these matters requires second generation design analysis studies. Further, S2-Glass/AS-Carbon is the only material combination found to date that offers designs without static interfacial pressure requirements and can use SMC hubs. The Kevlar 29/Kevlar 49 biannular rotors were designed to operate at 25,000 rpm and all require aluminum hubs. In these designs, hub/rim attachment can be a major problem and swept volumes are undesirably large.

Many of the Multi-material Multi-Ring-On-Ring designs are an extension of the first two design categories. In general, this design concept results in a better stress distribution and a more optimal usage of material. For example designs forty-six and fifty-five offer the best geometric properties of all rotors presented and yet achieve weights, even with SMC hubs, within the design limit.

CHART VI

SUMMARY OF FLYWHEEL DESIGNS

1.0 KW-HR USABLE ENERGY - 2:1 SPEED RATIO

DESIGN	FLYWHEEL DESIGN CONCEPT	MATERIAL	HUB TYPE	STATIC INTER-FERENCE PRESSURE REQUIRED	REFERENCE DESIGNS (DESIGN NO.)	RING DESCRIPTION AND DETAILS	DESIGN SPEED (RPM)	COST OF RINGS (1985 $)	ROTOR WEIGHT (LBS)	SWEPT VOLUME (CU.IN.)	STRESS PROFILE	RECOM-MENDED DESIGN NO.
A	SINGLE MATERIAL MULTI-RING-ON-RING	KEVLAR-49	ALU	YES	1-7	6-12 rings press fit† 0.2-0.5" thick OD = 24". ID = 16.8" - 20.0"	25,000	361-413 (413)*	52.0 - 53.7 (53.7)*	1767 - 2579 (1767)*	Increases with radial position. Inside-low; outside-high but below design limit. (See Fig.5.1)	5
			SMC	-	-	No feasible configuration available	-	-	-	-	-	-
	(DATA FROM CHART III)	AS-CARBON	ALU	YES	8	11 rings press fit. All 0.3" thick. OD = 24", ID = 17.4"	25,500	700	63.6	1970	Increases with radial position. Outside ring slightly above design limit.	-
			SMC	YES	9	7 rings press fit. All 0.9" thick. OD = 23", ID = 10.4"	23,500	851 (851)*	83.8 (83.8)*	1430 (1430)*	Inc. with radial position. Outside ring at design limit. (See Fig.5.2)	9
B	MULTI-MATERIAL BIANNULAR RING-ON-RING	S2-GLASS KEVLAR -49	SMC	YES	10-15	Two rings press fit, S2-Glass inside, Kevlar 49 outside. OD = 22-24" ID = 11.4-13.2"	22,500	340-430 (340)*	87.5 - 104.5 (87.5)*	1424 - 1910 (1425)*	High stress on inside S2-Glass ring-over design limit. Interference pressure at design limit for Kevlar. (See Fig.5.3)	11
			ALU	YES	16-17	Two rings press fit. S2-Glass inside, Kevlar 49 outside. OD=24", ID=17"	22,500	377-387 (387)*	66.1 (66.1)*	1987 - 2006 (2006)*	Stress on inside S2-Glass ring slightly over design limit. (See Fig.5.4)	17
	(DATA FROM CHART IV)	S2-GLASS AS-CARBON	SMC	YES	18-24 26-27 36-37	Two rings press fit, S2-Glass inside, AS-Carbon outside. OD=23-24". ID=10-13	22,500	469-657 (597)*	84.8 - 93.0 (85.5)*	1325 - 1473 (1363)*	Stresses in both ring materials can be below design limit. (See Fig.5.5)	20
				NO	28-35 25,38	Two rings, no inter ring pressure. S2-Glass inside AS-Carbon outside. OD = 23-24", ID = 12-13"	22,500	491-594 (594)*	85.0 - 92.8 (85.2)*	1335 - 1474 (1376)*	Stress on inside S2-Glass ring is high -- over design limit. (See Fig. 5.6)	34
		S2-G/AS-C and KEV29/KEV49	ALU	NO	39-41	Two rings, no inter ring pressure. S2-Glass inside AS-Carbon outside. OD = 23" ID = 17"	22,500	598 (479)*	69.9 (52.2)*	2114 (1981)*	Good stress patterns, both rings. (See Fig.5.7)	40
C	MULTI-MATERIAL MULTI-RING-ON-RING	AS-CARBON KEVLAR -49	ALU	YES	43	First 6 rings are AS-Carbon, last 2 are Kevlar -49, 0.3 - 0.4 thick. OD = 23" ID = 17"	25,000	571 (571)*	57.2 (57.2)*	1871 (1871)*	Good stress levels, both materials. (See Fig.5.8)	43
			SMC	YES	44	First 7 rings are AS-Carbon 0.9" thick. Last ring is Kevlar -49, 0.5" thick. OD=24", ID=10.4"	23,500	785 (785)*	77.7 (77.7)*	1344 (1344)*	Good stress levels, both materials. (See Fig.5.9)	44
	(DATA FROM CHART V)	S2-GLASS AS-CARBON KEVLAR -49	ALU	YES	45	3 rings press fit, 1st - S2-Glass, 2nd - AS Carbon 3rd - Kevlar -49. OD = 24" ID = 17.4"	22,500	531	64.7	1974	Good stress levels, all materials.	-
			SMC	YES	46-51	3 rings press fit. 1st - S2-Glass (thick); 2nd - AS-Carbon (thick); 3rd - Kevlar -49 (thin). OD = 24" ID = 10.6 - 12.0"	25,000	492-501 (498)*	70.1 - 70.5 (70.4)*	1148 - 1154 (1156)*	Stress in the inner S2 Glass ring tends to be high. (See Fig. 5.10)	46
			SMC	YES	52-56	5 rings press fit. Two S2-Glass; two AS-Carbon; one Kevlar -49. OD = 24" ID = 11-12"	25,000	489-498 (498)*	70.1 - 70.3 (70.2)*	1148 - 1153 (1152)*	Stress in the center AS Carbon rings tend to be over the design limit. (See Fig. 5.11)	55

*Actual value of ring cost, rotor weight and swept volume for the recommended rotor in the design class. † Implies interfacial pressure required.

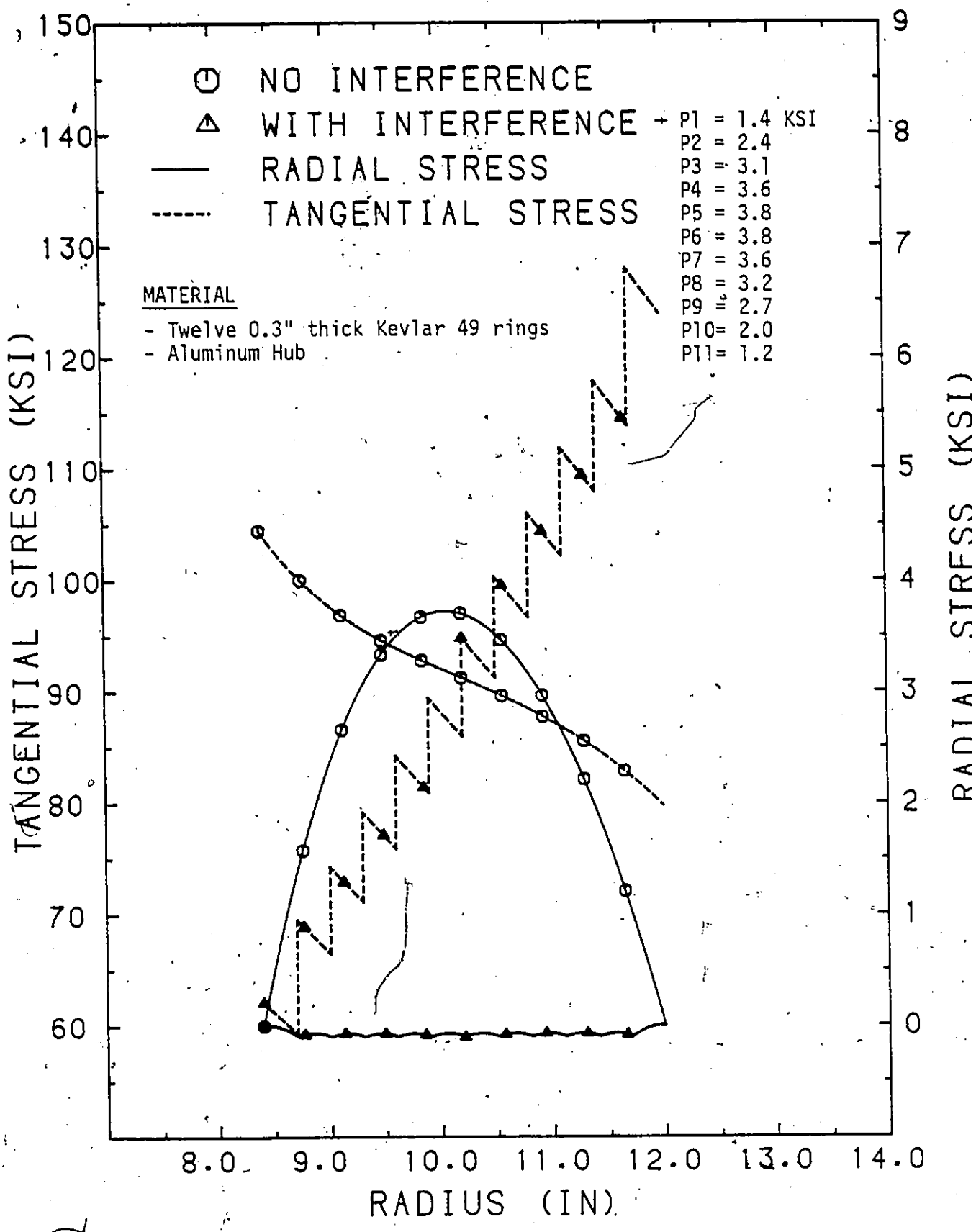

Fig. 5.1: Tangential and Radial Stress Patterns in a Single Material Multi-Ring-On-Ring Rotor at 25,000 RPM. (Design #5)

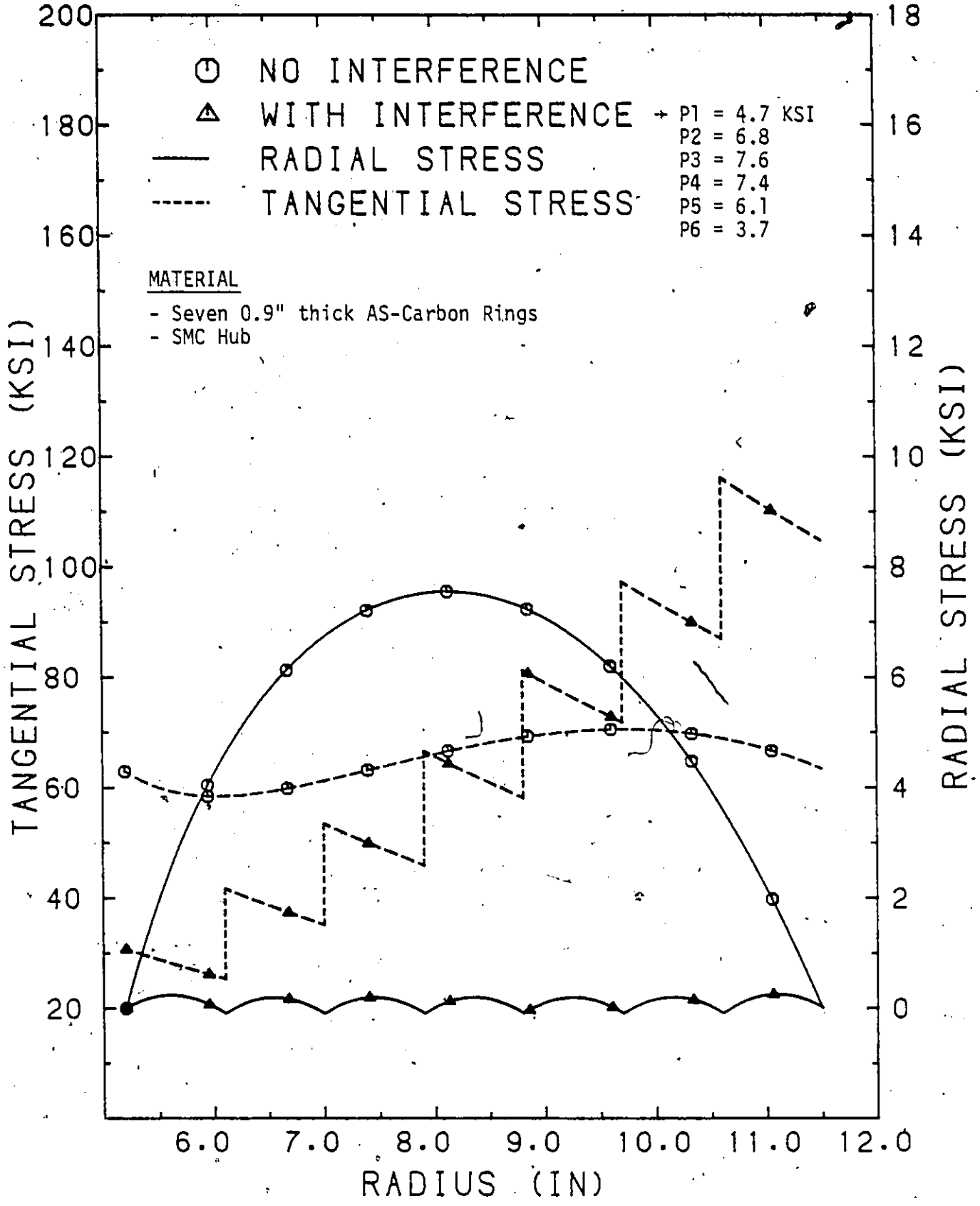

Fig. 5.2: Tangential and Radial Stress Patterns in a Single Material Multi-Ring-On-Ring Rotor at 23,500 RPM. (Design #9)

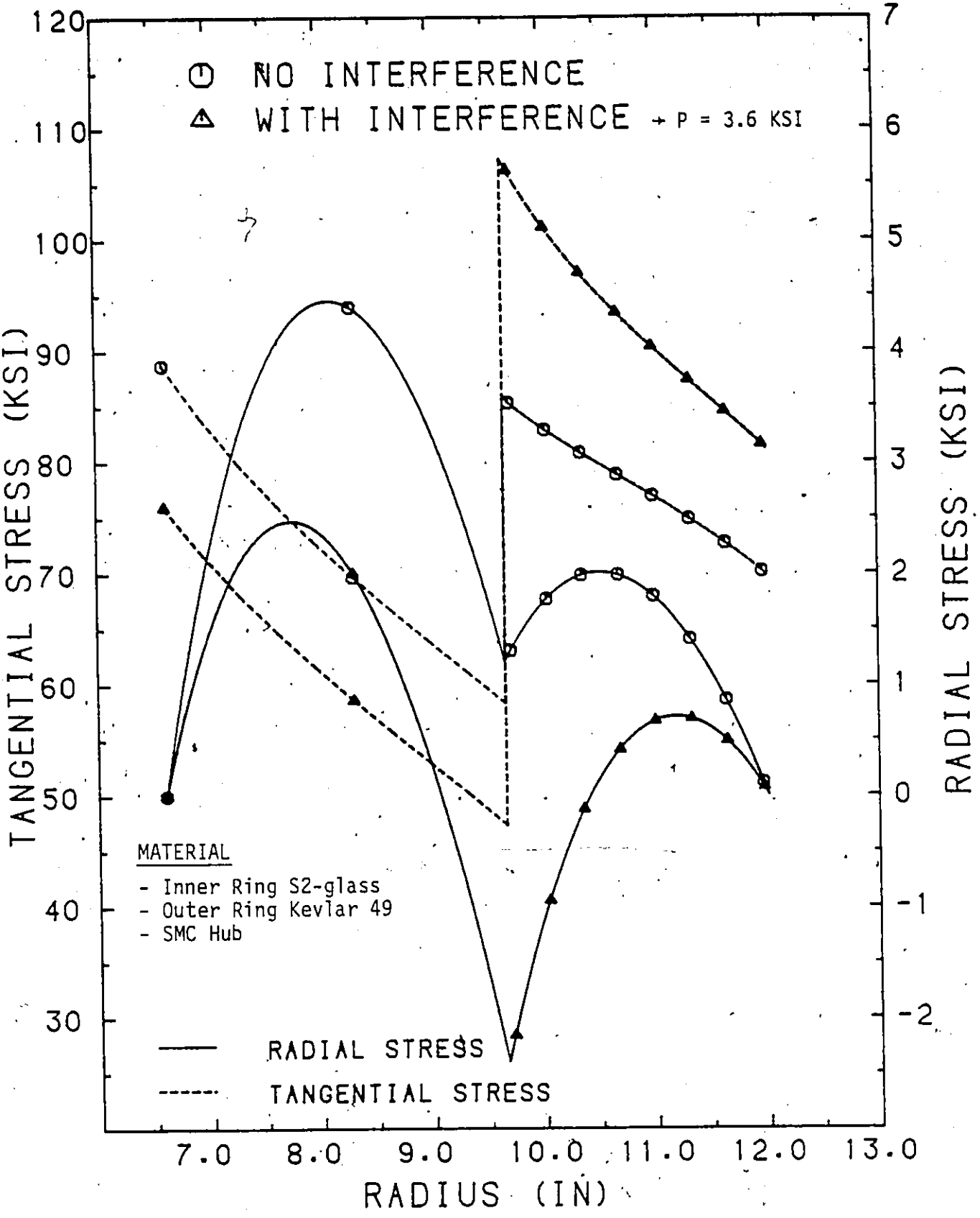

Fig. 5.3: Tangential and Radial Stress Patterns in a Multi-Material Biannular Ring-On-Ring Rotor at 22,500 RPM. (Design #11)

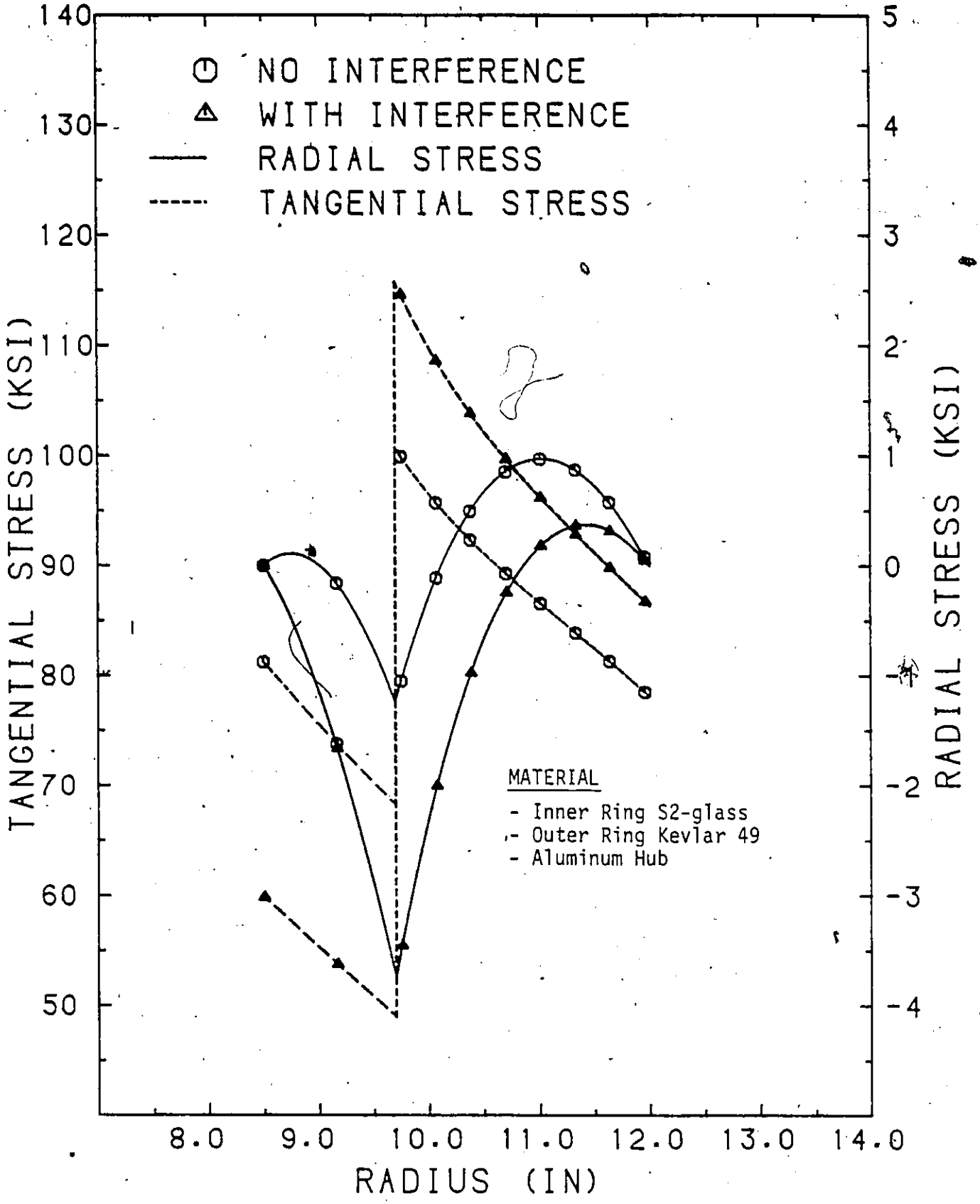

Fig. 5.4: Tangential and Radial Stress Patterns in a Multi-Material Biannular Ring-On-Ring Rotor at 22,500 RPM. (Design #17)

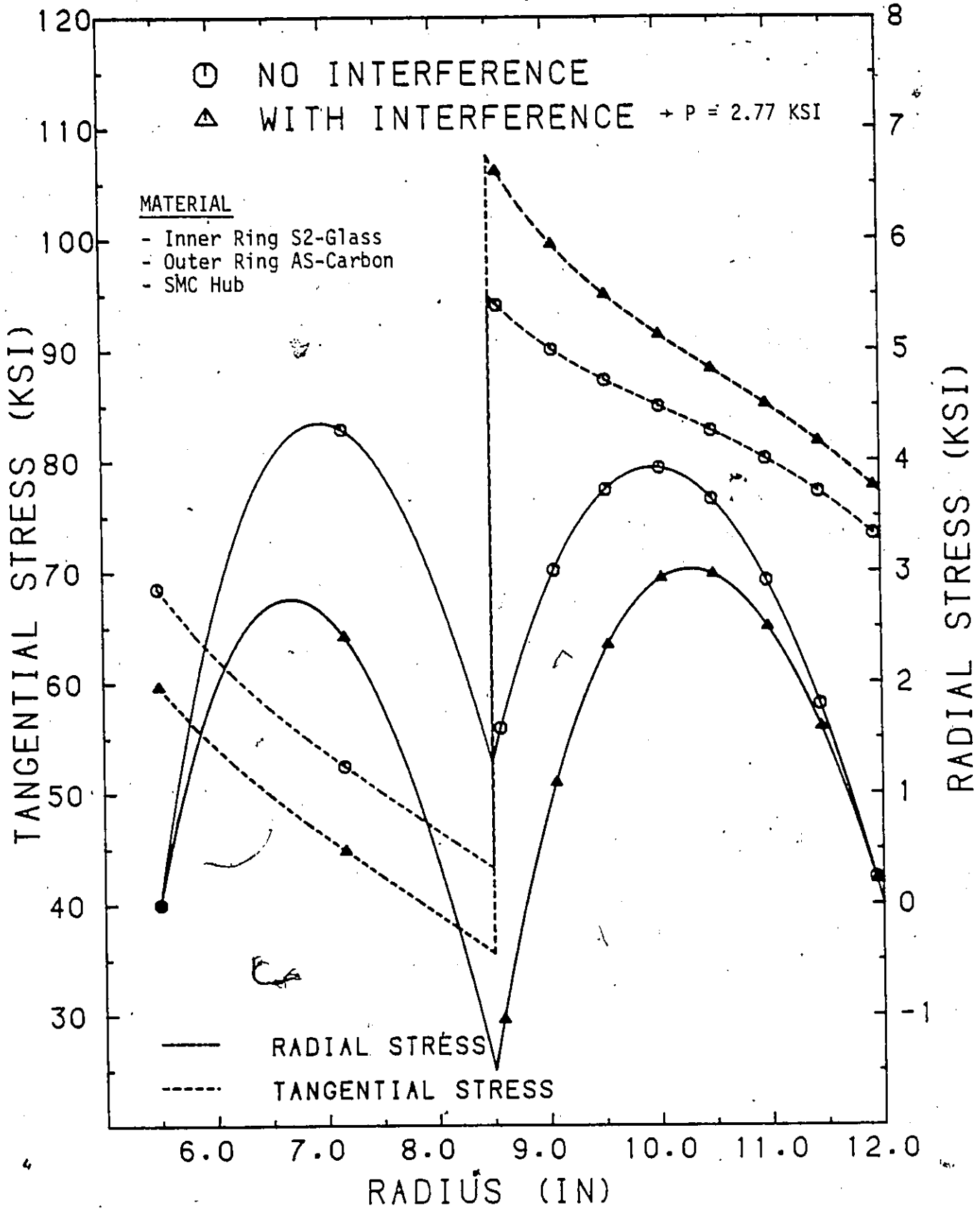

Fig. 5.5: Tangential and Radial Stress Patterns in a Multi-Material Biannular Ring-On-Ring Rotor at 22,500 RPM. (Design #20)

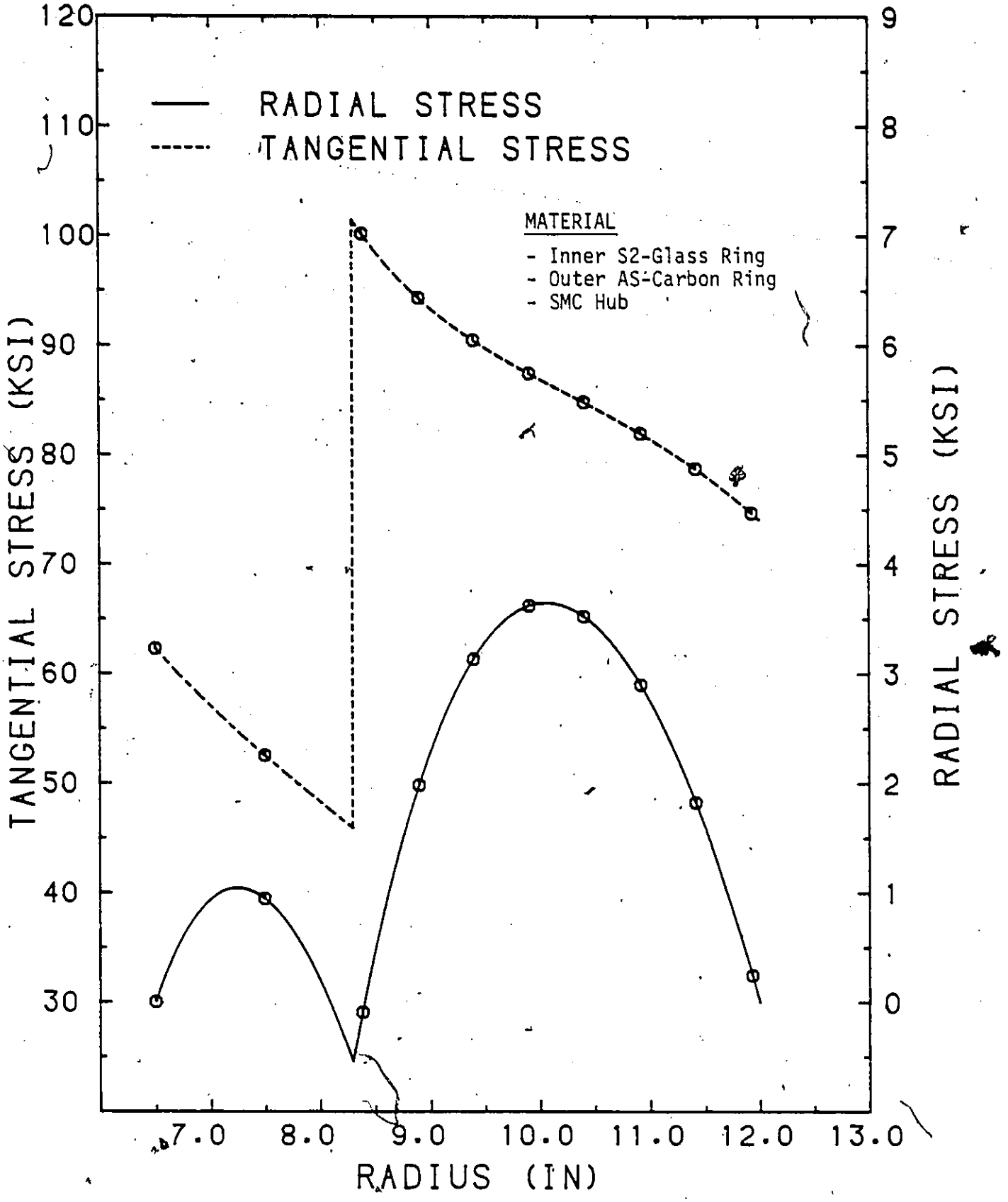

Fig. 5.6: Tangential and Radial Stress Patterns in a Multi-Material Biannular Ring-On-Ring Rotor at 22,500 RPM, with no Interference Pressure. (Design #34)

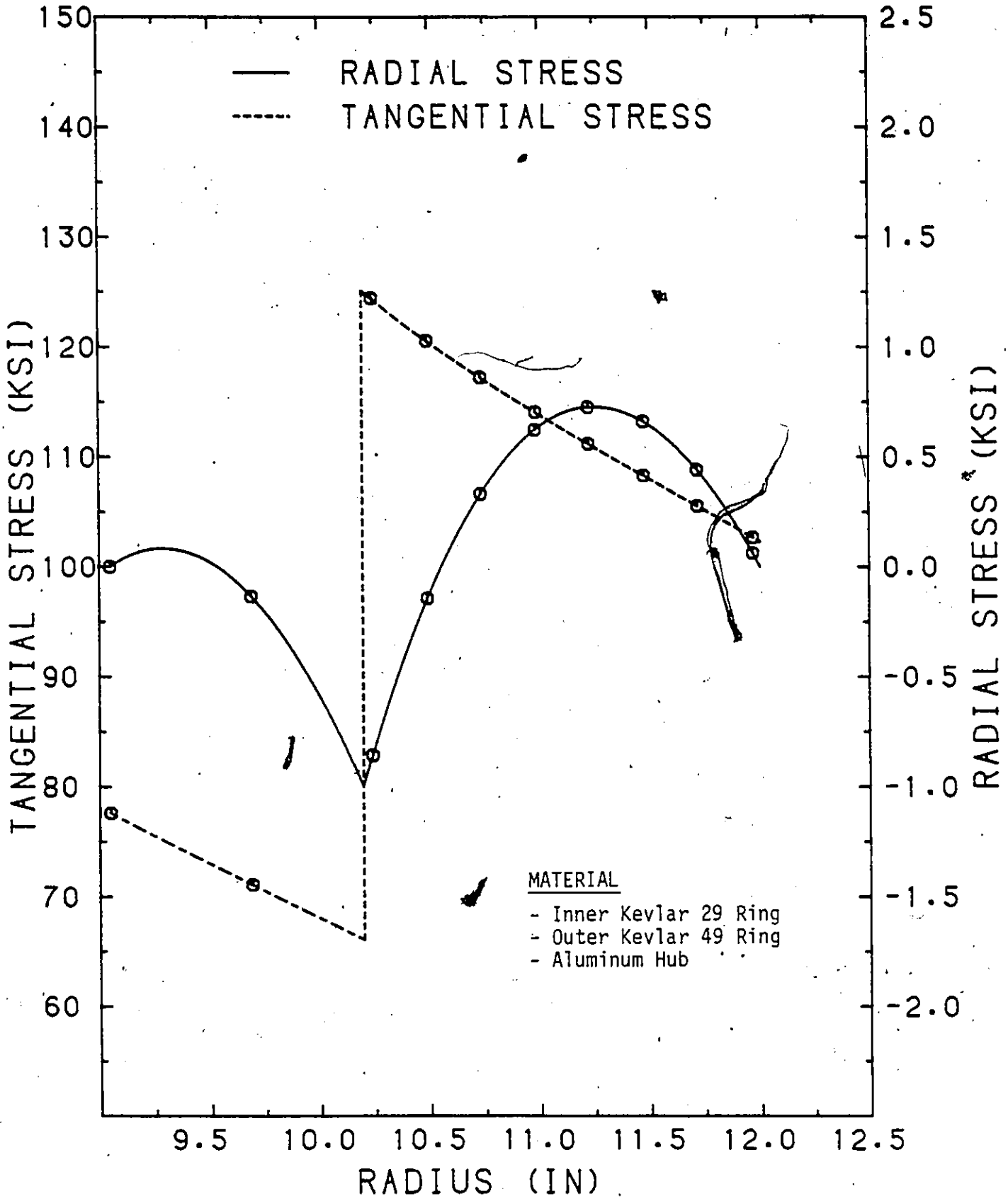

Fig. 5.7: Tangential and Radial Stress Patterns in a Multi-Material Biannular Ring-On-Ring Rotor at 25,000 RPM, with no Interference Pressure. (Design #40)

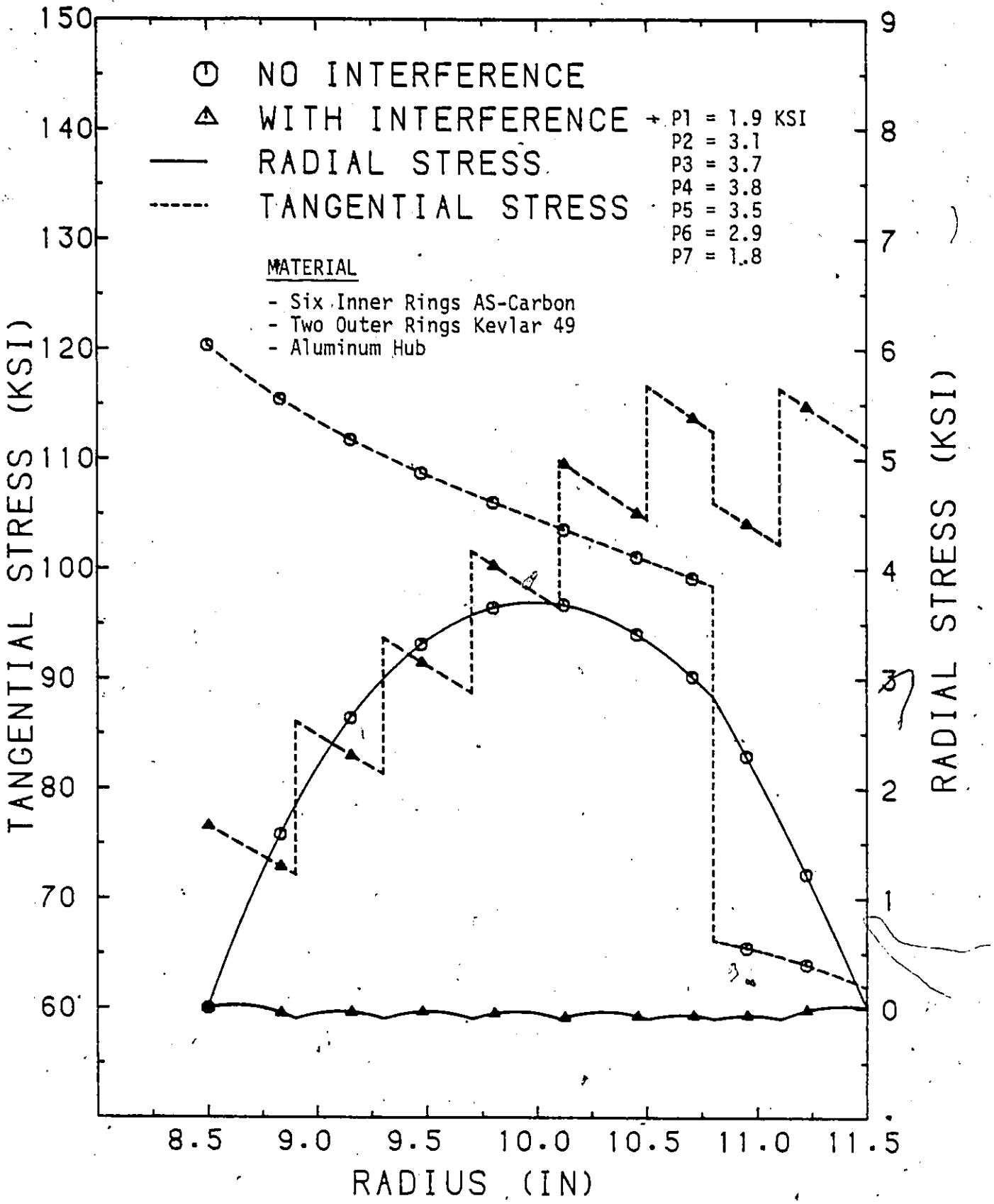

Fig. 5.8: Tangential and Radial Stress Patterns in a Multi-Material Multi-Ring-On-Ring Rotor at 25,000 RPM. (Design #43)

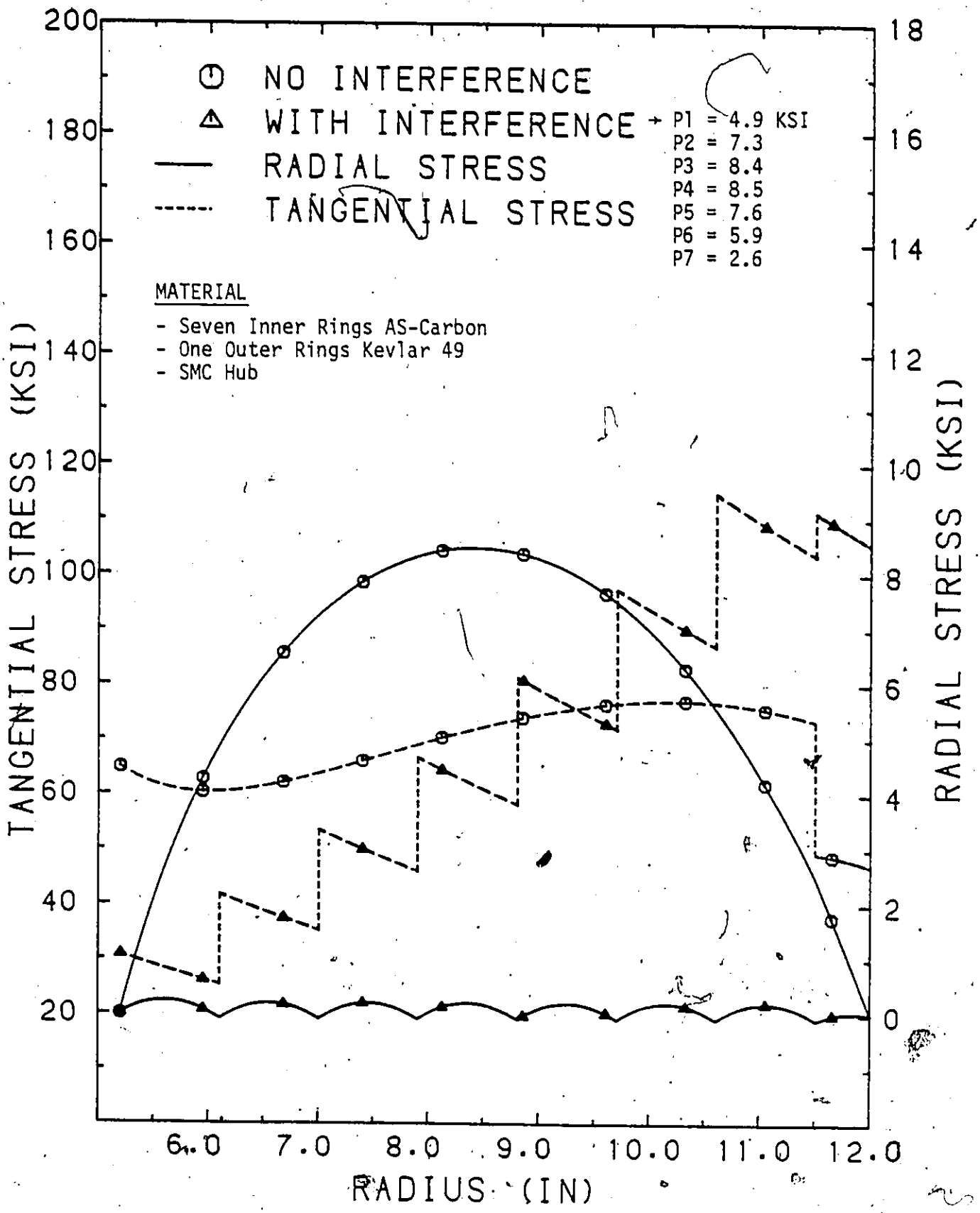

Fig. 5.9: Tangential and Radial Stress Patterns in a Multi-Material Multi-Ring-On-Ring Rotor at 23,500 RPM. (Design #44)

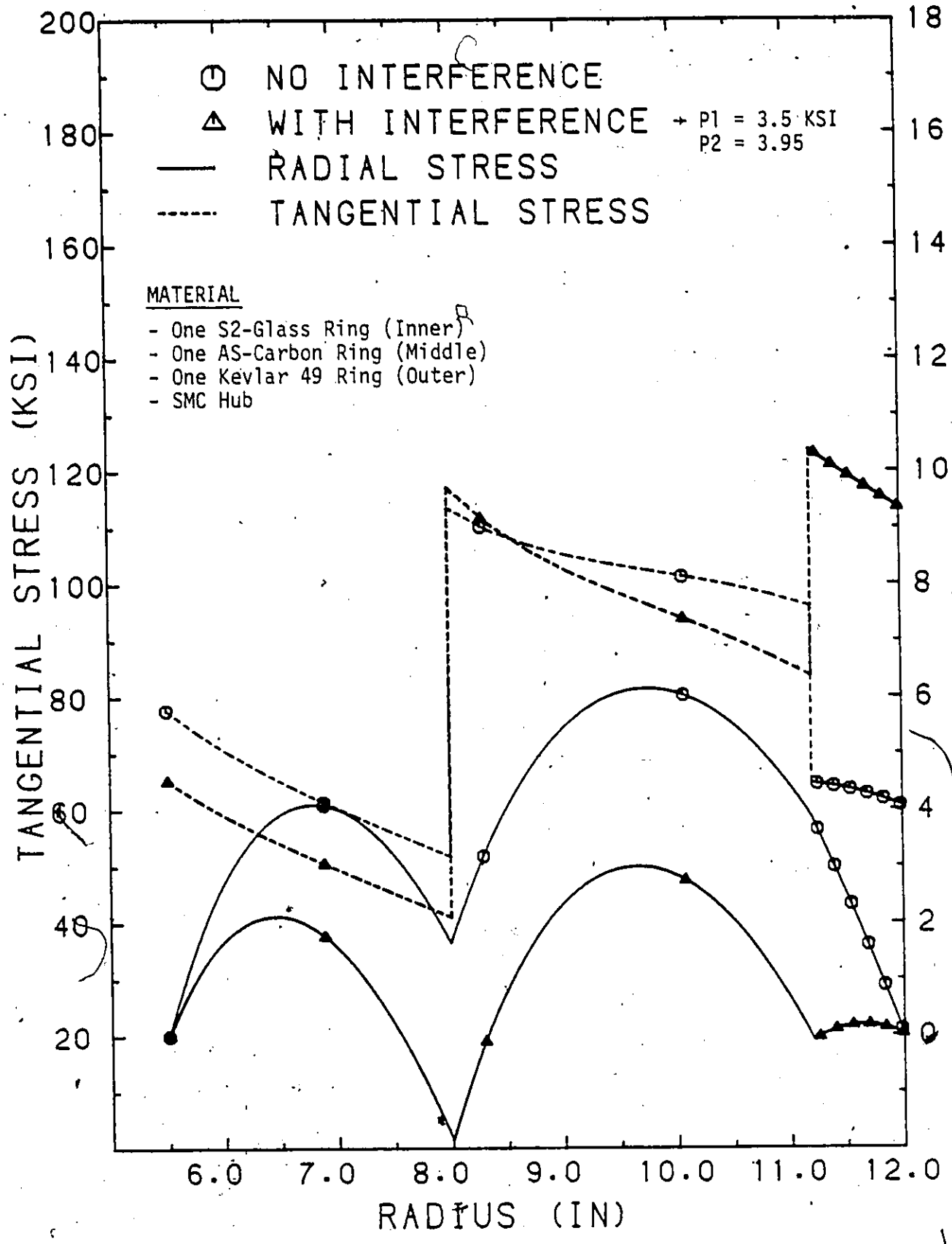

Fig. 5.10: Tangential and Radial Stress Patterns in a Multi-Material Multi-Ring-On-Ring Rotor at 25,000 RPM. (Design #46)

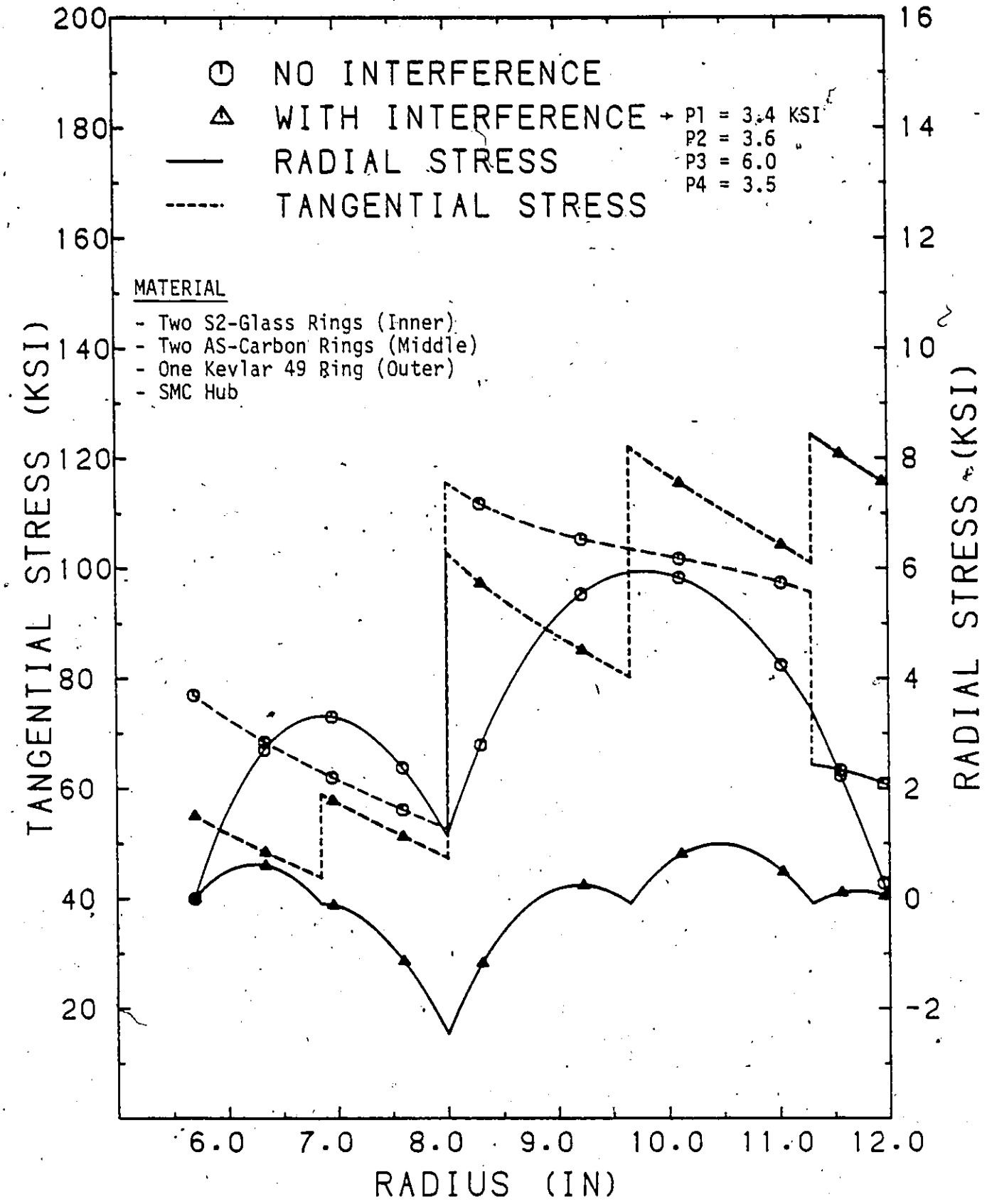

Fig. 5.11: Tangential and Radial Stress Patterns in a Multi-Material Multi-Ring-On-Ring Rotor at 25,000 RPM. (Design #55)

5.4 FINAL DESIGN SELECTION

It would be an error to try to make a final rotor selection at this stage of the analysis. Many questions must be carefully answered before such a decision should be attempted; namely: thick ring manufacture, precise material working strengths, SMC hub performance, interfacial pressure control, hub/rim attachment, failure analysis and residual stress/winding tension control.

However, some insight can be gained from an assessment of the defined rotor quantities (ring material cost, rotor weight and geometry) using a basic decision analysis. For this purpose, the rotor with the best specific property (eg. #11 for ring cost) was assigned a value of 10, that with the worst specific property (eg. #9 for ring cost) was assigned a value of 1, all other rotors received a value by direct linear interpolation. Table 5.1 lists rotor ratings vs. various rating criteria.

Surprisingly, the SMC hub rotors dominate the top rated groups under the various criteria. This is interesting since these rotors have an inherent weight disadvantage, on the other hand, however, they do have an inherent geometric advantage. It can be argued that 'weight' is the least important parameter (all rotor weights are reasonable) and provided that the rotor can be packaged in the vehicle, cost is the ultimate measure. Hence, the last criteria may be the most meaningful of the limited set of parameters being used.

By all measures however, designs 11, 46 and 55 with SMC hubs and 5 and 17 with aluminum hubs must be further considered. In addition, from the second rated group (Nos. 20, 34, 40 and 43), it is recommended that design 34 be carried further in the analysis because of its inherent attractiveness regarding manufacture as discussed in the previous section.

TABLE 5-1

ROTOR RATINGS

CRITERIA	TOP RATED GROUP	2ND RATED GROUP
Cost Only	11(SMC); 17(AL); 5(AL)	40(AL); 46(SMC); 55(SMC)
Cost + Geometry	46(SMC); 55(SMC); 11(SMC)	20(SMC); 34(SMC); 5(AL)
Cost + Geom. + Weight	46(SMC); 55(SMC); 5(AL)	40(AL); 11(SMC); 43(AL)
2 x Cost + Geom. + Weight	5(AL); 46(SMC); 55(SMC)	11(SMC); 40(AL); 17(AL)
2 x Cost + Geometry	11(SMC); 46(SMC); 55(SMC)	5(AL); 17(AL); 20(SMC); 34(SMC)
4 x Cost + 2 x Geom. + Wt.	11(SMC); 46(SMC); 55(SMC)	5(AL); 17(AL); 40(AL)

In summary, the following designs are recommended for second generation design analysis studies.

TABLE 5-2

FINAL RECOMMENDED FLYWHEEL DESIGNS

DESIGN NO.	DESIGN CONCEPT	HUB	MATERIALS
11	Biannular	SMC	S2-Glass; Kevlar 49
46	Triannular	SMC	S2-Glass; AS-Carbon Kevlar 49
55	Multi-Ring	SMC	S2-Glass; AS-Carbon Kevlar 49
5	Single Material	ALU	Kevlar 49
17	Biannular	ALU	S2-Glass; Kevlar 49
34	Biannular (P=0)	SMC	S2-Glass; AS-Carbon

CHAPTER 6
CONCLUSIONS AND RECOMMENDATIONS

6.1 CONCLUSIONS

After reviewing the detailed studies of the previous chapters, the conclusions from the design analysis of 1 Kw-Hr flywheels (usable energy with 2:1 speed range) are summarized as below.

1. Ring interfacial pressure, ring diameter, diameter ratio, density, specific tangential moduli and material moduli ratio 'K' were found to be the controlling parameters for hoop-wound fibre composite flywheel rotor design.

2. Only Kevlar 49 and AS-Carbon were found to be suitable fibre candidates for Single Material Multi-Ring-On-Ring designs because of their high tangential working strength. However, Kevlar 49 required the use of manufactured aluminum hubs whereas AS-Carbon could be designed for either aluminum or SMC hubs.

3. Despite its low cost, E-glass was eliminated as a feasible fibre candidate/or substitute for S2-glass. Because E-glass's low specific strengths cannot meet the stress levels of high speed composite flywheels.

4. From the computer analysis, multi-ring flywheel design concepts can meet all the design objectives (1 KW-Hr usable energy) with an operational speed of 25,000 rpm (maximum speed) and an outside diameter of 24" (maximum dimension). This result agrees

with the predicted result in the in-house analysis [1]. Further, from Chart VI, only the Multimaterial Multi-Ring-On-Ring designs made of S2-glass, AS-Carbon, and Kevlar 49, with an SMC hub could meet the above mentioned design objectives/constraints. Relaxing the weight constraint (80 to 90 lbs) allows for lower speed operation at 22,500 rpm where most of the Multimaterial Biannular ring designs become feasible. The use of aluminum hubs has the advantage of light weight but conversely, the swept volume will be larger (about 1,700 - 2,000 cu.in) than that of SMC hubs.

5. No final decision on flywheel design can or should be made at this stage of analysis. However, the most promising designs which warrant further analysis are:

   (i) SMC/S2 Glass/Kevlar 49 Biannular design eleven.

   (ii) SMC/S2 Glass/AS-Carbon/Kevlar 49 Triannular design forty-six.

   (iii) SMC/S2 Glass/AS-Carbon/Kevlar 49 Multiring design fifty-five.

   (iv) Alu/Kevlar 49 Single Material Multiring design five.

   (v) Alu/S2 Glass/Kevlar 49 Biannular design seventeen.

   (vi) SMC/S2 Glass/AS-Carbon Biannular (P=0) design thirty-four.

6. For the advanced materials data base, S2-Glass, AS-Carbon (or equivalent) and Kevlar 49 should be analyzed.

6.2 RECOMMENDATIONS

In view of the technical uncertainties involved in attempting to make a final selection on full-size flywheels, recommendations for future research and development are summarized as follows:

1. Thick ring winding techniques including residual stress.

2. SMC hub performance/production (stress level, quality control, etc.).

3. Control of interfacial pressures for Multi-Ring-On-Ring designs.

4. Establish a data base for the cost of production (hub, winding of rings).

5. Hub/rim attachment (shrink fitting, direct winding, etc.).

6. Failure analysis, especially benign failure modes.

BIBLIOGRAPHY

1. R.C. Flanagan, M.B. Munro, J. Wong, A. Miyase, J. McCrea; "Evaluation of and Program Recommendations for Anisotropic Material Flywheels". Report No. UOME-FP-8101-1, Contract No. OSU80-00043. Department of Mechanical Engineering, University of Ottawa, February 1981, 112 pp.

2. R.C. Flanagan; "Design and Evaluation of a Flywheel Hybrid Power Train for Minibus Vehicles: Parts I and II". DSS Contract No. OSU5-0201, Transport Canada, 1976, 92 pp and 75 pp.

3. R.C. Flanagan; "An Examination of the Potential for Innovative Automobile Power Trains". DSS Contract No. OST76-00038, Strategic Planning, Transport Canada, 1979, 195 pp.

4. M.B. Munro and R.C. Flanagan; "Evaluation of Non-Isotropic Materials for Canadian Flywheel Transportation Applications". Proceedings, Strength and Fracture of Composites - Canadian Fracture Conference 4, Alton, Ontario, 1980, pp. 69-74.

5. R.C. Clerk; "The Utilization of Flywheel Energy"; SAE Transactions, Vol. 72, 1964, pp. 508-543.

6. E.I. Danfelt, S. Hewes and T.W. Chou; "Optimization of Composite Flywheel Design"; Int. J. Mech. Sci., Vol. 19, 1977, pp. 69-78.

7. D.W. Rabenhorst; "Metals and Composites in Superflywheel Energy Storage Systems"; SAMPE Quarterly, Jan. 1975, p. 23.

8. G.F. Morganthaler and S.O. Bonk; "Composite Flywheel Stress Analysis and Materials Study". 12th National SAMPE Symposium, 1967, Paper D-5.

9. F.P. Gerstle and F. Biggs; "On Optimal Shapes for Anisotropic Rotating Discs"; Pro. 12th Annual Meeting of the Soc. Eng. Sci., 1975.

10. E.D. Reedy; "A Composite-Rim Flywheel Design". SAMPE Quarterly, Vol. 9, No. 3, 1978.

11. J.A. Kirk and R.A. Huntington; "Stress Redistribution for the Multi-ring Flywheel". ASME Paper 77-WA/DE-26, 1977, 12 pp.

12. J.A. Kirk and R.A. Huntington; "Stress Analysis and Maximization of Energy Density for a Magnetically Suspended Flywheel". ASME Paper 77-WA/DE-24, 1977, 8 pp.

13. R.L. Huddleston, J.J. Kelley, C.E. Knight, R.E. Pollard and D.W. Post; "Composite Flywheel Development Completion". Report No. Y-2117, Union Carbide - Nuclear Division, Oak Ridge, Tenn. 1978.

14. R.F. Post and S.F. Post; "Flywheels". Sci. American, Vol. 229, No. 6, 1973.

15. G.C. Pardoen, R.D. Nedenberg, B.E. Swartout; "Achieving Desirable Stress Rates in Thick Rim Rotating Disks by Variation of Properties". 1980 Flywheel Technology Symposium, pp. 159-167.

16. D.A. Towgood; "An Advanced Vehicular Flywheel System for the ERDA Electric Powered Passenger Vehicle". Proc. 1977 Flywheel Technology Symposium, p. 63.

17. L.J. Lawson; "Flywheel Trolley Coach Propulsion with a High-Capacity Composite Flywheel". Proc. 1980 Flywheel Technology Symposium, p. 153.

18. T.W. Place; "Composite Material Flywheel for UMTA Flywheel Trolley Coach". Proc. 1980 Flywheel Technology Symposium, p. 175.

19. J. Wang, R.C. Flanagan, M.B. Munro and A. Miyase; "Analysis and Design of 1.0 KW-Hr Anisotropic Material Flywheels". Report No. UOME-FP-8102-1, Contract No. OSU80-00043, Department of Mechanical Engineering, University of Ottawa, October 1981, 63 pp.

20. J. Wong, R.C. Flanagan and M. Munro; "Hoop-wound Fibre Composite Flywheel Design by Parameter Sensitivity". Proc. of the International Symposium on Mechanical Behaviour of Structured Media, Ottawa, May 18-21, 1981.

21. D.L. Satchwell; "High-Energy-Density Flywheel". Proceedings of 1978 Mechanical and Magnetic Energy Storage Contractors' Review Meeting, pp. 172.

22. F.C. Younger; "Tension-Balanced Spokes for Fibre-Composite Flywheel Rims". Proc. 1977 Flywheel Technology Symposium, p. 161.

23. F.C. Younger; "A Composite Flywheel for Vehicle Use". Proc. 1978 Mechanical and Magnetic Energy Storage Contractors' Review Meeting, p. 141.

24. T.M. Barlow et.al.; "Mechanical Energy Storage Technology Project: Annual Report for Calendar Year 1979". Lawrence Livermore Laboratory Report No. UCRL-50056-79, p. 74.

25. P.W. Hill et.al.; "Progress in Composite Flywheel Development". Proc. 1978 Mechanical and Magnetic Energy Storage Contractors' Review Meeting, p. 156.

26. P.C. Poubeau; "High-Speed Flywheels Operating on "One Active Axis", Magnetic Bearings". Proc. 1977 Flywheel Technology Symposium, p. 229.

27. G. Besel and E. Hau; "Flywheel Energy Accumulators for City Buses - Steel and Composite Design". Proc. 1980 Flywheel Technology Symposium, p. 4.

28. S.V. Kulkarni; "The Flywheel Rotor and Containment Technology Development Program of the U.S. Department of Energy". Proc. 1980 Flywheel Technology Symposium, Suppl. 1, p. 5.

29. D. Davis, A. Csomor and B. Ginsburg; "From Vehicle to Satellites: The Technology Revolution in High Performance Flywheels". Proc. 1980 Flywheel Technology Symposium, Suppl. 1, p. 93.

30. J.E. Notti; "Design and Test of Spacecraft Energy Momentum Flywheel". Proc. 1975 Flywheel Technology Symposium, p. 105.

31. D.E. Davis; "Advanced Composite Flywheel for Vehicle Application". Proc. 1978 Mechanical and Magnetic Energy Storage Contractors' Review Meeting, p. 168.

32. C.E. Knight et.al.; "Development of the "Bandwrap" Flywheel". Proc. 1977 Flywheel Technology Symposium, p. 137.

33. C.E. Knight and R.E. Pollard; "Prestressed Thick Flywheel Rims". Proc. 1977 Flywheel Technology Symposium, p. 183.

34. E.D. Reedy, Jr.; "Sandia Composite-Rim Flywheel Development". Proc. 1978, Mechanical and Magnetic Energy Storage Contractors Review Meeting, p. 87.

35. E.D. Reedy and H.K. Street; "Composite-Rim Flywheels: Spin Tests". SAMPE Quarterly, Vol. 10, No. 3, 1979, p. 36.

36. R.S. Steel and E.F. Babelay, Jr.; "Data Analysis Techniques Used at the Oak Ridge Y-12 Plant Flywheel Evaluation Laboratory". Proc. 1980 Flywheel Technology Symposium, p. 423.

37. T.M. Barlow et.al.; "Mechanical Energy Storage Technology Project - Annual Report for Calendar Year 1979". UCRL - 50056-79, May 1980, p. 63.

38. S.V. Kulkarni, R.G. Stone and R.H. Toland; "Prototype Development of Optimized Tapered - Thickness, Graphite/Epoxy Composite Flywheel". UCRL-52623, Nov. 1978.

39. R.P. Nimmer; "Laminated Composite Flywheel Failure Analysis". Proc. 1980 Flywheel Technology Symposium, p. 445.

40. R.P. Nimmer; "Laminated Flywheel Disc with Filament Wound Outer Ring". Proc. 1980 Flywheel Technology Symposium, p. 400.

41. D.P. McGuire and D.W. Rabenhorst; "Composite Flywheel Rotor/Hub Attachment Through Elastomeric Interlayers". Proc. 1979, Flywheel Technology Symposium, p. 155.

42. D.W. Rabenhorst; "Low-Cost Flywheel Demonstration Program". Report DOE/EC/1-5085, Applied Physics Lab., Johns Hopkins Univ., 1980, 86 pp.

43. D.S. Rabenhorst; "Low Cost Flywheel Demonstration". Proc. 1978 Mechanical and Magnetic Energy Storage Contractors Review Meeting, p. 44.

44. S. Renner-Smith; "Energy Storage: Search for the Perfect Flywheel". Popular Science, January 1980.

45. T.M. Barlow et.al.; "Mechanical Energy Storage Technology Project: Annual Report for Calendar Year 1979". Lawrence Livermore Laboratory Report No. UCRL-50056-79, p. 21.

46. C.E. Knight, Jr.; "Analysis of the Deltawrap Flywheel Design". Proc. 1977 Flywheel Technology Symposium, p. 131.

47. E.L. Lustenader, J.S. Hickey, W.R. Nial, A.B. Plunkett, E. Ritcher, F.G. Turnball, G. Chong; "Laboratory Evaluation of a Composite Material Flywheel Energy Storage System". SAE Paper No. 789683, presented at the 13th IECEC, San Diego, 1978.

48. D.E. Johnson; "Failure Modes of Bi-directionally Reinforced Flywheels". Proc. 1977 Flywheel Technology Symposium, p. 281.

49. T.M. Barlow, et.al.; "Mechanical Energy Storage Technology Project: Annual Report for Calendar Year 1979". Lawrence Livermore Laboratory Report No. UCRL-50056-79, p. 77.

50. D.W. Rabenhorst; "Flywheel Programs in Other Countries". Proc. 1977 Flywheel Technology Symposium, p. 27.

51. S. Post and F. Younger; "Design and Fabrication of a Flywheel Rotor for Automotive Use, Proc. 1980 Flywheel Technology Symposium, p. 168.

52. S.V. Kulkarni; "Composite-Laminate Flywheel-Rotor Development Program". Proc. 1979 Mechanical and Magnetic Energy Storage Contractors' Review Meeting, p. 388.

53. R.G. Stone; "The Laminated Disc Flywheel Program - A Rotor Development Project by LLL and G.E. Co.". Proc. 1978 Mechanical and Magnetic Energy Storage Contractors' Review Meeting, p. 68.

54. E.L. Lustenader and E.S. Zorzi; "A Status of the "Alpha-Ply" Composite Flywheel Concept Development". Proc. 23rd SAMPE Symposium and Exhibition, 1978, 712.

55. R.P. Nimmer; "Laminated Flywheel Disc with Filament Wound Outer Ring". Proc. 1979 Mechanical and Magnetic Energy Storage Contractors' Review Meeting, p. 399.

56. T.M. Barlow et.al.; "Mechanical Energy Storage Technology Project: Annual Report for Calendar Year 1979". UCRL-50056-79, May 1980, p. 70.

57. T.M. Barlow et.al.; "Mechanical Energy Storage Technology Project: Annual Report for Calendar Year 1979". UCRL-50056-79, May 1980, p. 87.

58. A.D. Sapowith; "AVCO Constant Stress Flywheel Design and Test Results". Proc. 1980 Flywheel Technology Symposium, Suppl. 1, p. 102.

59. D.W. Rabenhorst; "Flywheel Technology Development at APL". Proc. 1980 Mechanical and Magnetic Energy Storage Contractors' Review Meeting, Washington, D.C., Nov. 1980.

60. T.M. Barlow et.al.; "Mechanical Energy Storage Technology Project: Annual Report for Calendar Year 1979". UCRL-50056-79, May 1980, p. 18.

61. C.Y. Liu and C.C. Chamis; "Residual Stresses in Filament Wound Laminates and Optimum Programmed Winding Tension". Proceedings, Section 5-D, of the 20th Annual Meeting of the Society of the Plastic Industry, 1965.

62. E. Shiratori, K. Ikegami, T. Hattori and K. Shimizu; "Application of the Fibre Reinforced Composite to Rotating Discs". Bull. JSME, Vol. 18, No. 122, Aug. 1975, p. 784.

63. T. Hattori, K. Ikegami and E. Shiratori; "Rotating Strength of Glass-Carbon Fibre-Reinforced Hybrid Composite Discs, Bull. JSME, Vol. 21, No. 161, Nov. 1978, p. 1595.

64. M.R. Baer; "Aerodynamic Heating of High-Speed Flywheels in Low-Density Environments". Proc. 1978 Mechanical and Magnetic Energy Storage Contractors Review Meeting, p. 99.

65. J.J. Thompson; "A Note on Thermo-Elastic Stress in Axially Symmetric Anisotropic Cylinder". AAEC/E32, Aug. 1958.

66. T. Weng; "Thermal Stresses in Anisotropic Hollow Cylinders". J. Basic Engineering, Transaction of the ASME, Vol. 87, Series D, No. 2, p. 391.

67. D.B. Longcope, M.J. Forrestal and W.E. Warren; "Thermal Stresses in a Transversely Isotropic, Hollow, Circular Cylinder". AIAA Journal, Vol. 7, No. 11, p. 2174.

68. T.R. Tauchert; "Thermal Stresses in an Orthotropic Cylinder - Subject to a Radial, Steady-state Temperature Field". Southeastern Conference on Theoretical and Applied Mechanics, 7th Washington, D.C., March 21,22, 1974, Proc. Catholic University of America, p. 1.

69. R.L. Huddleston and B.R. Dewey; "Optimization of Elastic, Multilayer Cylindrical Vessel Loaded by Pressure and Radial Thermal Gradient". J. of Basic Engineering, ASME, pp. 885-892, Dec. 1972.

70. R.C. Reuter, Jr.; "Thermal Stresses in Composite Flywheels". 12th Annula Meeting, Society of Engineering Science, Austin, Texas, Oct. 1975.

71. R.C. Reuter, Jr.; "Fabrication and Thermal Stress in Composite Flywheels". 1975 Flywheel Technology Symposium, pp. 261-275.

72. C.T. Wang; "Applied Elasticity". McGraw-Hill Book Co., 1953, p.63.

73. S.G. Lekhnitskii; "Anisotropic Plates". Gordon and Beach Science Publishers, New York, 1968, pp. 152-3.

APPENDIX 'A'

FLYWHEEL DESIGN CONCEPTS

IDENTIFICATION

[REF. 1]

TABLE A-1: FLYWHEEL TERMINOLOGY IDENTIFICATION (Ref.1)

FLYWHEEL MANUFACTURER (Flywheel Name)	FLYWHEEL TYPE	FLYWHEEL NO. (See Table A-2&3)
Garrett AiResearch (In-house)	SINGLE MATERIAL MULTIRING ON RING 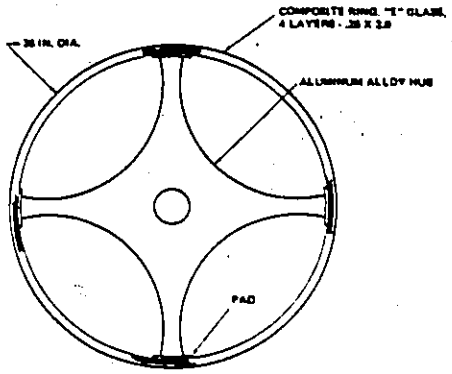 (Ref. 16)	1
Garrett AiResearch (Meradcom)	MULTIMATERIAL MULTIRING ON RING 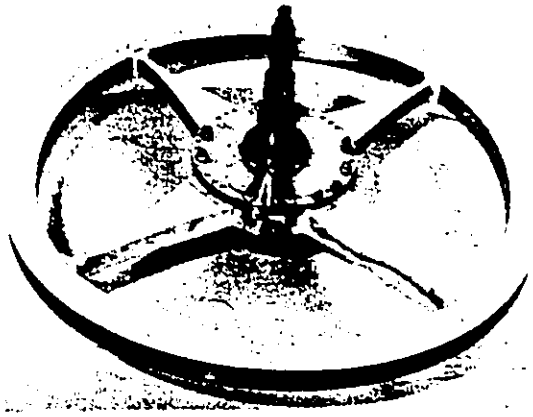 (Ref. 16)	2
Garrett AiResearch (High Energy Density)	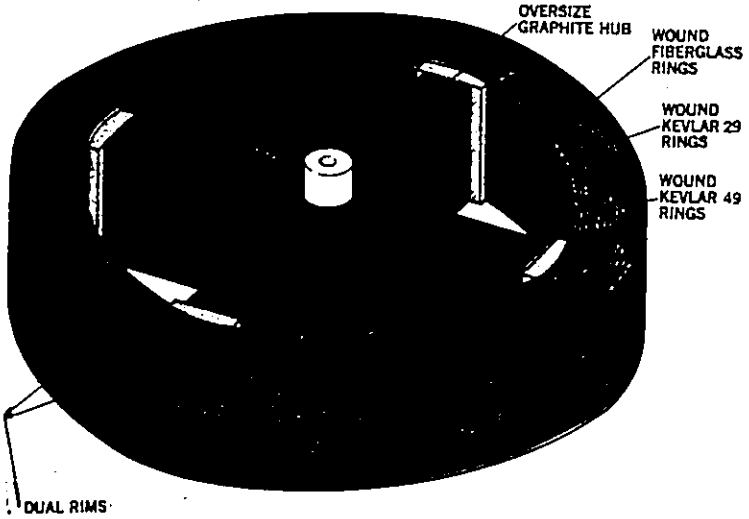 (Ref. 44)	4

FLYWHEEL MANUFACTURER (Flywheel Name)	FLYWHEEL TYPE	FLYWHEEL NO. (See Table A-2&3)
Garrett AiResearch (ESU)	 (Ref. 45)	5
Garrett AiResearch (UMTA Bus)	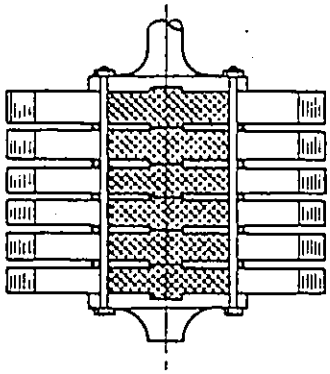 (Ref. 18)	6
Brobeck	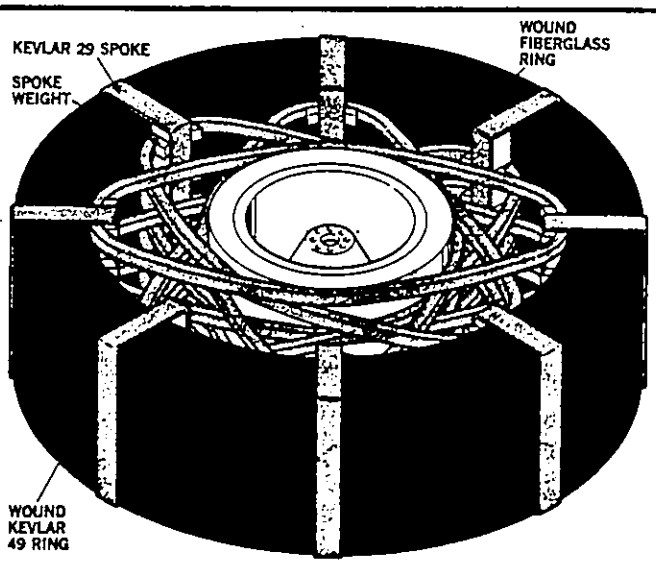 (Ref. 44)	7

FLYWHEEL MANUFACTURER (Flywheel Name)	FLYWHEEL TYPE	FLYWHEEL NO. (See Table A-2&3)
Hercules	WOUND DISK 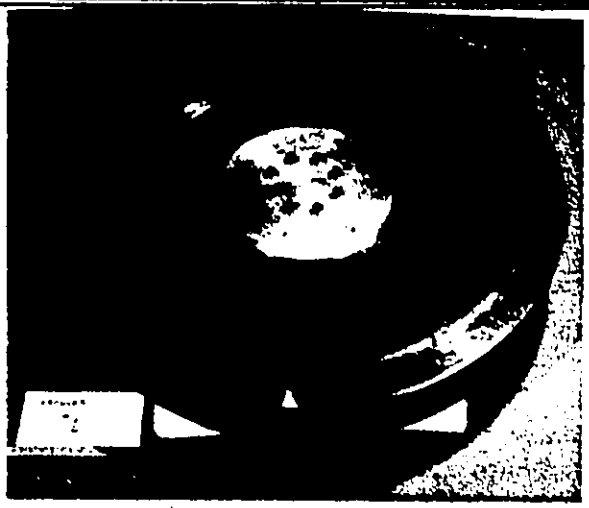 (Ref. 24)	8
	SINGLE/MULTIRING WITH OVERWRAP 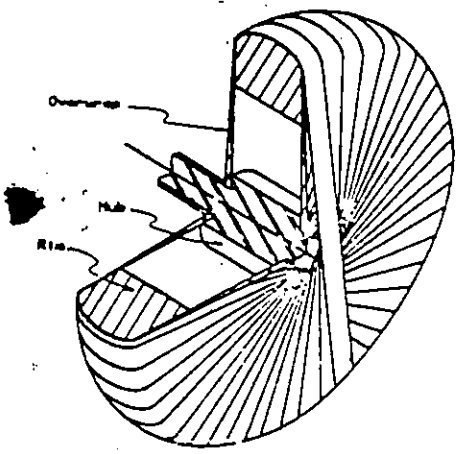 (Ref. 46)	
MAN	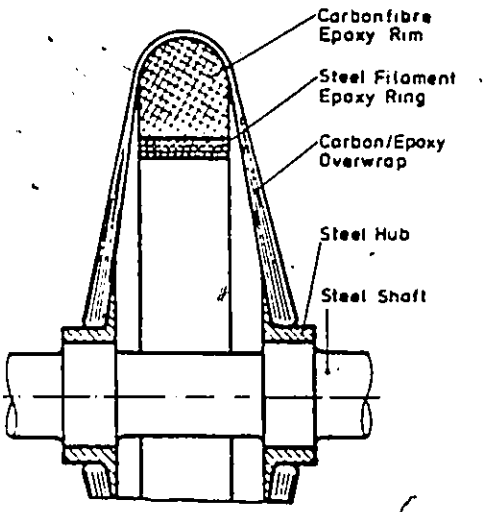 (Ref. 27)	10

FLYWHEEL MANUFACTURER (Flywheel Name)	FLYWHEEL TYPE	FLYWHEEL NO. (See Table A-2&3)
Rocketdyne (RPE-10)	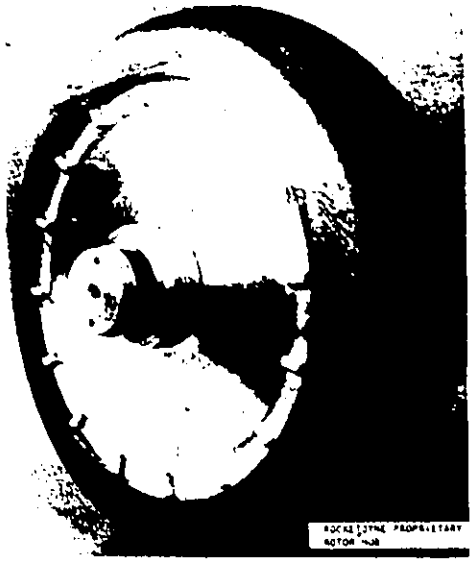 (Ref. 28)	11
Rocketdyne (In-house design)	TAPE WRAP 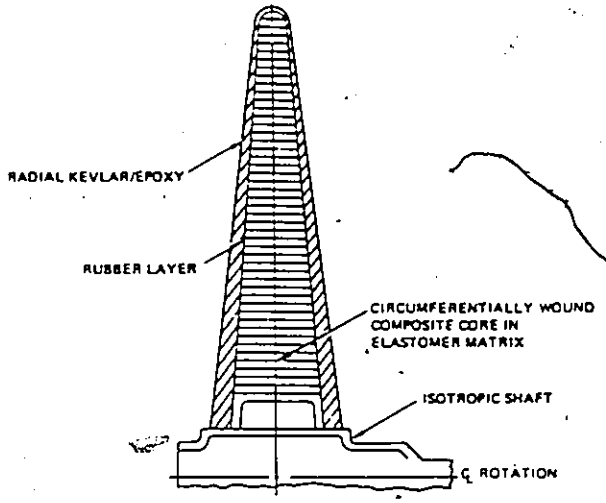 (Ref. 31)	12

FLYWHEEL MANUFACTURER (Flywheel Name)	FLYWHEEL TYPE	FLYWHEEL NO. (See Table A-2&3)
	THICK RIM WITH BANDWRAP	
Union Carbide	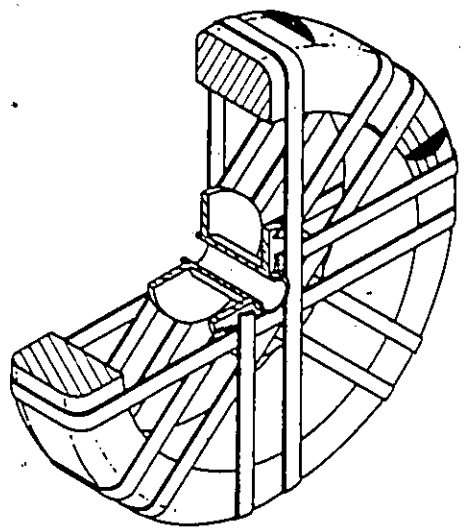 (Ref. 33)	14-18
Sandia Labs (Wagon wheel)	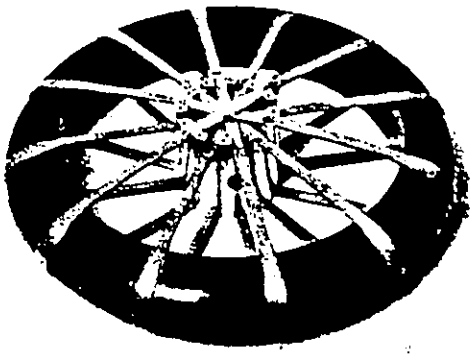 (Ref. 10)	19
Sandia Labs (Pinwrapped)	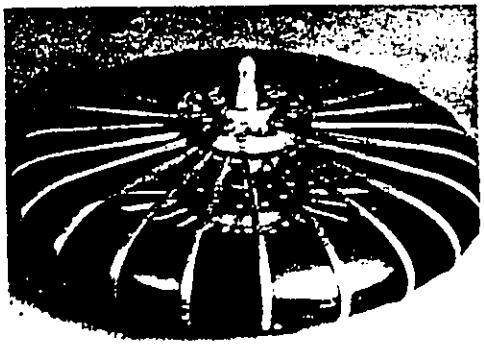 (Ref. 35)	20

FLYWHEEL MANUFACTURER (Flywheel Name)	FLYWHEEL TYPE	FLYWHEEL NO. (See Table A-2&3)
LLL (Tapered disk)	LAMINATED DISK 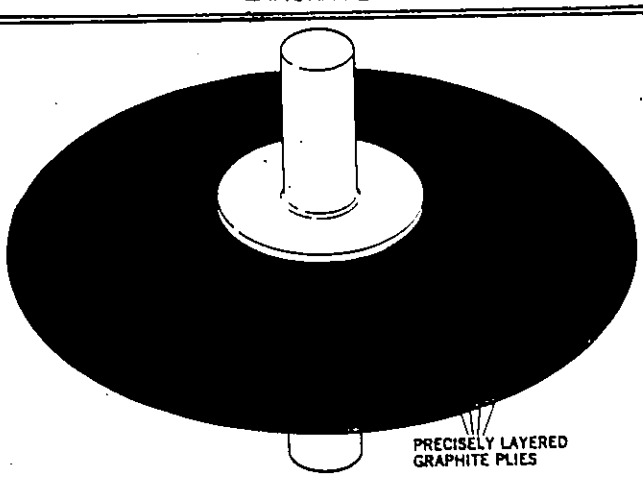 (Ref. 44)	21
General Electric (Constant thickness, bolted hub)	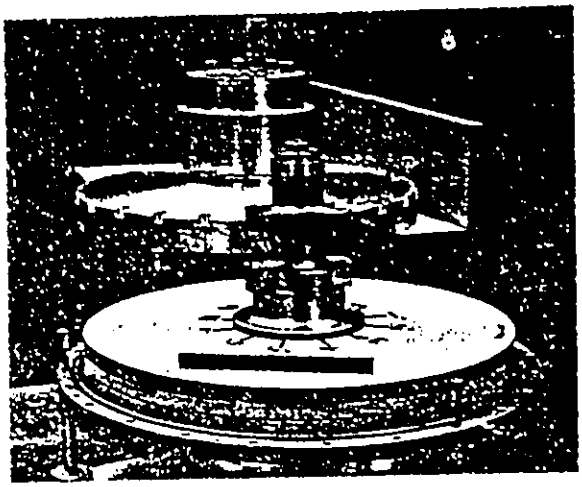 (Ref. 47)	22
LLL(GE) (Constant thickness, bonded hub)	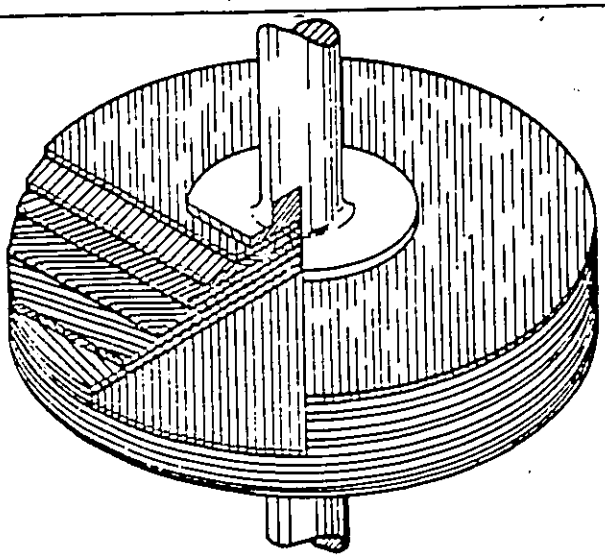 (Ref. 42)	23-31

FLYWHEEL MANUFACTURER (Flywheel Name)	FLYWHEEL TYPE	FLYWHEEL NO. (See Table A-2&3)
AVCO (Bidirectionally reinforced disk)	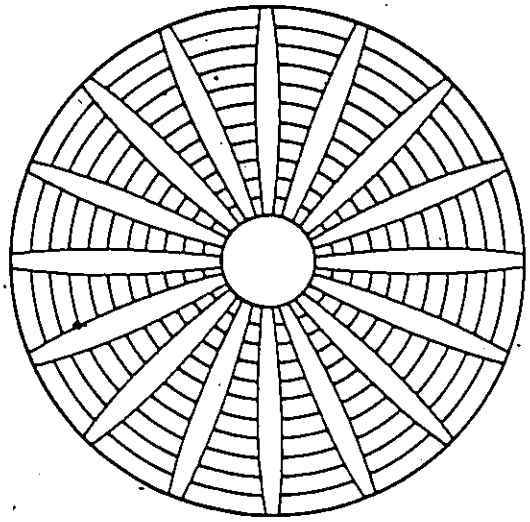 (Ref. 48)	32
General Electric	LAMINATED DISK/RIM 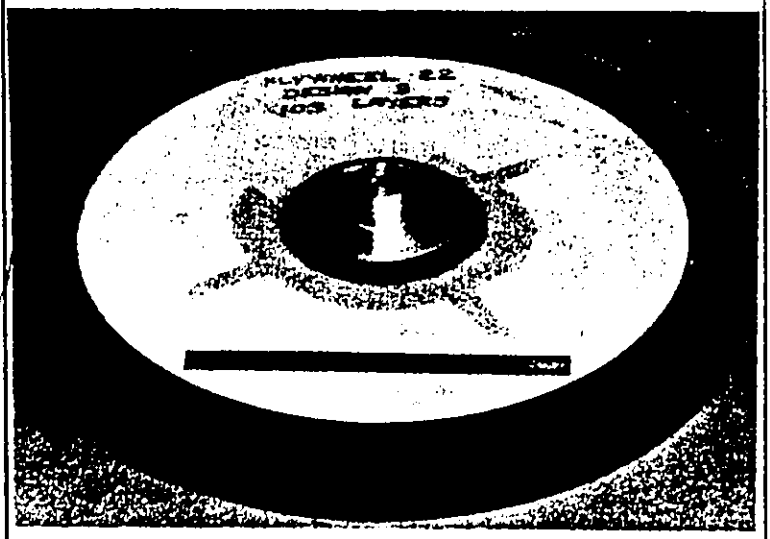 (Ref. 49)	33-35

FLYWHEEL MANUFACTURER (Flywheel Name)	FLYWHEEL TYPE	FLYWHEEL NO. (See Table A-2&3)
	BARE FILAMENT/TAPE	
APL (Steel wire)	 (Ref. 42)	36
APL (Vinyl-glass)	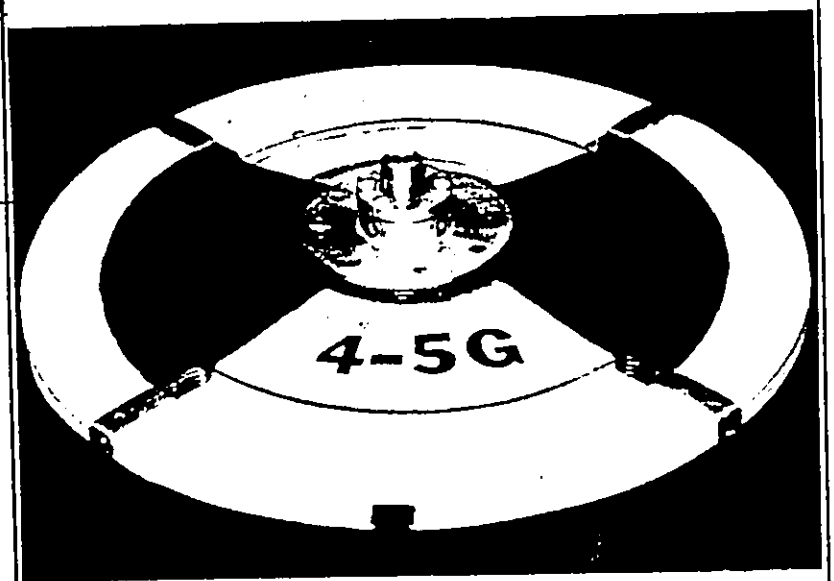 (Ref. 42)	37

FLYWHEEL MANUFACTURER (Flywheel Name)	FLYWHEEL TYPE	FLYWHEEL NO. (See Table A-2&3)
APL (Metglas)	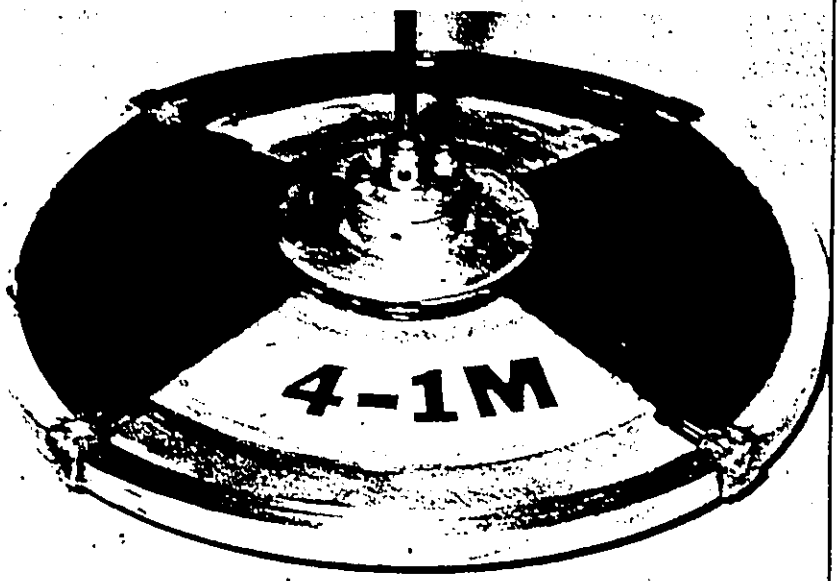 (Ref. 42)	39
APL (Kevlar)	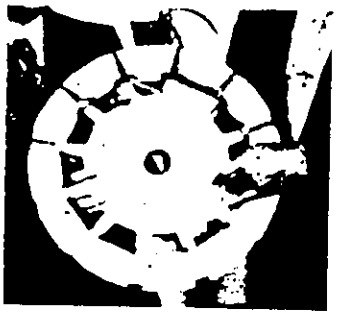 (Ref. 50)	40

TABLE A-2 (Ref. 1)

FLYWHEEL DESIGN DATA BASE

FLY-WHEEL NO.	BACKGROUND		DESIGN CONCEPT			FLYWHEEL DESIGN OBJECTIVE						REF.
	Flywheel Manufacturer (Flywheel Name)	Year Built	Design Description	Design Details	Manufacturing Details	Maximum Operating Speed (rpm)	Flywheel Mass (Kg)	Flywheel Size: Outside Diameter (cm)	Flywheel Size: Height (cm)	Energy Stored (Kw-hr)	Specific Energy (whr/Kg)	
SINGLE MATERIAL MULTIRING ON RING												
1.	Garrett AiResearch (In-house)	1974	Single material multiring	Rim - (4) 0.6 cm thick E glass rings Hub - 4 spoke aluminum	- wet filament winding - separator between rings - subcircular mount		10.4	66	5.1			1 16 17
2.	Garrett AiResearch (Meradcom)	1976	Single material multiring	Rim - (8) rings of Kevlar 49/epoxy Hub - 4 spoke aluminum	- wet filament winding - separator between rings - subcircular mount			107	3.8 (est.)	2.4		1 16 17 18
MULTIMATERIAL MULTIRING ON RING												
3.	Garrett AiResearch (Near Term Electric Vehicle)	1976	Multimaterial multiring	Rim - (1) S2 glass/epoxy ring (inner) (3) Kevlar 29/epoxy (5) Kevlar 49/epoxy Hub - 4 spoke aluminum	- wet filament winding - separate cure each ring with teflon sheet inserted between rings - subcircular mount	25,000	20.6 (Note 2)	58.5	10.7	1.00 @ 25,000 0.75 for 2:1 speed range	48.5	1 16 17 18
4.	Garrett AiResearch (High Energy Density)	1977	Multimaterial multiring	Rim - (2) rings S2/epoxy (inner) (5) rings Kevlar 29/epoxy (8) rings Kevlar 49/epoxy - all rings approx. 0.38 cm thick - dual rims Hub - multi-slat graphite /epoxy cruciform Shaft attachment - aluminum	- same as for Near Term Electric Vehicle (NTEV) - slat fabricated from prepreg - slats bonded together to form cruciform hub - sub circular mount - elastomeric bond to hub	30,000	16.7	58.7	10.9	1.43 kwh @ 30,000	86	1 17

Note 1: Actual mass of manufactured flywheel (unless otherwise noted).
Note 2: Calculated from Mass = Energy Stored ÷ Specific Energy.
Note 3: Conflicting data reported in the literature.

TABLE A-2

FLYWHEEL DESIGN DATA BASE

Fly-wheel No.	BACKGROUND		DESIGN CONCEPT			FLYWHEEL DESIGN OBJECTIVE						REF
	Flywheel Manufacturer (Flywheel Name)	Year Built	Design Description	Design Details	Manufacturing Details	Maximum Operating Speed (rpm)	Flywheel Mass (Kg)	Flywheel Size: Outside Diameter (cm)	Flywheel Size: Height (cm)	Energy Stored (Kw-hr)	Specific Energy (whr/Kg)	
5.	Garrett AiResearch (ESU)	1978	Multimaterial multiring	- same as HTEV	- same as HTEV	42,000	6.6	34.7	6.9	0.25 @ 42,000	37.9	1 17
6.	Garrett AiResearch (UMTA Bus)	1980	Multimaterial multiring	- (6) Meradcom type units attached together (See flywheel No. 2)		12,500	557	106.7	59	15.0 @ 12,500	37 (Note 3) 26.9 (Note 2)	1 17 18
7.	Broebeck	1979	Multimaterial multiring rim with tension balanced spokes	Rim - S2 glass/epoxy (inner), 4.9 cm thick - Kevlar 49/epoxy (outer), 5.6 cm thick Spokes - (16) individual Kevlar 29/epoxy Hub - aluminum with Kevlar 49/epoxy overwrap Loading weights - aluminum Spacers - balsa wood	- wet filament winding in 5 separately cured layers - wet filament wound - assembly in special fixture - Kevlar 49/ epoxy overwraps to hold weights and spacers in place	56,000	11.2	34.9	12.6	0.975 @ 56,000	87.1	1 61
WOUND DISC												
8.	Hercules, Inc.	1980	Contoured rim (wound disk)	Rim - AS carbon/polysulphone resin Hub - aluminum	- continuous winding from prepreg tape - elastomeric bonded to rim	32,620	20.3 (Note 3)	58.8	2.5(hub) 7.3 (outer rim)	1.270 total @ 32,620	62.5	1 25
SINGLE/MULTIRING WITH OVERWRAP												
9.	Aerospatiale	1977	Thick rim with cyclo-profile overwrap	Rim - carbon/epoxy Overwrap - cycloprofile of Kevlar/epoxy Hub - aluminum	- wet filament winding - wet wound		10.5	35	21 (at hub)	0.042 @ 24,000 0.022 available	4.0 (Note 2)	26

Note 1: Actual mass of manufactured flywheel (unless otherwise noted).
Note 2: Calculated From Mass = Energy Stored ÷ Specific Energy.
Note 3: Conflicting data reported in the literature.

TABLE A-2

FLYWHEEL DESIGN DATA BASE

Fly-wheel No.	BACKGROUND: Flywheel Manufacturer (Flywheel Name)	BACKGROUND: Year Built	DESIGN CONCEPT: Design Description	DESIGN CONCEPT: Design Details	DESIGN CONCEPT: Manufacturing Details	FLYWHEEL DESIGN OBJECTIVE: Maximum Operating Speed (rpm)	FLYWHEEL DESIGN OBJECTIVE: Flywheel Mass (Kg)	FLYWHEEL DESIGN OBJECTIVE: Flywheel Size: Outside Diameter (cm)	FLYWHEEL DESIGN OBJECTIVE: Flywheel Size: Height (cm)	FLYWHEEL DESIGN OBJECTIVE: Energy Stored (Kw-hr)	FLYWHEEL DESIGN OBJECTIVE: Specific Energy (whr/Kg)	REF.
10.	MAN, Germany	1980	Multiring multimaterial with overwrap	Rim - outer, carbon/ epoxy - inner, steel wire/ epoxy	- wet filament wound in 7 mm thick layers and are cured individually	28,500	32	52	6(est)	0.750 @ 28,500	23.5	27
				Hub - steel, integral with shaft	- inner and outer ring press fitted together							
				Overwrap - 3 separate layers of carbon/epoxy								
11.	Rocketdyne (RPE-10)	1980	Overwrapped multiring multimaterial with Twin-Disk hub	Rim - 17 rings, AS carbon (inner), HTS carbon (outer)	- wet wound on aluminum ring - prestress varied from ring to ring	22,000	54 (Note 2)	72(est)	25(est)	1.79 @ 22,000	33.2	1 28 29
				Overwrap - carbon/ epoxy, 5 layers, each 0.08 cm thick	- wet winding of 5 star pattern							
				Hub - aluminum, 2 disks (constant stress)	- aluminum ring attached to disks with 32 radial pins	32,500 (burst)				3.91 @ 32,500	72.5	
	TAPE WRAP											
12.	Rocketdyne Division, Rockwell International (In-house design)	1975	Tapered circumferential wound core with tape wrap	Hub - aluminum Core - E glass/epoxy	- wet wound on hub	12,300		45.6	8(est)		6.6	30
					- rubber layer applied							
				Tape wrap - Kevlar 49/ epoxy	- wet wound	18,000 (burst)					14.3	
13.	Rocketdyne (IPACS)	1977	Tapered circumferential wound core with tape wrap	Hub - aluminum		35,000	24 (Note 2) 27.3 (Note 3)	68.5 (est)	13(est) at hub	1.48 @ 35,000	61.7	31 29 30
				Core - Kevlar/nitrile circumferentially wrapped	- wet wound in 6 rings (reduced tension) on hub							
					- nitrile rubber interface							
				Wrap - Kevlar 49/Dow 332 resin	- 9 layers of roving @ 1.4 kg tension							

Note 1: Actual mass of manufactured flywheel (unless otherwise noted).
Note 2: Calculated From Mass = Energy Stored ÷ Specific Energy.
Note 3: Conflicting data reported in the literature.

TABLE A-2
FLYWHEEL DESIGN DATA BASE

Fly-Wheel No.	BACKGROUND: Flywheel Manufacturer (Flywheel Name)	BACKGROUND: Year Built	DESIGN CONCEPT: Design Description	DESIGN CONCEPT: Design-Details	DESIGN CONCEPT: Manufacturing Details	FLYWHEEL DESIGN OBJECTIVE: Maximum Operating Speed (rpm)	FLYWHEEL DESIGN OBJECTIVE: Flywheel Mass (Kg) [1]	FLYWHEEL DESIGN OBJECTIVE: Flywheel Size: Outside Diameter (cm)	FLYWHEEL DESIGN OBJECTIVE: Flywheel Size: Height (cm)	FLYWHEEL DESIGN OBJECTIVE: Energy Stored (Kw-hr)	FLYWHEEL DESIGN OBJECTIVE: Specific Energy (whr/Kg)	REF.
THICK RIM WITH BAND WRAP												
14.	Union Carbide (UCCMD-1)	1976	Thick rim with band wraps	Rim - Kevlar 49/epoxy	- wet filament winding - edges machined	40,000	12.7 (Note 2) 11.2	50.0	10.0	1.12 @ 40,000	88	1 32
				Bandwraps - Kevlar 49/epoxy Hub - aluminum	- wet filament winding of bandwraps for rim to hub attachment							
15.	Union Carbide (UCCMD-2)	1977	Thick rim with band wraps	Rim - Kevlar 49/epoxy, (10) rings (individual prestress), catenary outer radius	- wet winding (3 weeks)	35,100	7.1 (Note 2)	50.0	10.0	0.50 @ 35,100	- 88	1 13 33
				Bandwraps, Hub } as above No.14	- as above No. 14							
16.	Union Carbide (UCCMD-3)	1978	Thick rim with band wraps	Rim - outer half Kevlar 49/epoxy - inner half Kevlar 29/epoxy - equal thicknesses	- wet winding	38,600 (est.)	7.1	50.0	10.0	0.63 @ 38,600 (est.)	- 88	1
				Bandwraps, Hub } as above No.14	- as above No. 14							
17.	Union Carbide (UCCMD-4)	1978	Thick rim with band wraps	As above No. 16	- as above No. 14	38,600 (est.)	7.1	50.0	10.0	0.63 @ 38,600 (est.)	- 88	1
18.	Union Carbide (UCCMD-5)	1978	Thick rim with band wraps	As above except Kevlar 29/epoxy bandwraps(No.16)	- as above No. 14			50.0	10.0		- 88	1
19.	Sandia Labs (Wagon wheel)	1978	Thick rim with band wraps	Rim - semi - elliptical - 3617 denier Thornel 300 graphite/epoxy	- wet filament winding at 1.8 kg tension	31,000	11.4	50.8	15.2	0.56 @ 31,000 0.50 available for 3:1 speed reduction	49	10 35
				Overwraps - 4560 denier Kevlar 49/epoxy	- wet wound							
				Hub - aluminum								
20.	Sandia Labs (Pinwrapped)	1978	Thick rim with band wraps	Rim - AS graphite/epoxy	- wet filament winding	31,000	11.4	50.8	15.2	0.56 @ 31,000 0.50 available with 3:1 speed reduction 0.90 @ 40,000	49	10 35
				Spokes - (24), wrapped around pins on hub, Kevlar 49/epoxy	- wet filament winding							
				Hub - aluminum								

Note 1: Actual mass of manufactured flywheel (unless otherwise noted).
Note 2: Calculated From Mass = Energy Stored ÷ Specific Energy
Note 3: Conflicting data reported in the literature.

TABLE A-2

FLYWHEEL DESIGN DATA BASE

Fly-Wheel No.	BACKGROUND: Flywheel Manufacturer (Flywheel Name)	BACKGROUND: Year Built	DESIGN CONCEPT: Design Description	DESIGN CONCEPT: Design Details	DESIGN CONCEPT: Manufacturing Details	FLYWHEEL DESIGN OBJECTIVE: Maximum Operating Speed (rpm)	FLYWHEEL DESIGN OBJECTIVE: Flywheel Mass (Kg) [1]	FLYWHEEL DESIGN OBJECTIVE: Flywheel Size: Outside Diameter (cm)	FLYWHEEL DESIGN OBJECTIVE: Flywheel Size: Height (cm)	FLYWHEEL DESIGN OBJECTIVE: Energy Stored (Kw-hr)	FLYWHEEL DESIGN OBJECTIVE: Specific Energy (whr/Kg)	REF.
LAMINATED DISK												
21.	LLL	1977	Tapered thickness laminated disk	Disk - 160 layers of Narmco 5213 with Celion 6000 graphite fibres (0/±45/±90) Hub - aluminum	- vacuum bag and press moulding - contour machined - elastomeric bond	50,000 (burst)	5.2	61	2.5 (hub)	0.625 @ 50,000	120	28 52 53
22.	General Electric	1977	Constant thickness laminated disk	Disk - Alpha 3 cross ply of Scotch ply 1002 (E glass/polyester) prepreg to thickness of 2.5 cm Ring - circumferential, 1 cm thick, of Kevlar 49 type 326 tape Hub - bolted through disk	- vacuum bag and press moulding - three 2.5 cm thick x 76 cm dia. disks epoxied together - machined diameter to 74 cm - 1.25 cm diameter hole at centre - (6) 1.5 cm diameter hole on 20.3 cm diameter bolt circle	15,000	60	76	7.6	1.3 @ 15,000;1.0 for 15,000 to 7,500 rpm spin down	21.7	47 54
	LLL(GE)	1978, 1979	Constant thickness laminated disk	Disk - graphite/epoxy (Celion 6000 - Narmco 5213) prepreg Hub - aluminum	- vacuum bag and press moulding - elastomeric bonded							39 55 56
23.				(a) 0/±45/90		53,500	0.92	31	0.72	0.048 @ 53,500	52.5	
24.				(b) 0/±45/90		48,800	1.106	34	0.72	0.058 @ 48,800 (Note 2)	52.5	
25.	LLL(GE)	1978, 1979	Constant thickness laminated disk	Disks - S2 glass/epoxy (0/90/30/-60/60/-30) Hub - aluminum	- vacuum bag and press moulding - elastomeric bonded		2.88	40	1.16			39

Note 1: Actual mass of manufactured flywheel (unless otherwise noted.)

Note 2: Calculated From Mass = Energy Stored ÷ Specific Energy.

TABLE A-2

FLYWHEEL DESIGN DATA BASE

Fly-Wheel No.	BACKGROUND: Flywheel Manufacturer (Flywheel Name)	BACKGROUND: Year Built	DESIGN CONCEPT: Design Description	DESIGN CONCEPT: Design Details	DESIGN CONCEPT: Manufacturing Details	FLYWHEEL DESIGN OBJECTIVE: Maximum Operating Speed (rpm)	FLYWHEEL DESIGN OBJECTIVE: Flywheel Mass (Kg)	FLYWHEEL DESIGN OBJECTIVE: Flywheel Size: Outside Diameter (cm)	FLYWHEEL DESIGN OBJECTIVE: Flywheel Size: Height (cm)	FLYWHEEL DESIGN OBJECTIVE: Energy Stored (Kw-hr)	FLYWHEEL DESIGN OBJECTIVE: Specific Energy (whr/Kg)	REF.
	General Electric	1978	Constant thickness laminated disk	Disk - S2/epoxy prepreg. Hub - aluminum	- hydroclave - elastomeric bonded							39 55
26.				(a) 0/-45/45/90			1.79	22.4	2.41	0.094	53	
27.				(b) 0/-45/45/90			1.81	22.4	2.54	0.096	53	
28.				(c) α - 9			1.58	22.4	2.14	0.084	53	
29.				(d) α - 9			1.58	22.4	2.15	0.084	53	
30.				(e) α - 9			3.2	28.5	2.69	0.170	53	
31.	LLL	1980	Constant thickness laminated disk	Disk - S2 glass/epoxy prepreg. Hub - aluminum	- vacuum bag and press moulding - elastomeric bonded			38.1				1
32.	AVCO	1978	Bidirectionally reinforced, constant thickness disk	- stacked sequence of 0.043 cm thick hoop layers(Kevlar 49),hoop layers alternating with radial layers of (144) 0.016 cm thick Kevlar 49 tapered members Hub - segmented steel spider			8.45	49.5	3.8			48 56 57 58
LAMINATED DISK/RIM												
33. and 34.	General Electric	1979	Laminated disk with rim	Disk - S2 glass/epoxy α ply construction (3HSP-252 prepreg.) Rim - graphite (Thornel 300)/epoxy Hub - aluminum	- hydroclave - wet filament winding - rim press fitted to disk - Lord elastomeric bond	Disk 1 46,000 (approx) Disk 2 46,000 (approx)		37.0 38.4	2.5 2.5		54 54	1 40

Note 1: Actual mass of manufactured flywheel (unless otherwise noted).

TABLE A-2

FLYWHEEL DESIGN DATA BASE

Fly-Wheel No.	BACKGROUND		DESIGN CONCEPT			FLYWHEEL DESIGN OBJECTIVE						REF.
	Flywheel Manufacturer (Flywheel Name)	Year Built	Design Description	Design Details	Manufacturing Details	Maximum Operating Speed (rpm)	Flywheel Mass (Kg)	Flywheel Size: Outside Diameter (cm)	Flywheel Size: Height (cm)	Energy Stored (Kw-hr)	Specific Energy (whr/Kg)	
35.	General Electric	1980	Laminated disk with rim	Disk - as above #33, 34 Rim - graphite (Thornel 300)/epoxy Hub - aluminum	- wet filament winding - rim press fitted to disk - Lord elastomeric bond	46,000		45	2.5			1
BARE FILAMENT/TAPE												
36.	APL	1980	Bare steel wire flywheel	- 0.03 cm dia steel wire Hub - plywood	- continuously wound - (4) radial wraps for fibre to hub attachment							1 42 59
37.	APL	1980	Vinyl-glass flywheel	- 50/50 vinyl coated E glass fibre Hub - plywood	- continuously wound - (4) radial wraps for fibre to hub attachment							1 42 59
38.	APL	1980	Polymer-glass flywheel	- 10/90 polymer coated E glass fibre Hub - plywood	- continuously wound - (4) radial wraps for fibre to hub attachment							1 42 59
39.	APL	1980	Metglas flywheel	- 1.25 cm wide x 0.08 cm thick ribbon Hub - plywood	- continuously wound - (4) radial wraps for fibre to hub attachment							1 42 59
40.	APL	1978	Kevlar flywheel	- Kevlar 49 fibre Hub-12-spoked aluminum	- continuously wound -(12) radial wraps for fibre to hub attachment							1 50

TABLE A-3 (Ref. 1)

FLYWHEEL PERFORMANCE DATA BASE

FLY-WHEEL NO.	BACKGROUND: Flywheel Manufacturer (Flywheel Name)	BACKGROUND: Year Tested	FLYWHEEL TEST PROGRAM	FLYWHEEL PERFORMANCE DATA: Failure Mode	Failure (or Maximum) Speed (rpm)	Stored Energy (Kwhr)	Specific Energy @ Failure Speed (whr/Kg)	Specific Energy % of Design	COMMENTS	REF
SINGLE MATERIAL MULTIRING OR RING										
1.	Garrett AiResearch (In-house)	1974	- quill shaft - AiResearch facilities - non-destructive		17,000	0.20	19.3		- no signs of deterioration	1 16 17
2.	Garrett AiResearch (MERADCOM)	1976	- straddle mtd., ball bearings - AiResearch facilities - non-destructive		15,000	2.04	46 (Note 1)	85	- no signs of deterioration	1 16 17 18
MULTI MATERIAL MULTIRING OR RING										
3.	Garrett AiResearch (Near Term Electric Vehicle)	1976	- Flywheel No. 1 - AiResearch facilities - rigid mounting in final ass'y - air introduced	- outer 3 rings disintegrated and jammed between remainder of flywheel and outer housing - stopped in 2 seconds	25,280	0.91	44	91	- housing temperature increased gradually to 175°F	1 16 17 18
			- Flywheel No. 2 - AiResearch facilities - rigid mounting in final ass'y - 1000 cycles between 25,000 and 13,000 rpm	- separation between S2 glass and Kevlar 29 rings					- no spin burst test conducted	
4.	Garrett AiResearch (High Energy Density)	1980	- quill shaft - ORFEL facilities - burst test	- rim lifted off 2 spokes (opposite) - rims migrated in opposite directions - rim spun around in bottom of chamber, outer 2 rings only removed, remainder of rim intact - carbon pieces pierced 0.6 cm thick aluminum crash ring in 2 places	27,780	1.25	75	87	- Failure actually occurred @ 23,400 rpm as flywheel was being slowed down.	1 28
5.	Garrett AiResearch (ESU)	1979	- rigid mount in complete assembly - AiResearch facilities - 100 cycles between 0 and 42,000 rpm @ 250°F	- no degradation of unit					- no spin burst test conducted	1 60
6.	Garrett AiResearch (UMTA)	1980							- not tested as yet	1

Note 1: Conflicting data reported in the literature.

TABLE A-3

FLYWHEEL PERFORMANCE DATA BASE

FLY-WHEEL NO.	BACKGROUND: Flywheel Manufacturer (Flywheel Name)	BACKGROUND: Year Tested	FLYWHEEL TEST PROGRAM	FLYWHEEL PERFORMANCE DATA: Failure Mode	Failure (or Maximum) Speed (rpm)	Stored Energy (Kwhr)	Specific Energy @ Failure Speed (whr/Kg)	Specific Energy % of Design	COMMENTS	REF.
7.	Broebeck	1980	- quill shaft - ORFEL facility - burst test	- Kevlar 49 overwraps bowed into cantenary shape and most failed - spokes slipped as predicted by modal analysis - according to Broebeck, failure was due to underdesigned hub - one half of rim was intack after test, remainder was fibrous	30,000	0.29	25.4	29		1 28 51
WOUND DISK										
8.	Hercules, Inc.	1980	- quill shaft - ORFEL facility - burst test	- circumferential cracks developed, test stopped - post test inspection revealed finger size pieces missing from outer surface, no unbalance developed	22,320	0.76	37.4	60		1 28
SINGLE/MULTI RING WITH OVERWRAP										
9.	Aerospatiale								- test data not available	
10.	MAN	1980	- quill shaft - burst test	- increasing imbalance, stopped test at 22,000 - believed due to creep in bonding of hub and overwrap	22,000	0.45	14	60	- burst speed; 35,000 (predicted)	27
11.	Rocketdyne (RPE-10)	1980	- quill shaft - ORFEL facility - non destructive	- one aluminum disk shifted with respect to other disk @ 22,920 rpm	22,920	1.94	36		- will be tested on dual bearing mount late 1980 - capacity of ORFEL facility was 2 Kw-hr	1 28
TAPE WRAP										
12.	Rocketdyne (In-house design)	1975	- quill shaft - Rocketdyne facilities - burst test	- excessive vibration - quill shaft broke and rotor fell into pit - outer tip of flywheel failed	20,000		17.6	123		29
13.	Rocketdyne (IPACS)	1978	- dual bearing support - Rocketdyne facilities - non-destructive	- dynamic instability @ 10,000 - assumed to be eccentric shift in core - creep in core found					- similar to flywheel No. 12 - about 25% design objective achieved - concept discontinued	29
			- as above but quill shaft and burst test	- failure not specified	17,610					

TABLE A-3

FLYWHEEL PERFORMANCE DATA BASE

FLY-WHEEL NO.	BACKGROUND: Flywheel Manufacturer (Flywheel Name)	BACKGROUND: Year Tested	FLYWHEEL TEST PROGRAM	FLYWHEEL FAILURE DATA: Failure Mode	Failure (or Maximum) Speed (rpm)	Stored Energy (Kwhr)	Specific Energy @ Failure Speed (whr/Kg)	Specific Energy % of Design	COMMENTS	REF.
THICK RIM WITH BAND WRAP										
14.	Union Carbide (UCCND-1)	1977	- quill shaft - ORFEL facility - burst test	- bowing of bandwraps at outer radius - rim delamination	18,000	0.25	22.2	25		1 32
15.	Union Carbide (UCCND-2)	1978	- as above	- band failure	27,000 (est.)	0.35 (est.)	49.3	56		1 13 33
16.	Union Carbide (UCCND-3)	1978	- as above	- band failure	26,220	0.3	42.2	48		1
17.	Union Carbide (UCCND-4)	1978	- as above - momentum transfer measured	- band failure - average torque of 150,000 ft-lb measured over 3.45 msec.	20,940	0.2	26.9	31		1 36
18.	Union Carbide (UCCND-5)	1978	- as above	- band failure - average torque of 5,000 ft-lb measured over 4-5 msec.			24.2	28		1 36
19.	Sandia Labs (Wagon Wheel)	1979	- quill shaft - Sandia facilities - burst test	No. 1 - runout increased with speed - loud noise, test stopped @ 17,000 rpm - lead balancing tape had blown off - post test radiograph found circumferential crack in rim No. 2 - runout again excessive - shaft broke @ 22,100 - one half of rim worn off, producing fine dust - remainder of rim intact - post test x-ray revealed numerous circumferential cracks in rim - spokes shredded	22,100	0.29	25.3	52	- fabricated by Brunswick Corporation	10 35

TABLE A-3

FLYWHEEL PERFORMANCE DATA BASE

FLY-WHEEL NO.	BACKGROUND: Flywheel Manufacturer (Flywheel Name)	BACKGROUND: Year Tested	FLYWHEEL TEST PROGRAM	FLYWHEEL FAILURE DATA: Failure Mode	Failure (or Maximum) Speed (rpm)	Stored Energy (Kwhr)	Specific Energy @ Failure Speed (whr/Kg)	Specific Energy % of Design	COMMENTS	REF.
20.	Sandia Labs (Pinwrapped)	1979	- quill shaft - Sandia facilities - burst test	No. 1 - excessive runout - vacuum lost at 29,000 rpm No. 2 - excessive runout - shaft broke @ 30,100 rpm - rim spun around in bottom of tank removing only 0.25 cm - no voids or fractures found in rim	30,100	0.532 @ 30,100	42 (Note 1)	95 (Note 1)	- fabricated by Hercules, Inc.	10 35
LAMINATED DISK										
21.	LLL	1977	- quill shaft - APL facilities - burst test	- catastrophic, fracture initiated near centre - 12 large sections - hub not damaged - 2 inner steel containment rings severely damaged	36,000	0.325	62.6	52	- fabricated by Babcock & Wilcox, quality was questioned	52 28 53
22.	General Electric	1977	- quill shaft - GE facilities - burst test	- catastrophic - large pieces	14,200	1.17	19.3	90	- post test analysis revealed large air voids	47 54
23.	LLL (GE)	1978 1979	- quill shaft - GE facilities - burst	- shaft failure, large sections of composite	44,500	0.033	36.3	70		39 55 56
24.	LLL (GE)	1978 1979	- quill shaft - GE facilities - nondestructive		35,000	0.030	27.4	52		39 55 56
			- burst	- catastrophic failure, large sections of composite	48,200 (Note 1)	0.057	51.5	98		
25.	LLL (GE)	1978 1979	- non-destructive		30,100	0.081	28.24			39

Note 1: Conflicting data reported in the literature.

TABLE A-3

FLYWHEEL PERFORMANCE DATA BASE

FLY-WHEEL NO.	BACKGROUND: Flywheel Manufacturer (Flywheel Name)	BACKGROUND: Year Tested	FLYWHEEL TEST PROGRAM	FLYWHEEL FAILURE DATA: Failure Mode	Failure (or Maximum) Speed (rpm)	Stored Energy (Kwhr)	Specific Energy @ Failure Speed (whr/Kg)	Specific Energy % of Design	COMMENTS	REF.
	General Electric	1978 1979	- quill shaft - GE facilities - burst test							39 55
26.			- Disk (a)	- catastrophic, fibrous debris	65,000	0.072	40.1	76		
27.			(b)	- large orbit prior to failure	37,500	0.024	13.4	25		
28.			(c)	- fibrous debris	58,000	0.050	31.9	60		
29.			(d)	- turbine bearing seized	53,000	0.042	26.6	50		
30.			(e)	- large shaft orbit prior to failure	49,000	0.119	37.2	70		
31	LLL	1980	- quill shaft - APL facility - burst test	- catastrophic - 1.25 cm deep crease in 1.25 cm thick steel containment ring	50,000		66.4			1
32	AVCO	1979	- quill shaft - U.S. Army facility - burst test	- reduction in speed at failure, believed to be from inside to outside - benign failure	38,000	0.6	71			48 57 58
LAMINATED DISK/RIM										
33. and 34.	General Electric	1980	- quill shaft - GE facilities - burst test	Disk 1 - circumferential crack in graphite rim @ 33,000 rpm (no TV monitoring) - Close to 46,000 rpm measured 8g vertical accelerations on turbine shaft - @ 46,000 quill shaft pulled out of aluminum hub and flywheel spun to stop in bottom of tank - flywheel remained intact, circumferential crack still present	46,000 (approx.)		54	100	- during design graphite/epoxy transverse strength assumed to be 49 MPa - subsequent coupon tests after manufacture found strength to be 22 MPa	1 27
				Disk 2 - again circumferential crack at 33,000 rpm, monitored on TV and pressure rise in chamber recorded. - same events at 46,000 as in Disk 1 above except elastomeric bond failed - flywheel intact with circumferential crack visible	46,000 (approx.)		57.2	106		

TABLE A-3

FLYWHEEL PERFORMANCE DATA BASE

FLY-WHEEL NO.	BACKGROUND: Flywheel Manufacturer (Flywheel Name)	BACKGROUND: Year Tested	FLYWHEEL TEST PROGRAM	FLYWHEEL FAILURE DATA: Failure Mode	Failure (or Maximum) Speed (rpm)	Stored Energy (Kwhr)	Specific Energy @ Failure Speed (whr/Kg)	Specific Energy % of Design	COMMENTS	REF.
35.	General Electric	1980	- quill shaft - ORFEL facilities - burst test						- flywheel designed with thinner graphite outer ring, more catastrophic failure expected @ 46,000 rpm - maximum speed of 28,000 to date - relative motion between hub and disk	1
BARE FILAMENT/TAPE										
36.	APL (Steel wire)	1980	- quill shaft - APL facilities - burst test	- tangled mass - large proportion of unfailed wire - failed particles were small - no damage to containment			29		NOTE: In the past few years APL has tested over 100 bare filament or tape flywheels. The specific energies listed represent those highest obtained as of November, 1980.	1 42 59
37.	APL (Vinyl-glass)	1980	- quill shaft - APL facilities - burst test	- bulk of glass fibres not broken - failed fibre, extremely small particles - no damage to containment			33			
38.	APL (Polymer-glass)	1980	- quill shaft - APL facilities - burst test	- bulk of glass fibres not broken - failed fibre, extremely small particles - no damage to containment			44			
39.	APL (Metglas)	1980	- quill shaft - APL facilities - burst test	- all failed particles on the order of 5-10 cm long - no damage to containment			33			
40.	APL	1978	- quill shaft - APL facilities - burst test	- tangled mass with no structural integrity			90			1 50

APPENDIX 'B'

FLYWHEEL TECHNOLOGY ASSESSMENT

[REF. 1]

TABLE B-1: MAJOR IMPACT PARAMETERS

For the road vehicle transportation application, in the process of flywheel assessment and identification, the major impact parameters were established [1] as follows:

i)	Safety	Failure mode
		Ease of Containment
		Prefailure Indicators
ii)	Geometry	Geometric Compatibility
		Weight Compatibility
		Flywheel Stability
		Effective Shape Factor
iii)	Cost	Material Cost
		Manufacture Cost
		Industrial Implementation
		Quality Control/Inspection
iv)	Technology	State-of-the-Art
		Technology Level Required
		Technical Risk

TABLE B-2

RATING CRITERION (Ref.1)

1. Each 'Flywheel Design Concept' is numerically rated on a relative basis from '0-10' for each 'Impact Parameter' according to the following guide:

PARAMETER / VALUE	0-2	3-4	5-6	7-8	9-10
Failure Mode	V.Poor	Poor	Average	Good	V.Good
Ease of Containment	V.Hard	Hard	Average	Easy	V.Easy
Pre-failure Indicators	No	-	Possible	-	Yes
Geometric Compatibility	V.Poor	Poor	Average	Good	V.Good
Weight Compatibility	V.Poor	Poor	Average	Good	V.Good
Flywheel Stability	V.Poor	Poor	Average	Good	V.Good
Effective Shape Factor	V.Poor	Poor	Average	Good	V.Good
Material Cost	V.High	High	Average	Low	V.Low
Manufacture Cost	V.High	High	Average	Low	V.Low
Industrial Implementation	V.Hard	Hard	Average	Easy	V.Easy
Q.C./Inspection	V.Hard	Hard	Average	Easy	V.Easy
State of the Art	V.Low	Low	Average	High	V.High
Technology Required	V.High	High	Average	Low	V.Low
Technical Risk	V.High	High	Average	Low	V.Low

2. Each 'Impact Parameter' is assigned a weight between '0-120' dependendent on its' perceived importance relative to the road vehicle application. The impact parameter 'score' equals the numerical rating received times the weight factor.

3. Any flywheel design concept receiving a '0' rating in any category is judged unsatisfactory for the application and will be a basis for elimination.

4. Each of the four major rating criteria viz; safety, geometry, cost and technology carry equal total weight (200 points) in the assessment. Thus:

   (a) Maximum possible score is 8000 points.
   (b) Average score is 4000-4800 points.
   (c) Design concepts scoring less than 4000 will be eliminated.

TABLE B-3

TECHNOLOGY SUMMARY OF

FLYWHEEL DESIGN CONCEPT - MAJOR ENERGY STORAGE UNIT (Ref.1)

FLY-WHEEL CODE	FLYWHEEL DESIGN CONCEPT	TYPICAL FLYWHEEL [1]		MANUFACTURING COST, DEVELOPMENT AND TECHNOLOGY LEVELS [1]	CRITICAL ELEMENTS [2]	SAFETY FACTORS [3]	EFFECTIVE SHAPE FACTOR [4]	VEHICLE COMPATIBILITY [5]
		Manufacturer	Flywheel Number					
A	Single Material (i) Thin ring (ii) Thick ring	LLL/Garrett	Ref.	The thin ring design is well established with low technology and capital cost requirements. Thick ring designs require high technology-very thick rings require a design or materials breakthrough re radial failure, i.e. high to very high technical risk. Overwrap is low to average development, high technology and capital costs.	- Ring/hub attach. - Swept volume	- Thin ring yields a gross rotor failure, not prone to containment protrusion. - Thick ring may be designed for radial failure, perhaps benign with pre-failure unbalance. Requires much R&D . - Overwrap not signicantly different.	- Excellent for thin rings. Full utilization of material strength. Low material costs. - Poor to very poor for thick rings with current technology re. radial stress capability and failure. High material costs.	- Thin ring volume requirements are excessive for transportation application. - With current technology, poor weight and volume potential for thick rings. Somewhat better with overwrap.
B	Single Material Ring with Overwrap or Bandwrap	Aerospatial Union Carb. Sandia	9 14,15 19,20		- Ring/hub attach. - Swept volume - Overwrap - Quality Control - Inspection			
C	Single Material Multi-Ring with Overwrap or Bandwrap			Single material multi-ring designs are not well developed. Ring on ring designs (bare or overwrapped) require R&D and extensive testing to determine the required prestress for ring compatibility. The inter-ring design requires very low modulus inter-wraps, is not developed and is judged difficult to assemble with questionable rotor dynamic stability and very high technical risk. Overwrap is low to average development. Technology level and costs judged average to high for ring-on-ring designs and very high for inter-ring designs and multi-ring with overwrap/bandwrap.	- Ring/hub attach. - Ring radial compatibility - Overwrap - Quality Control - Inspection	- Single material multi-rings lend to sequential failure from the outside ring inward. - Good failure mode in that only part of the rotor energy need be contained. Reasonably easy to contain, not prone to protrusion. - May result in lumping and hence high momentum transfer. (Note 6).	- Tangential stress patterns do not lend to efficient material usage. Outside ring will control rotor stress levels and hence material selection. Average to poor shape factors, high material costs. - Inter-wrap design somewhat worse in both shape factors and material costs	- Good, both physical size and weight can meet the transportation application.
D	Single Material Multi-Ring with Low-modulus Inter-Ring Wraps	None	None		- Ring/hub attach. - Inter-ring bond - Dynamic Stability - Assembly			- Average, both physical size and weight can meet the transportation application.
E	Single Material Multi-Ring-on-Ring	Garrett	1		- Ring/hub attach. - Ring radial compatibility - Quality Control			- Good, both physical size and weight can meet the transportation application.

Note: 1. See Table A-2 and A-3.

2. See Table A-2 and A-3; further (i) Ring/hub attachment by 'sub-circular' design - Garrett AiResearch Patent.
(ii) Ring/hub attachment by 'twin-disc' design - Rocketdyne Patent.
(iii) Shaft/disc attachment by 'bonded' design - Lord Kinematics Patent.

3. See Table A-2 and A-3.

4. A measure of energy density-more effectively interpreted as the efficiency of material usage and directly related to rotor design stress patterns.

5. Relative to the transportation application.

6. High momentum transfer may be a function of hub stability. Evidence exists that for stable hubs, lumping results in a controlled, hence desirable. 'braking' of the rotor.

TABLE B-3 - TECHNOLOGY SUMMARY OF

FLYWHEEL DESIGN CONCEPT - MAJOR ENERGY STORAGE UNIT

FLY-WHEEL CODE	FLYWHEEL DESIGN CONCEPT	TYPICAL FLYWHEEL 1		MANUFACTURING COST, DEVELOPMENT AND TECHNOLOGY LEVELS 1	CRITICAL ELEMENTS 2	SAFETY FACTORS 3	EFFECTIVE SHAPE FACTOR 4	VEHICLE COMPATIBILITY 5
		Manufacturer	Flywheel Number					
F	Multi-Material Multi-Ring with Overwrap or Bandwrap	MAN Rocketdyne Union Carb.	10 11 16,17,18	Average to high development level for ring-on-ring designs, average on overwrap designs and very low on inter-ring designs. Easier to achieve radial ring compatibility and desirable stress patterns/efficient use of material than single material designs. Technology levels and costs as in designs C, D and E, however, quality control should be somewhat easier due to the partial control of radial compatibility by material selection.	- Ring/hub attach. - Overwrap - Quality Control - Inspection	- Multi-material multi-rings tend to seqential failure of outermost ring of each material. Thus, internal failure of one ring can be designed for - may lead to benign failure mode. - Design for outer most ring failure, same as C, D and E.	- Good to very good. By appropriate choice of materials, a desirable stress distribution can be obtained with efficient material usage. Material costs average to low. - Inter-ring design somewhat higher cost, average shape.	- Good to very good in both physical size and weight.
G	Multi-Material Multi-Ring with Low Modulus Inter-Ring Wraps.	None	None		- Ring/hub attach. - Inter-ring bond - Dynamic Stability - Assembly			- Average to good in both physical size and weight.
H	Multi-Material Multi-Ring-on-Ring	Garrett Broebeck	2 to 6 7		- Ring/hub attach. - Quality Control			- Good to very good in both physical size and weight.
I	Shaped Central Core with Tape-wrap. (Note 7)	Rocketdyne	12,13	Average development level with high technology requirements to resolve the radial strength problems - likely require advanced design or new materials breakthrough. Moderately high cost. Overwrap as in 'A'	- New materials - Advanced design - Radial failure - Quality Control - Inspection	- Tend to radial circumferential failure and outside tip rupture. - Good failure mode. - Easy to contain.	- Depends dominantly on design. In principal, the multi-material, multi-ring core should be very good. Single material, poor, etc.	- Depends dominantly on design. Average to good geometrically, average to poor in weight.
J	Bare Filament/ Tapes	APL	36 to 40	Low development and average technology levels. Very questionable for the transportation application re. energy density, rotor stability and filament/tape alignment, requires considerable R&D/testing. Low cost potential. Very high technical risk.	- Rotor stability - Long term material alignment - Ring securement - Ring/hub attach. - Material availability. (Metglas, vinylglass) - Energy density	- Tend to be gross rotor failures, not prone to protrusion. - Average failure mode and containment.	- Similar to single material ring on ring. - Average to poor (very poor for wound disc design) shape factor, corcorresponding material cost.	- Metal tapes cannot meet weight requirements. - Material availability and flywheel stability are questionable for vehicle applications.
K	Wound Disc (Note 8)	Hercules	8	Very low development level with very high technology requirements to resolve radial strength problems - new resins required. Very high technical risk.	- New resin req'd - Radial failure	- Similar to rotor design 'I'.	- Very poor even with new resin break through. - High to very high material costs.	- In principal, average geometry, and very poor weight if design can be accomplished.

Note: 7. Central core must be continuous from the shaft and may be single or multi-ring, single or multi-material. Otherwise, the design is classified under design code 'B', 'C' or 'F'.

8. Disc must be continuously wound and may be contoured. Otherwise the design is classified under design code 'E' or 'H'.

TABLE B-3 - TECHNOLOGY SUMMARY OF

FLYWHEEL DESIGN CONCEPT - MAJOR ENERGY STORAGE UNIT

FLY-WHEEL CODE	FLYWHEEL DESIGN CONCEPT	TYPICAL FLYWHEEL [1] Manufacturer	TYPICAL FLYWHEEL [1] Flywheel Number	[1] MANUFACTURING COST, DEVELOPMENT AND TECHNOLOGY LEVELS	[2] CRITICAL ELEMENTS	[3] SAFETY FACTORS	[4] EFFECTIVE SHAPE FACTOR	[5] VEHICLE COMPATIBILITY
L	Laminated Disc	GE LLL(GE) LLL AVCO	22,26-30 23 to 25 31 32	Low to average development level. Promise of high energy storage requires very high technology and considerable R&D to realize. Quality control and inspection could be a problem and safety is a real problem. Manufacturing costs are high for disc, very high for shaped disc.	- Shaft attachment - Failure mode - Containment - Q.C./ Inspection	- Typically catastrophic failure, large chunks difficult to contain. Prone to protrusion and hence implosion/explosion.	- Average provided technology can be advanced to Q.I. material goals.	- In principal, good in volume, average to poor in weight.
M	Shaped Laminated Disc	LLL	21		- Shaft attachment - Failure mode - Containment - Cost - Machining - Q.C./Inspection		- Very good provided technology can be advanced.	- In principal, good to very good but diameter restrictions will be very difficult to meet.
N	Laminated Disc With Ring (Note 9)	GE	33 to 35	Similar to 'L' and 'M' but safety can be improved - will require extensive R&D and testing to establish. Very high technology levels and costs are required.	- Shaft attachment - Failure mode - Containment - Cost - Machining - Q.C./Inspection - Ring/disc attach. - Assembly	- Prone to catastrophic failure. Rated only slightly better than 'L' and 'M' since safe failure is not likely. (Note 9)	Same as 'L'	Same as 'L'
O	Shaped Laminated Disc/Ring. (Note 9)	LLL	None				Same as 'M'	- In principal, good to very good.
P	SMC Disc	None	None	Manufacturing procedures are well established but have not been applied to flywheel technology. Technology level average, costs low to very low but safety and energy storage capability will restrict the application to road vehicles. Lend well to mass production.	- Shaft attachment - Failure mode - Safety - Q.C./Inspection - Energy density	- Similar to 'L' and 'M' perhaps less prone to protusion	- Average	- Available stress levels will not permit either volume or weight goals to be met.
Q	Shaped SMC Disc	None	None				- Very Good	
R	SMC Disc with Ring (Note 9)	None	None	Somewhat safer with better energy storage than designs 'P' and 'Q', however the principal advantages of low cost, low technology and ease of mass production will be lost.	- Same as 'N' and 'O' - Energy density	- Similar to 'N' and 'O', perhaps less prone to protrusion.	- Average	- Somewhat better than 'P' and 'Q' but goals will not be met.
S	Shaped SMC Disc/ Ring (Note 9)	None	None				- Very Good	

Note: 9. Laminated or SMC disc must be the dominant energy storage component of the rotor. Otherwise the design is classified under design code 'A-ii', 'E' or 'H'.

TABLE B-4

FLYWHEEL PERSPECTIVE RATING - ROAD VEHICLE APPLICATION (Ref.1)

IMPACT PARAMETER / Weight / FLYWHEEL DESIGN CONCEPT CODE	SAFETY			GEOMETRY				COST FACTORS				TECHNOLOGY			RATINGS	
	Failure Mode	Ease of Containment	Pre-failure Indicators	Geometric Compatibility	Weight Compatibility	Flywheel Stability	Effective Shape Factor	Material Cost	Manufacture Cost	Industrial Implementation	Quality Control Inspection	State of the Art	Technology Level Required	Technical Risk	Total Rating Score	Basis For Elimination
	40	120	40	50	50	50	50	50	80	30	40	50	50	100		
Design 'A-1'	5	5	1	0	9	5	9	8	7	7	7	8	7	7	4890	Yes
Design 'A-11'	8	7	5	3	3	5	3	3	7	7	3	3	1	2	3500	Yes
Design 'B'	6	5	5	3	4	5	4	3	4	4	3	4	2	3	3150	Yes
Design 'C'	6	6	1	7	7	5	5	4	2	4	3	2	2	5	3500	Yes
Design 'D'	7	7	1	5	5	2	4	3	2	4	3	1	2	2	2860	Yes
Design 'E'	7	7	1	7	7	6	5	4	5	5	5	3	4	6	4310	No
Design 'F'	7	7	5	8	8	5	8	5	2	4	2	4	2	5	4180	No
Design 'G'	8	8	5	6	6	2	5	4	2	4	3	1	2	2	3380	Yes
Design 'H'	8	8	5	8	8	6	8	6	5	5	5	6	5	6	5180	No
Design 'I'	7	7	5	6	4	5	5	3	2	4	3	2	1	2	3220	Yes
Design 'J'	5	5	1	3	3	1	4	4	8	8	3	4	5	2	3240	Yes
Design 'K'	7	8	5	5	2	5	2	2	6	5	5	2	1	1	3320	Yes
Design 'L'	1	1	1	7	5	8	5	5	3	3	2	4	3	3	2760	Yes
Design 'M'	1	1	1	2	9	8	9	4	1	2	2	4	2	2	2520	Yes
Design 'N'	3	1	1	7	6	6	5	5	2	3	2	3	2	3	2610	Yes
Design 'O'	3	1	1	9	9	6	9	4	1	1	2	2	1	2	2670	Yes
Design 'P'	2	2	1	0	0	8	5	8	9	8	3	3	5	6	3490	Yes
Design 'Q'	2	2	1	0	0	8	9	8	9	8	3	3	5	6	3690	Yes
Design 'R'	4	2	1	0	0	6	5	6	5	4	3	2	3	2	2380	Yes
Design 'S'	4	2	1	0	0	6	9	6	5	4	3	2	3	2	2580	Yes

TABLE B-5 - TECHNOLOGY SUMMARY OF

FLYWHEEL HUB CONCEPTS FOR MULTIRING TYPE FLYWHEELS (Ref.1)

HUB CODE	HUB DESIGN CONCEPT	SAMPLE HUB 1		SAFETY FACTORS	GEOMETRIC FACTORS	MANUFACTURING COST, DEVELOPMENT AND TECHNOLOGY LEVELS	CRITICAL ELEMENTS
		Manufacturer	Flywheel Number				
A	Metallic hub with integral shaft.	Garrett Rocketdyne	1,2,3,6 11	Consistently very stable hub. Has never initiated failure of flywheel on the contrary, bunching of outer rings between flywheel and containment acted as low momentum transfer brake. Containment of metallic hub fragments is difficult.	Very high torsional and flexural rigidity. Moderate radial compatibility requires special design eg. sub-circular, twin-disc.	High development level. Moderate to high technology level depending on sophistication of hub design. Manufacturing and quality control/inspection techniques are well developed resulting in low-moderate manufacturing costs and technical risk.	- radial compatibility
B	Spoke type composite material hub (with bonded shaft attachments)	Garrett Broebeck	4,5 7	Typically lack of hub integrity and poor hub/rim attachment have initiated failures. Containment can be serious problem in radial spoke hub due to piercing of containment ring by spoke fragments.	Poor to moderate torsional rigidity. Very poor to poor flexural rigidity noted in spin tests. Garrett designs require subcircular mount. Broebeck hub designed for radial compatibility.	Low development level as designs are quite sophisticated. Manufacturing costs are very high and inspection techniques not fully developed. Very high technical risk.	- hub integrity - containment - rigidity - manufacturing cost - quality control/ inspection
C	Laminated disc type composite material hub (with bonded shaft attachments).	LLL GE LLL(GE)	21,31 26-30,33 34,35 23-25	Has not been designed as hub. Disc itself would be very stable. Elastomeric bonding has failed at least once, thus initiating flywheel failure. Fragments could require substantial containment.	Very good torsional and flexural rigidity due to quasi-isotropic layup. Radial compatibility is poor possibly requiring cryogenic press fitting unless subcircular mount is employed. Bolted shaft attachments more rigid than bonded.	Discs are low to average development level. Quality control and inspection could be problem. High technology level required resulting in high manufacturing costs and moderate-high technical risk. Bonding of shaft attachment less difficult than bolting due to problems in drilling composite.	- containment - radial compatibility - manufacturing cost - quality control - inspection
D	Laminated disc type composite material hub (with bolted shaft attachments).	GE	22	Has not been designed as hub. Disc would be very stable. Bolt holes significantly increase stress levels, i.e. smaller hub diameter. Same as C re failure.			
E	SMC disc (with bonded shaft attachments).	none	none	Has not been designed as hub. Same as C except failure fragments probably easier to contain. Material working stress levels less than C, i.e. smaller hubs. Disc is stable to very stable.	Good to very good torsional and flexural rigidity. Radial compatibility better than C,D due to lower modulus. Subcircular mount possibly not required. (Requires R&D to define). Bolted and integral shafts more rigid than bonded.	Technology level as well as development level are average except for untried integral shaft design. Comments on quality control/inspection and bonding vs bolting as in C, D. Moderate technical risk since R&D required is not a major commitment. Lend well to mass production-promise of very low cost.	- quality control - inspection - requires R&D program to define 'radial compatibility' and 'integral shaft' design.
F	SMC disc (with bolted shaft attachments).	none	none	Has not been designed as hub. Very stable. Same as D re stress levels. Same as E re containment. Material working stress levels less than E.			
G	SMC disc (with integral shaft.	none	none	Preliminary concept only. Stress levels probably similar to F. Same as E re containment.			
H	Bandwrap on metallic hub and shaft.	Union Carbide Sandia	14-18 19,20	Bandwrap failure has consistantly initiated flywheel failure. Lack of hub integrity has allowed contact of rim with containment resulting in very high momentum transfer. Bandwraps could pierce containment.	Poor to moderate torsional and flexural rigidity. Radial compatability good as rim expands radially against bandwraps.	Average development level with high technology requirements. High manufacturing costs due to specialized equipment and procedure.	- integrity - containment - rigidity - manufacturing cost - quality control - inspection
I	Overwrap on metallic hub and shaft.	Aerospatial MAN	9 10	Overwrap has better integrity than bandwrap re system failure. During catastrophic failure sections of overwrap could pierce containment.	Good torsional and flexural rigidity on continuous overwrap. Radial compatibility very good for same reason as H.	Same as H except even higher technology requirements.	

Note 1: See Table A-2 and A-3.

TABLE B-6

FLYWHEEL HUB RATINGS - ROAD VEHICLE APPLICATION (Ref.1)

IMPACT PARAMETER / Weight / HUB DESIGN CONCEPT CODE	SAFETY		GEOMETRY		COST FACTORS						TECHNOLOGY			RATINGS	
	Integrity 150	Ease of Containment 50	Rigidity 100	Radial Compatibility 100	Material Cost 40	Manufacturing Cost 70	Assembly Cost 20	Industrial Implementation 30	Quality Control Inspection 40	State-of-the Art 50	Technology Level Required 50	Technical Risk 100	Total Rating Score	Basis for Elimination
Design A	8	4	8	4	6	6	7	8	6	8	5	8	5330	No
Design B	2	3	2	5	3	1	4	1	2	2	2	2	1930	Yes
Design C	6	4	6	3	2	2	6	4	2	4	2	4	3240	Yes
Design D	7	4	8	3	2	2	6	4	2	4	2	4	3590	Yes
Design E	5	5	6	6	6	9	7	6	3	6	6	5	4560	No
Design F	4	5	7	6	6	8	7	6	3	6	6	5	4440	No
Design G	4	5	7	6	6	9	8	6	3	4	5	4	4330	No
Design H	1	3	4	8	2	1	9	3	4	2	2	2	2480	Yes
Design I	4	4	5	9	2	1	9	2	4	2	2	2	3150	Yes

TABLE B-7

FIBRES RATING FOR MULTIRING FLYWHEEL

IMPACT PARAMETER (Weight) / FIBRE	1985 MATERIAL COST (100) (Constant Dollars)		TENSILE FATIGUE STRENGTH (50)		TRANSVERSE TENSILE STRENGTH (50)		RESISTANCE TO CREEP (% OF UTS) (20)		TOTAL RATING SCORE	TENSILE MODULUS (Note 5)	DENSITY (Note 5)	TENSILE MODULUS DENSITY
	Can.$/Kg.	Rating[1]	MPa	Rating[2]	MPa	Rating[2]	%	Rating[2]		GPa	(gm/cc)	
E-GLASS	2	10	250	2.5	7	1.6	62	7.8	1361	42	2.00	21
S2-GLASS	8	8.7	325	3.3	40	10	62	7.8	1691	54	1.97	27
HIGH MODULUS CARBON	50	0	800	8	40	10	80	10	1100	198	1.59	125
HIGH STRENGTH CARBON	50	0	800	8	40	10	80	10	1100	144	1.54	94
INTERMEDIATE CARBON	40	2.1	800	8	40	10	80	10	1310	120	1.56	77
KEVLAR 29	50	0	1000	10	10	2.5	75	9.4	813	36	1.34	27
KEVLAR 49	30	4.2	1000	10	10	2.5	75	9.4	1233	72	1.34	54
REFERENCE	Chart VIII		Chart XIII		Charts IX & X		Chart XIV & Ref.75		2200 (max)	Charts IX, X	Chart VIII	

Note 1: Highest cost=0, lowest cost =10; other values based on linear interpolation.

Note 2: Maximum value = 10; other values based on linear interpolation.

Note 3: Volume Fraction approximately 60%.

Note 4: For 1000 hours @ 25°C, 50% probability.

Note 5: Cannot be rated. Included for comparative purposes as an aid in fibre selection.

APPENDIX 'C'

DERIVATION OF EQUATIONS

C.1 PRE-STRESS DUE TO WINDING TENSION

The equilibrium equation in the radial direction is simply [72,73].

$$\frac{d\sigma_r}{r} + \frac{\sigma_r - \sigma_\theta}{r} = 0 \qquad \ldots\ldots (C.1.1)$$

From Figure C.1, the boundary conditions at $r = \rho$ are.

$$\begin{aligned} \sigma_r(\rho) &= 0 \\ \sigma_r(b_m) &= -P(\rho) \\ \sigma_\theta(\rho) &= T(\rho) \\ u(\rho) &= 0 \end{aligned} \qquad \ldots\ldots (C.1.2)$$

Where:

ρ = radial position of the outermost filament during winding at a particular instant

b_m = outside radius of mandrel

$P(\rho)$ = the pressure exerted on the mandrel surface due to filament winding when $r = \rho$

$T(\rho)$ = Tension at ρ

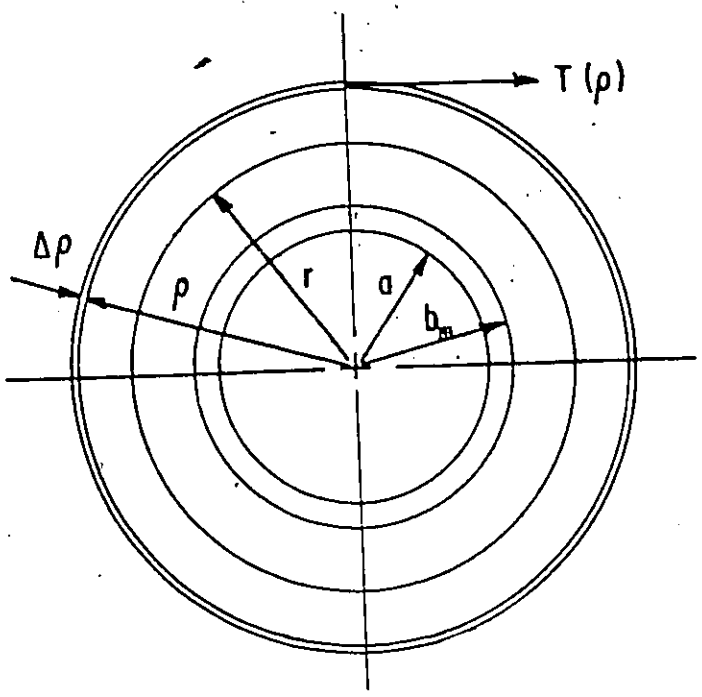

Figure C.1: Schematic Diamgram of Composite Ring During Winding

The stress and displacement of the isotropic mandrel for $a_m \leq r \leq b_m$ will be

$$\sigma_{rm}(r) = \frac{b_m^2 P(\rho)}{b_m^2 - a_m^2} \left(1 - \frac{a_m^2}{r^2}\right)$$

$$\sigma_{\theta m}(r) = \frac{-b_m^2 P(\rho)}{(b_m^2 - a_m^2)} \left(1 + \frac{a_m^2}{r^2}\right) \qquad \ldots\ldots(C.1.3)$$

$$U_m(r) = \frac{b_m^2 P(\rho)}{E_m(b_m^2 - a_m^2)} \left[(1+\nu_m) r \; (1+\nu_m) \frac{a_m^2}{r}\right]$$

Where a_m = inside radius of mandrel.

ν_m = Poisson ratio of mandrel.

Now, if a thin filament of thickness $\Delta\rho$ with tension $T(\rho)$ is wound on the top of the outermost filament at ρ , a compressive force of $T(\rho)\ \Delta\rho/\rho$ is exerted at ρ. Consequently, the interfacial pressure between the mandrel and the filament-wound ring will be increased to

$$\overline{P}(\rho) = P(\rho) + \Delta P(\rho)$$

Similarly, for the new displacement, stresses and strains for the filament-wound element become:-

$$\begin{aligned}
\overline{u}(r) &= u(r) + \Delta u(r) \\
\overline{\sigma}_r(r) &= \sigma_r(r) + \Delta\sigma_r(r) \\
\overline{\sigma}_\theta(r) &= \sigma_\theta(r) + \Delta\sigma_\theta(r) \qquad \ldots\ldots\ldots (C.1.4) \\
\overline{\varepsilon}_r(r) &= \varepsilon_r(r) + \Delta\varepsilon_r(r) \\
\overline{\sigma}_\theta(r) &= \sigma_\theta(r) + \Delta\varepsilon_\theta(r)
\end{aligned}$$

Therefore, the equilibrium equation C.1.1 becomes

$$\frac{d\overline{\sigma}_r}{dr} + \frac{\overline{\sigma}_r - \overline{\sigma}_\theta}{r} = 0 \qquad \ldots\ldots\ldots (C.1.5)$$

Substituting equation C.1.4 into equation C.1.5 and combining with equation C.1.1 we have

$$\frac{d\Delta\sigma_r}{dr} + \frac{\Delta\sigma_r - \Delta\sigma_\theta}{r} = 0 \qquad \ldots\ldots\ldots (C.1.6)$$

By assuming a linear orthotropic material property, similar to the stress-strain and strain-displacement relation in Appendix C.4, we have:

$$\Delta\varepsilon_r(r) = \frac{d\,\Delta u(r)}{dr}$$

$$\Delta\varepsilon_\theta(r) = \frac{\Delta u(r)}{r} \qquad \ldots\ldots\ldots (C.1.7)$$

$$\Delta\sigma_r(r) = \frac{E_r}{1-\nu_r\nu_\theta}\left(\Delta\varepsilon_r + \nu_\theta\Delta\varepsilon_\theta\right)$$

$$\Delta\sigma_\theta(r) = \frac{E_\theta}{(1-\nu_r\nu_\theta)}\left(\Delta\varepsilon_\theta + \nu_r\Delta\varepsilon_r\right)$$

Substituting equation (C.1.7) into equation (C.1.6) and simplify, yields:

$$\frac{d^2\Delta u(r)}{dr^2} + \frac{1}{r}\frac{d\,\Delta u(r)}{dr} - K^2\frac{\Delta u(r)}{r^2} = 0$$

Solving, we have:

$$\Delta u(r) = C_1 r^K + C_2 r^{-K} \qquad \ldots\ldots (C.1.8)$$

Substituting equation C.1.8 into equation C.1.7 and applying the following new boundaries conditions:

$$\text{at } r = \rho \qquad \bar{\sigma}_r(\rho) = \Delta\sigma_r(\rho) = \frac{-T(\rho)\,\Delta\rho}{\rho}$$

$$\text{at } r = b_m \qquad \Delta\sigma_r(b_m) = -\Delta P(\rho)$$

We have,

$$\Delta u(r) = \frac{1-\nu_\theta\nu_r}{E_r(\rho^{2K}-b_m^{2K})}\left[\frac{b_m^{K+1}\,\Delta P(\rho) - \rho^K T(\rho)\,\Delta\rho}{\beta-B}\, r^K + \frac{\rho^K b_m^K(\rho^K b_m\,\Delta P(\rho) - T(\rho) b_m^K\,\Delta\rho)}{\alpha+B}\, r^{-K}\right] \quad \ldots\ldots \text{(C.1.9)}$$

Where:

$$\alpha = K - \nu_\theta - B$$

$$\beta = K + \nu_\theta + B$$

$$B = \frac{E_\theta}{E_m(b_m^2 - a_m^2)}\left[(1-\nu_m)b_m^2 + (1+\nu_m)a_m^2\right]$$

Equation C.1.9 gives the incremental radial displacement at r when an incremental layer $\Delta\rho$ was wound on ρ . $\Delta P(\rho)$ could be solved by considering the continuity of interface between the filament and the mandrel.

Hence, $$\Delta u(b_m) = \Delta u_m(b_m) = \frac{b_m B}{E_\theta}\,\Delta P(\rho) \qquad \ldots\ldots \text{(C.1.10)}$$

(From Eq. C.1.3)

Solving equation C.1.9 and C.1.10, we have:

$$\Delta P(\rho) = \frac{2Kb_m^{K-1} \rho^K T(\rho)\,\Delta\rho}{\beta\rho^{2K} + \alpha b_m^{2K}} \quad \ldots\ldots (C.1.11)$$

Substituting equation C.1.11 into C.1.9.

$$\Delta u(r) = \frac{b_m^K \rho^K T(\rho)\,\Delta\rho}{E_\theta\,(\beta\rho^{2K} + \alpha b_m^{2K})} \left[\alpha(\beta - B)\left(\frac{b_m}{r}\right)^K - \beta(\alpha+\beta)\left(\frac{r}{b_m}\right)^K\right]$$

$\ldots\ldots (C.1.12)$

Substituting equation C.1.12 into equation C.1.7, we have,

$$\Delta\sigma_r(r) = \frac{-b_m^{K-1} \rho^K T(\rho)\,\Delta\rho}{\beta\rho^{2K} + \alpha b_m^{2K}} \left[\alpha\left(\frac{b_m}{r}\right)^{K+1} + \beta\left(\frac{r}{b_m}\right)^{K-1}\right]$$

$\ldots (C.1.13)$

$$\Delta\sigma_\theta(r) = \frac{Kb_m^{K-1} \rho^2 T(\rho)\Delta\rho}{\beta\rho^{2K} + \alpha b_m^{2K}} \left[\alpha\left(\frac{b_m}{r}\right)^{K+1} - \beta\left(\frac{r}{b_m}\right)^{K-1}\right]$$

Integrating equations C.1.11, C.1.12 and C.1.13, the total interfacial pressure, radial displacement and stresses are as follows:

$$P(\rho) = \int_{b_m}^{c} \Delta P(\rho) = 2Kb_m^{K-1} \int_{b_m}^{c} \frac{\rho^K T(\rho)\,d\rho}{\beta\rho^{2K} + \alpha b_m^{2K}} = 2Kb_m^{K-1} f(b_m)$$

Equation continued...

$$u(r) = \left[\alpha(\beta-B)\left(\frac{b_m}{r}\right)^K - \beta(\alpha+B)\left(\frac{r}{b_m}\right)^K\right] \frac{b_m}{E_\theta} f(r)$$

$$\sigma_r(r) = -\left[\alpha\left(\frac{b_m}{r}\right)^{K+1} + \beta\left(\frac{r}{b_m}\right)^{K-1}\right] b_m^{K-1} f(r) \qquad \ldots(C.1.14)$$

$$\sigma_\theta(r) = T(r) + \left[\alpha\left(\frac{b_m}{r}\right)^{K+1} - \beta\left(\frac{r}{b_m}\right)^{K-1}\right] K b_m^{K-1} f(r)$$

Where: $$f(r) = \int_r^c \frac{\rho^K T(\rho)}{\beta\rho^{2K} + \alpha b_m^{2K}} d\rho$$

C = outside radius of the filament-wound ring

Also it should be noted that the term 'T(r)' in $\sigma_\theta(r)$ is the initial condition given by equation C.1.2.

Equation C.1.14 gives the residual stresses of the filament-wound composite ring after completion of winding. The total residual stress after the ring was taken away from mandrel could be obtained by super-imposing a negative p(ρ) on the inside radius of the ring.

Therefore, after super-imposing -p(p) on the inside radius of the composite ring, we have:

$$\sigma_r(r) = \frac{2KB^{2K}C^{K-1}f(b_m)}{C^{2K}-b_m^{2K}}\left[\left(\frac{c}{r}\right)^{K+1} - \left(\frac{r}{c}\right)^{K-1}\right]$$

$$- b_m^{K-1} f(r)\left[\alpha\left(\frac{b_m}{r}\right)^{K+1} + \beta\left(\frac{r}{b_m}\right)^{K-1}\right] \qquad \ldots(C.1.15)$$

(Equation contined)....

$$\sigma_\theta(r) = T(r) + Kb_m^{K-1} f(r) \left[\alpha \left(\frac{b_m}{r}\right)^{K+1} - \beta \left(\frac{r}{b_m}\right)^{K-1}\right]$$

$$- \frac{2K^2 b_m^{2K} C^{K-1} f(b_m)}{C^{2K} - b_m^{2K}} \left[\left(\frac{c}{r}\right)^{K+1} + \left(\frac{r}{c}\right)^{K-1}\right] \quad \ldots (C.1.15)$$

C.2 RESIDUAL STRESS DUE TO ANISOTROPIC SHRINKAGE

The anisotropic shrinkage of filament-wound composite consists of two components, namely: (1) chemical shrinkage when the resin sets, and (2) thermal shrinkage when cooled from curing temperature to room temperature.

The equilibrium equation in radial direction is simply (plane stress):

$$\frac{d\sigma_r}{dr} - \frac{\sigma_\theta - \sigma_r}{r} = 0 \quad \ldots (C.2.1)$$

Also, the strain-displacement and stress-strain relations are as follows:

$$\varepsilon_r = \frac{du}{dr}$$

$$\varepsilon_\theta = \frac{u}{r} \quad \ldots (C.2.2)$$

and

$$\varepsilon_r = \frac{\sigma_r}{E_r} - \frac{\nu_\theta \sigma_\theta}{E_\theta} + \varepsilon_{ro}$$

$$\varepsilon_\theta = \frac{\sigma_\theta}{E_\theta} - \frac{\nu_r \sigma_r}{E_r} + \varepsilon_{\theta o} \quad \ldots (C.2.3)$$

Where ε_{ro} and $\varepsilon_{\theta o}$ are the radial and circumferencial free shrinkage respectively after the ring was cured and removed from the mandrel.

Substituting equation C.2.2 and C.2.3 into equation C.2.1, and applying the boundary conditions.

$$\begin{aligned} \text{at} \quad r &= a, \quad \sigma_r = o \\ r &= b, \quad \sigma_r = o \end{aligned} \qquad \ldots \text{(C.2.4)}$$

Solving, we have:

$$u = \left\{ \frac{\varepsilon_{ro}-\varepsilon_{\theta o}}{K^2-1} \left[(K-\nu_\theta)\left(\frac{C^{K+1}-1}{C^{2K}-1}\right) C^{K-1} \left(\frac{r}{a}\right)^{K-1} - (K+\nu_\theta)\left(\frac{C^{K-1}-1}{C^{2K}-1}\right)\left(\frac{r}{a}\right)^{-K-1} + (\nu_\theta - K^2) \right] + \varepsilon_{ro} \right\} r \qquad \ldots \text{(C.2.5)}$$

$$\varepsilon_{rR} = \frac{K^2(\varepsilon_{ro}-\varepsilon_{\theta o})}{K^2-1} \left[(1-\sqrt{\nu_r \nu_\theta}) \frac{C^{K+1}-1}{C^{2K}-1} C^{K-1} \left(\frac{r}{a}\right)^{K-1} + (1+\sqrt{\nu_r \nu_\theta})\left(\frac{C^{K-1}-1}{C^{2K}-1}\right) \left(\frac{r}{a}\right)^{-K-1} + (\nu_r - 1) \right] \qquad \ldots \text{(C.2.6)}$$

$$\varepsilon_{\theta R} = \frac{\varepsilon_{ro}-\varepsilon_{\theta o}}{K^2-1} \left[(K-\nu_\theta) \frac{C^{K+1}-1}{C^{2K}-1} C^{K-1} \left(\frac{r}{a}\right)^{K-1} - (K+\nu_\theta)\left(\frac{C^{K-1}-1}{C^{2K-1}}\right)\left(\frac{r}{a}\right)^{-K-1} + (\nu_\theta - 1) \right] \qquad \ldots \text{(C.2.7)}$$

$$\sigma_{rR} = \frac{(\varepsilon_{ro}-\varepsilon_{\theta o})E_\theta}{K^2-1}\left[\frac{C^{K+1}-1}{C^{2K}-1}\; C^{K-1}\left(\frac{r}{a}\right)^{K-1} + \left(\frac{C^{K-1}-1}{C^{2K}-1}\right)\left(\frac{r}{a}\right)^{-K-1} - 1\right] \quad \ldots\ldots(C.2.8)$$

$$\sigma_{\theta R} = \frac{(\varepsilon_{ro}-\varepsilon_{\theta o})KE_\theta}{K^2-1}\left[\left(\frac{C^{K+1}-1}{C^{2K}-1}\right) C^{K-1}\left(\frac{r}{a}\right)^{K-1} - \left(\frac{C^{K-1}-1}{C^{2K}-1}\right)\left(\frac{r}{a}\right)^{-K-1} - \frac{1}{K}\right] \quad \ldots\ldots(C.2.9)$$

Where: $C = \frac{a}{b}$

$K = \sqrt{\frac{E_\theta}{E_r}}$

Where: $\varepsilon_{rR} = \varepsilon_r - \varepsilon_{ro}$

$\varepsilon_{\theta R} = \varepsilon_\theta - \varepsilon_{\theta o}$

C.3 THERMAL STRESS

The equilibrium equation in the radial direction is:

$$\frac{d\sigma_r}{dr} + \frac{\sigma_r-\sigma_\theta}{r} = 0 \quad \ldots\ldots(C.3.1)$$

For uniform temperature change, the stress-strain relationship is:

$$\varepsilon_r = \frac{\sigma_r}{E_r} - \frac{\nu_\theta\sigma_\theta}{E} + \alpha_r T \quad \ldots\ldots(C.3.2)$$

$$\varepsilon_\theta = \frac{\sigma_\theta}{E_\theta} - \frac{\nu_r\sigma_r}{E_r} + \alpha_\theta T$$

From C.3.2, the tangential and radial stress can be written as:

$$\sigma_r = \frac{E_r}{1-\nu_r\nu_\theta}\left[(\varepsilon_r - \alpha_r T) + \nu_\theta(\varepsilon_\theta - \alpha_\theta T)\right]$$

$$\sigma_\theta = \frac{E_\theta}{1-\nu_r\nu_\theta}\left[(\varepsilon_\theta - \alpha_\theta T) + \nu_r(\varepsilon_r - \alpha_r T)\right] \quad \ldots (C.3.3)$$

Also, strain-displacement relations are,

$$\varepsilon_r = \frac{du}{dr} \qquad \varepsilon_\theta = \frac{u}{r} \quad \ldots (C.3.4)$$

Substituting equation C.3.3 and C.3.4 into the equilibrium equation C.3.1,

$$\frac{d^2u}{dr^2} + \frac{1}{r}\frac{du}{dr} - K^2\frac{u}{r^2} = \left[\alpha_r + \nu_\theta(\alpha_\theta - \alpha_r) - K^2\alpha_\theta\right]\frac{T}{r} \quad \ldots (C.3.5)$$

Where $K^2 = \frac{E_\theta}{E_r} = \frac{\nu_\theta}{\nu_r}$

Solving, we have:

$$u = C_1 r^K + C_2 r^{-K} + \frac{\alpha_r + \nu_\theta(\alpha_\theta - \alpha_r) - K^2\alpha_\theta}{1-K^2} Tr \quad \ldots (C.3.6)$$

Where: C_1 and C_2 (constants)

Applying boundary conditions,

$$\text{at } r = a, \quad \sigma_r = -P_a$$
$$r = b, \quad \sigma_r = -P_b \qquad \ldots\ldots(C.3.7)$$

Therefore, after substituting equation C.3.7 into C.3.6, we have

$$C_1 = \frac{(K^2-\nu_\theta^2)(\alpha_\theta-\alpha_r)\,T}{(1-K^2)(\nu+K)\,a^{K-1}} \quad \frac{1-C^{-K-1}}{1-C^{-2K}}$$

$$\frac{P_a(1-\nu_r\nu_\theta)}{(\nu_\theta+K)E_r\,a^{K-1}} \quad \frac{1}{1-C^{-2K}} + \frac{P_b(1-\nu_r\nu_\theta)}{(K+\nu_\theta)E_r b^{K-1}} \quad \frac{1}{C^{2K}-1}$$

and $C_2 = \frac{(K^2-\nu_\theta^2)(\alpha_\theta-\alpha_r)\,T}{(1-K^2)(\nu_\theta-K)a^{-K-1}} \quad \frac{1-C^{K-1}}{1-C^{2K}} + \frac{P_a(1-\nu_r\nu_\theta)}{(\nu_\theta-K)E_r a^{-K-1}} \quad \frac{1}{C^{2K}-1}$

Where: $C = \frac{a}{b}$

Substituting the value of C_1 and C_2 into equation C.3.6 yields

$$u = \frac{aT}{1-K^2}\left\{(\alpha_\theta-\alpha_r)(K-\nu_\theta)\,\frac{1-C^{-K-1}}{1-C^{-2K}}\,\left(\frac{r}{a}\right)^K - (\alpha_\theta-\alpha_r)(K+\nu_\theta)\right.$$

$$\left.\frac{1-C^{K-1}}{1-C^{2K}}\left(\frac{r}{a}\right)^{-K} + [\nu_\theta(\alpha_\theta-\alpha_r) + \alpha_r - K^2\alpha_\theta]\left(\frac{r}{a}\right)\right\} - \frac{P_a(1-\nu_r\nu_\theta)}{E_r}$$

(Equation continued)....

$$a\left[\frac{1}{(\nu_\theta+K)(1-C^{-2K})}\left(\frac{r}{a}\right)^{K}+\frac{1}{(\nu_\theta-K)(1-C^{2K})}\left(\frac{r}{a}\right)^{-K}\right]$$

$$-\frac{P_b(1-\nu_r\nu_\theta)b}{E_r}\left[\frac{1}{(K+\nu_\theta)(1-C^{2K})}\left(\frac{r}{a}\right)+\frac{1}{(\nu_\theta-K)(1-C^{-2K})}\left(\frac{r}{a}\right)^{-K}\right]$$

. . . . .(C.3.8)

Now, subsituting the value of 'u' into equation C.3.4 yields ε_r and ε_θ . Thereafter, the tangential and radial stress can be obtained by substituting equation C.3.4 into equation C.3.3, viz:

$$\sigma_r = \frac{E_r(K^2-\nu_\theta^2)(\alpha_\theta-\alpha_r)T}{(1-\nu_r\nu_\theta)(1-K^2)}\left[\frac{1-C^{-K-1}}{1-C^{-2K}}\left(\frac{r}{a}\right)^{K-1}+\frac{1-C^{K-1}}{1-C^{2K}}\left(\frac{r}{a}\right)^{-K-1}-1\right]-P_a$$

$$\left[\frac{1}{1-C^{-2K}}\left(\frac{r}{a}\right)^{K-1}+\frac{1}{1-C^{2K}}\left(\frac{r}{a}\right)^{-K-1}\right]-P_b\left[\frac{1}{1-C^{2K}}\left(\frac{r}{b}\right)^{K-1}+\right.$$

$$\left.\frac{1}{1-C^{2K}}\left(\frac{r}{b}\right)^{K-1}\right] \qquad \text{. . . . . (C.3.9)}$$

$$\sigma_\theta = \frac{E_r(K^2-\nu_\theta^2)(\alpha_\theta-\alpha_r)T}{(1-\nu_r\nu_\theta)(1-K^2)}\left[K\frac{1-C^{-K-1}}{1-C^{-2K}}\left(\frac{r}{a}\right)^{K-1}-K\frac{1-C^{K-1}}{1-C^{2K}}\left(\frac{r}{a}\right)^{-K-1}\right.$$

$$\left.-1\right]-KP_a\left[\frac{1}{1-C^{-2K}}\left(\frac{r}{a}\right)^{K-1}-\frac{1}{1-C^{2K}}\left(\frac{r}{a}\right)^{-K-1}\right]-KP_b\left[\frac{1}{1-C^{2K}}\left(\frac{r}{a}\right)^{K-1}\right.$$

$$\left.-\frac{1}{1-C^{-2K}}\left(\frac{r}{b}\right)^{-K-1}\right] \qquad \text{. . . . .(C.3.10)}$$

C.4 CENTRIFUGAL STRESS

The following equation represents the equilibrium of an infinitestimal element in radial direction (plane stress) [72,73]:

$$\frac{d\sigma_r}{dr} + \frac{1}{r}\frac{d\tau_{r\theta}}{d\theta} + \frac{\sigma_r-\sigma_\theta}{r} + F_r = 0 \qquad \ldots\ldots (C.4.1)$$

Where F_r = body force per unit volume in the radial direction.

In case of rotation: $F_r = \rho\omega^2 r$

Also, for rotational symmetry: $\frac{d\tau_{r\theta}}{d\theta} = 0$

Therefore, equation C.4.1 becomes

$$\frac{d\sigma_r}{d_r} + \frac{\sigma_r-\sigma_\theta}{r} + \rho\omega^2 = 0 \qquad \ldots\ldots (C.4.2)$$

Strain-displacement equation is [72,73]:

$$\varepsilon_r = \frac{du}{dr}$$

$$\varepsilon_\theta = \frac{u}{r} + \frac{1}{r}\frac{dv}{d\theta} = \frac{u}{r} \quad \left(\because \frac{dv}{d\theta} = 0\right) \qquad \ldots\ldots (C.4.3)$$

Stress-strain equations [73]:

$$\varepsilon_r = \frac{\sigma_r}{E_r} - \frac{\nu_\theta \sigma_\theta}{E_\theta}$$

$$\varepsilon_\theta = \frac{\sigma_\theta}{E_\theta} - \frac{\nu_r \sigma_r}{E_r} \qquad \ldots\ldots(C.4.4)$$

$$\text{also} \quad K^2 = \frac{E_\theta}{E_r} = \frac{\nu_\theta}{E_r}$$

Rearranging equation C.4.4 yields:

$$\sigma_r = \frac{E_r}{1-\nu_r\nu_\theta}(\varepsilon_r + \nu_\theta \varepsilon_\theta)$$

$$\sigma_\theta = \frac{E_\theta}{1-\nu_r\nu_\theta}(\varepsilon_\theta + \nu_r \varepsilon_r) \qquad \ldots\ldots(C.4.5)$$

Substituting equation C.4.3 and C.4.5 into equation C.4.2, after simplification, yields:

$$\frac{d^2u}{dr^2} + \frac{1}{r}\frac{du}{dr} - K^2\frac{u}{r^2} = -\frac{(1-\nu_r\nu_\theta)}{E_r}\rho\omega^2 r \qquad \ldots\ldots(C.4.6)$$

Solving, we have:

$$u = C_1 r^K + C_2 r^{-K} - \frac{\rho\omega^2(1-\nu_r\nu_\theta)}{9E_r - E_\theta} r^3 \qquad \ldots\ldots(C.4.7)$$

Where C_1 and C_2 are constants. Now, applying the boundary conditions to equation C.4.7:

$$\text{at} \quad r = a, \quad \sigma_r = -P_a \text{ (negative for compression)}$$
$$r = b, \quad \sigma_r = -P_b \qquad \ldots\ldots (C.4.8)$$

C_1 and C_2 can be determined. Then, radial displacement, radial stress and tangential stress are obtained by substituting C_1 and C_2 into equation C.4.7, C.4.3 and C.4.5. Hence, we have:

$$u = \frac{\gamma\omega^2 b^3}{gE_\theta(9-K^2)}\left\{(3+\nu_\theta)\left[(K-\nu_\theta)\frac{1-C^{K+3}}{1-C^{2K}}\left(\frac{r}{b}\right)^K - (K+\nu_\theta)\frac{1-C^{K-3}}{1-C^{2K}}C^{K+3}\left(\frac{b}{r}\right)^K\right]\right.$$
$$\left. - (K^2-\nu_\theta^2)\left(\frac{r}{b}\right)^3\right\} + \frac{P_a b C^{K+1}}{E_\theta(1-C^{2K})}\left[(K-\nu_\theta)\left(\frac{r}{b}\right)^K + (K+\nu_\theta)\left(\frac{b}{r}\right)^K\right]$$
$$- \frac{P_b\, b}{E_\theta(1-C^{2K})}\left[(K-\nu_\theta)\left(\frac{r}{b}\right)^K + (K+\nu_\theta)C^{2K}\left(\frac{b}{r}\right)^K\right]$$
$$\ldots\ldots (C.4.9)$$

$$\sigma_r = \frac{\gamma\omega^2 b^2(3+\nu_\theta)}{g(9-K^2)}\left[\frac{1-C^{K+3}}{1-C^{2K}}\left(\frac{r}{b}\right)^{K-1} + \frac{1-C^{K-3}}{1-C^{2K}}C^{K+3}\left(\frac{b}{r}\right)^{K+1}\right.$$
$$\left. - \left(\frac{r}{b}\right)^2\right] + \frac{P_a C^{K+1}}{1-C^{2K}}\left[\left(\frac{r}{b}\right)^{K-1} - \left(\frac{b}{r}\right)^{K+1}\right] + \frac{P_b}{1-C^{2K}}$$
$$\left[-\left(\frac{r}{b}\right)^{K-1} + C^{2K}\left(\frac{b}{r}\right)^{K+1}\right] \qquad \ldots\ldots (C.4.10)$$

$$\sigma_\theta = \frac{\gamma\omega^2 b^2}{g(9-K^2)}\left\{(3+\nu_\theta)K\left[\frac{1-c^{K+3}}{1-c^{2K}}\left(\frac{r}{b}\right)^{K-1} - \frac{1-c^{K-3}}{1-c^{2K}}c^{K+3}\left(\frac{b}{r}\right)^{K+1}\right]\right.$$

$$\left. - (K^2+3\nu_\theta)\left(\frac{r}{b}\right)^2\right\} + \frac{P_a c^{K+1}}{1-c^{2K}}\left[\left(\frac{r}{b}\right)^{K-1} + \left(\frac{b}{r}\right)^{K+1}\right] -$$

$$- \frac{P_b K}{1-c^{2K}}\left[\left(\frac{r}{b}\right)^{K-1} + c^{2K}\left(\frac{b}{r}\right)^{K+1}\right] \quad \ldots\ldots(C.4.11)$$

Equations C.4.9 to C.4.11 give the radial displacement, radial and tangential stress of a single anisotropic ring as in figure C.2. Similarly, the radial displacement, radial stress and tangential stress in a particular ring of a multiring rotor (Figure C.3) can be written as follows:-

$$u^{(m)} = \frac{\gamma_m\omega^2 a_m^3}{gE_\theta^{(m)}(9-K_m^2)}\left\{(3+\nu_\theta^{(m)})\left[(K_m-\nu_\theta^{(m)})\frac{1-c_m^{k_m+3}}{1-c_m^{2k_m}}\left(\frac{r}{a_m}\right)^{k_m}\right.\right.$$

$$\left.\left. - (K_m+\nu_\theta^{(m)})\frac{1-c_m^{k_m-3}}{1-c_m^{2k_m}}c_m^{k_m+3}\left(\frac{a_m}{r}\right)^{k_m}\right] - [K_m^2 - (\nu_\theta^{(m)})^2]\left(\frac{r}{a_m}\right)^3\right\}$$

$$+ \frac{q_{m-1}a_m c_m^{k_m+1}}{E_\theta^{(m)}(1-c_m^{2k_m})} \times \left[(K_m-\nu_\theta^{(m)})\left(\frac{r}{a_m}\right)^{k_m} + (K_m+\nu_\theta^{(m)})\left(\frac{a_m}{r}\right)^{k_m}\right]$$

$$- \frac{q_m a_m}{E_\theta^{(m)}(1-c_m^{2k_m})}\cdot\left[(K_m-\nu_\theta^{(m)})\left(\frac{r}{a_m}\right)^{k_m} + (K_m+\nu_\theta^{(m)})c_m^{2k_m}\left(\frac{a_m}{r}\right)^{k_m}\right]$$

$$\ldots\ldots(C.4.12)$$

$$\sigma_r^{(m)} = \frac{\gamma_m \omega^2}{g} a_m^2 \frac{3+\nu_\theta^{(m)}}{9-K_m^2} \left[\frac{1-c_m^{K_m+3}}{1-c_m^{2K_m}} \left(\frac{r}{a_m}\right)^{K_m-1} \right.$$

$$+ \frac{1-c_m^{K_m-3}}{1-c_m^{2K_m}} c_m^{K_m+3} \left(\frac{a_m}{r}\right)^{K_m+1} - \left(\frac{r}{a_m}\right)^2 \left. \right] + \frac{P_{m-1} c_m^{K_m+1}}{1-c_m^{2K_m}} \left[\left(\frac{r}{a_m}\right)^{K_m-1} \right.$$

$$\left. - \left(\frac{a_m}{r}\right)^{K_m+1} \right] + \frac{P_m}{1-c_m^{2K_m}} \left[- \left(\frac{r}{a_m}\right)^{K_m-1} + c_m^{2K_m} \left(\frac{a_m}{r}\right)^{K_m+1} \right]$$

. . . . (C.4.13)

$$\sigma_\theta(m) = \frac{\gamma_m \omega^2}{g} \cdot \frac{a_m^2}{9-K_m^2} \left\{ (3+\nu_\theta^{(m)}) K_m \left[\frac{1-c_m^{K_m+3}}{1-c_m^{2K_m}} \left(\frac{r}{a_m}\right)^{K_m-1} \right. \right.$$

$$\left. - \frac{1-c_m^{K_m-3}}{1-c_m^{2K_m}} c_m^{K_m+3} \left(\frac{a_m}{r}\right)^{K_m+1} \right] - (K_m^2 + 3\nu_\theta^{(m)}) \left(\frac{r}{a_m}\right)^2 \left. \right\}$$

$$+ \frac{P_{m-1} c_m^{K_m+1} K_m}{1-c_m^{2K_m}} \left[\left(\frac{r}{a_m}\right)^{K_m-1} + \left(\frac{a_m}{r}\right)^{K_m+1} \right] - \frac{P_m K_m}{1-c_m^{2K_m}}$$

$$\left[\left(\frac{r}{a_m}\right)^{K_m-1} + c_m^{2K_m} \left(\frac{a_m}{r}\right)^{K_m+1} \right]$$

. . . . (C.4.14)

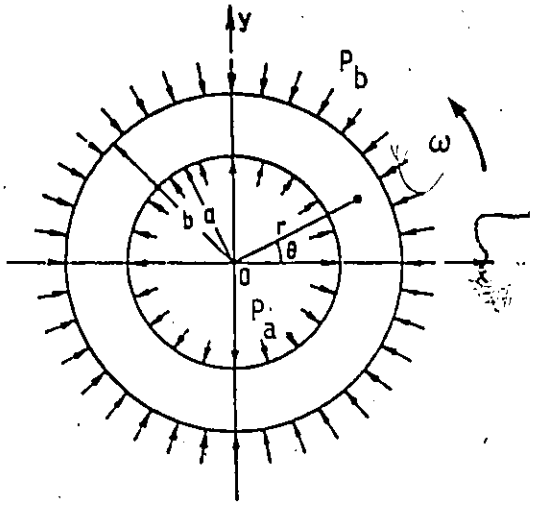

Fig. C.2: Schematic diagram of Single Ring Rotor

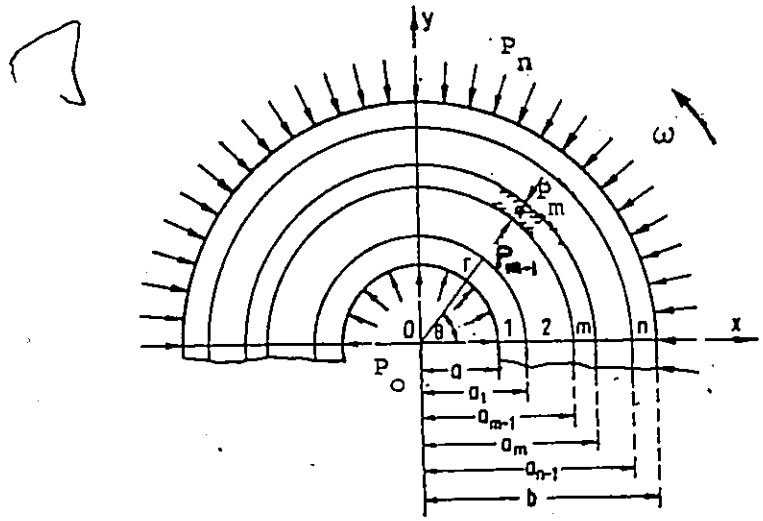

Fig. C.3: Schematic diagram of Multi-Ring Rotor

Now, the unknown pressures P_m are determined from the continuity of radial displacement of points on the contact surface,

$$\text{at} \quad r = a_m - 1, \quad u_r^{(m-1)} = u_r^{(m)} \qquad \ldots\ldots (C.4.15)$$

Substituting equation C.4.12 into C.4.15, n-1 equations of unknown pressures P_m are obtained,

$$P_{m+1}\ a_{m+1}\ \alpha_{m+1} + P_m\ a_m\ \beta_m + P_{m-1}\ a_{m-1}\ \alpha_m = \omega^2 a_m^3 \delta_m \qquad \ldots\ldots (C.4.16)$$

Where,

$$\delta_m = \frac{\rho_m}{9-K_m^2}\left(\frac{1+3\nu_r^{(m)}}{E_r^{(m)}} - \frac{3+\nu_\theta^{(m)}}{E_\theta^{(m)}}\ K_m\ \frac{1-2c_m^{K_m+3}+c_m^{2K_m}}{1-c_m^{2K_m}}\right)$$

$$\left\{ - \frac{\rho_{m+1}}{9-K_{m+1}^2}\left(\frac{1+3\nu_r^{(m+1)}}{E_r^{(m+1)}} + \frac{3+\nu_\theta^{(m+1)}}{E_\theta^{(m+1)}}\ K_{m+1}\ \frac{1-2c_{m+1}^{K_{m+1}-3}+c_{m+1}^{2K_{m+1}}}{1-c_{m+1}^{2K_{m+1}}}\right)\right. \qquad \ldots\ldots (C.4.17)$$

$$\alpha_m = \frac{2K_m}{E_\theta^{(m)}}\ \frac{c_m^{K_m}}{1-c_m^{2K_m}}$$

$$\beta_m = \frac{1}{E_\theta^{(m)}}\left(\nu_\theta^{(m)} - K_m\ \frac{1+c_m^{2K_m}}{1-c_m^{2K_m}}\right) - \frac{1}{E_\theta^{(m+1)}}\left(\nu_\theta^{(m+1)} + K_{m+1}\right.$$

$$\left.\frac{1+c_{m+1}^{2K_{m+1}}}{1+c_{m+1}^{2K_{m+1}}}\right) \qquad \ldots\ldots (C.4.18)$$

Therefore, for n-1 unknown pressures, n-1 equations could be obtained from equation C.4.16. After solving for the n-1 unknown P_m (m= 1,2,.....n-1), the values of radial displacement, radial and tangential stress in each ring can be obtained by substituting the values of P_m into equations C.4.12 to C.4.14.

APPENDIX 'D'

MATERIAL PROPERTIES

[REF. 19]

APPENDIX 'D'

MATERIAL PROPERTIES

The material properties listed in Chart I were calculated by the rule of mixtures for a Volume Fraction ranging from 0.55 to 0.70 as follows:-

Density (ρ): $\rho_{composite} = \rho_{fibre} V_f + \rho_{resin} (1-V_f)$ . . . . .(D.1)

Tensile Modulus (Both Tangential and Transverse):

$$E_{composite} = E_{fibre} V_f + E_{resin} (1-V_f) \quad . . . . .(D.2)$$

Table D.1 gives the density, tangential and transverse moduli of the five different identified fibres and the resin.

Where E_{11f}, E_{22f} = tangential and radial modulus, respectively, of fibre.

E_{11r}, E_{22r} = tangential and radial modulus, respectively, of resin.

Sample Calculation:

(i) For E-glass, with $V_f = 0.60$

From equation D.1,

$$\rho_{E\text{-glass}} = (2.72)(0.6) + (1.20)(1-0.6)$$

$$= \underline{2.112 \text{ gm/c.c}} \quad (0.0763 \text{ lb/cu.in})$$

Sample calculations continued:

(ii) Also, from equation D.2:

$$E_{11,\ \text{E-glass}} = E_{11f,\ \text{E-glass}}\ V_f + E_{11r,\ \text{E-glass}}\ (1-V_f)$$

$$= (83)(0.6) + (21)(1-0.6)$$

$$= \underline{58.2\ \text{GPa}}\ \ (8.439\ \text{MSI})$$

TABLE D-1

FIBRE AND RESIN PROPERTIES

PROPERTIES \ MATERIALS	E-GLASS	S2-GLASS	KEVLAR 29	KEVLAR 49	AS-CARBON
FIBRE DENSITY (gm/c.c.)	2.72[1]	2.49[1]	1.44[1]	1.44[1]	1.82[1]
RESIN DENSITY (gm/c.c.)	1.20[1]	1.20[1]	1.20[1]	1.20[1]	1.20[1]
E_{11_f} (GPa)	83[1,2]	93.2[1]	81.7[1]	124[1]	182[1,3]
E_{11_r} (GPa)	21[1,2]	2.6[1]	-5.3[1]	-10.5[1]	27[1]
E_{22_f} (GPa)	32	29	6	6	12
E_{22_r} (GPa)	-19[4]	-3	1	1	1

Notes:
1. Experimental result from University of Ottawa. (Ref. [19]).
2. Up to 50% of ultimate strength.
3. Up to 40% of ultimate strength.
4. The -ve value is obtained from the intercept of best fitting straight line.

APPENDIX 'E'

COST OF MATERIALS

[REF. 19]

APPENDIX 'E'

COST OF MATERIALS

The costs of the five identified materials and SMC (S2-glass) used in the analysis are calculated by the rule of mixtures. The following table gives the cost and density of each fibre and resin.

TABLE E-1

COST[1] AND DENSITY[2] OF FIBRE AND RESIN

FIBRE	FIBRE COST (1985 $/Kg)	RESIN COST (1985 $/Kg)	FIBRE DENSITY (gm/c.c.)	RESIN DENSITY (gm/c.c.)
E-GLASS	2.0	3.6	2.72	1.20
S2-GLASS	8.0	3.6	2.49	1.20
KEVLAR 29	50.0	3.6	1.44	1.20
KEVLAR 49	30.0	3.6	1.44	1.20
AS-CARBON	40.0	3.6	1.82	1.20

Notes: 1. Data from in-house study [1].
2. From Table D-1 of Appendix D.

Sample Calculation:

(i) Calculate the cost of E-glass, V_f = 0.60

Cost of E-glass (60%) = Fibre cost x V_f x Fibre Density +

Resin cost x (1 - V_f) x Resin Density

$$= \left(\frac{2.0}{1000}\ \$/gm\right)(0.6)(2.72\ gm/c.c.) +$$

$$\left(\frac{3.6}{1000}\ \$/gm\right)(1-0.6)(1.2\ gm/c.c.)$$

$$= \underline{\underline{\$4.992 \times 10^{-3}/c.c.}}$$

From Appendix D:

Density of E-glass (60%) = 2.112 gm/c.c.

$$\therefore \text{Cost of E-glass (60\%} = \frac{\$4.992 \times 10^{-3}/c.c.}{2.112\ gm/c.c}$$

$$= \underline{\underline{\$2.3636/Kg\ (\$1.074/lb)}}$$

(ii) Calculate the cost of SMC (S2-glass, R65)

V_f = 48.5%

% by weight (fibre) = 65%

Cost of SMC (S2-glass, R65)

= Fibre cost x % by weight + cost of resin x (1-% by weight)

= ($8.0/Kg)(0.65) + ($3.6/Kg)(1 - 0.65)

= $6.46/Kg ($2.94/lb)